OPTICALLY STIMULATED LUMINESCENCE DATING OF FLUVIAL SEDIMENTS: APPLICATIONS AND IMPLICATIONS TO PALEOSEISMOLOGY AND PALEOCLIMATOLOGY

A thesis submitted to
The Maharaja Sayajirao University of Baroda, Vadodara
For the award of the degree of
Doctor of Philosophy
In
Geology

By
MANOJ KUMAR JAISWAL

Physical Research Laboratory
Ahmedabad– 380 009, INDIA

October 2005

DECLARATION

This is to certify that the contents of this thesis comprise original research work of the candidate and have at no time been submitted for any other degree.

Prof. S. Ganapathi

I/C Head of the Department
Department of Geology
Faculty of Science
M.S. University of Baroda
Vadodara–390 002, Gujarat

Guide:

Dr. S.K. Gupta
Planetary and Geosciences Division
Physical Research Laboratory
Ahmedabad- 380 009, Gujarat

Co-Guide:

Dr. S. J. Patel
Department of Geology
Faculty of Science
M.S. University of Baroda,
Vadodara–390 002, Gujarat

Author:

Manoj Kumar Jaiswal

Abstract

The dynamic Himalaya is the result of collision of the Indian and the Asian plate. The signatures of climatic and tectonic events during its evolution are preserved in the form of various geomorphic features. This thesis deals with the methodological aspects of luminescence dating of fluvial sediments in the Himalaya. The results are then used to understand some aspects of the past climate and seismic events in Himalaya.

Optically Stimulated Luminescence (OSL) dating relies on the premise that daylight exposure of the constituent minerals during their pre-depositional transport photo-bleaches the geological signal to a zero or near zero level. In case of fluvial sediments, the daylight is attenuated due to variety of factors such as depth of water column and turbidity. This implies that the fluvial sediments are in general partially and heterogeneously bleached at the time of their deposition. Luminescence dating methods such as the Single Aliquot Regeneration (SAR) method now enable an understanding of the bleaching history of a sample and help in the isolation of the most bleached grains for age estimation.

The present study examined the feasibility of using OSL dating for a variety of fluvial environments from Himalayan terrain. The basic effort was towards examining the validity of the basic assumptions of luminescence dating technique using samples with age constraints. In this process new protocols were developed, tested and applied. The aim and scope of the thesis can be summarized in two broad categories–

1. Methodological aspects

Sensitivity changes during the measurement of natural OSL is not accounted for, in conventional SAR protocol. Such a change could imply systematic offsets in SAR ages. This aspect was examined for a large variety of sediments using 110^{o}C TL peak as a surrogate for OSL sensitivity. Results indicated that sensitivity changes could range from 20-50% and therefore corresponding offsets in ages could occur.

A practical handicap in applying SAR protocol is that it consumes considerable measurement time. This implies a low data throughput. Recently, a practical solution towards increasing the data throughput was suggested. This involved construction of a Standard Growth Curve (SGC) from a small set of growth curves, on which sensitivity corrected natural luminescences from large number of aliquots are read to estimate the paleodose. This process minimizes time by eliminating the need of carrying out a full SAR cycle that comprises the construction of a growth curve for each aliquot. A detailed investigation suggested that reliable SGC-SAR based ages can be obtained for cases where regression coefficient of SGC is greater than 0.9.

2. Feasibility of sediment dating from Himalayan terrain, chronology and its Implications–

Breaching of a landslide induced natural lake is quite common in Himalayas and results in flash

floods. This provides high velocity, high bed load and high suspension load flows. A feasibility study for the dating of sediments transported under these conditions was examined using samples of a known catastrophic flood event in Himalaya. This was the 1970 flood in the Alaknanda basin. A suite of samples at various distances downstream from the origin of flood over a distance of ~250 km were collected. No systematic change in bleaching was found although mean grain size of the sample decreased as the distance of travel of the sediment. However samples deposited during receding phase of flood has indicated significant bleaching up to 90% and gave a notional luminescence age of ~ 400 a, indicating the magnitude of 'zero error' in luminescence dating of such sediments.

The extent of daylight bleaching for the slack water deposit in Raiwala near Haridwar was also examined. The difference between mean and least 10% of paleodoses suggested that samples were partially bleached and the SAR protocol could still provide realistic ages. Almost 1.5 meter of sediment was deposited in a time period of ~2.3ka to ~800 years having 14 flood couplets in total. The results accorded well with paleoclimate records.

Fan sediments comprise gravel and coarse-grained sands. Typical transport distance in the case of Himalaya fans sediments is of the order of few km and the bleaching in such sediments is expected to be partial. It has been suggested that mega fan aggradation in Ganga plain occurred during the time of the initiation of humid climate that was preceded by a long arid phase when huge amount of sediment from the Himalaya were transported into the Ganga plain. The data suggested that the mega fan sediments are relatively better bleached as compared to piedmont fan sediments. Our results concluded that the studied section of the mega fan sedimentation postdate the Last Glacial Maximum and occurred in three episodes during ~14 – 8 ka. This accorded well with the paleoclimate records. The possible cause of well-bleached mega-fan sediment is explained by the prolonged daylight exposure during weathering in arid period. Chronology of the younger piedmont fan suggests its formation during ~2 – 1 ka.

During tectonic uplift of the riverbed, the river incises into the bedrock and leaves a thin veneer (~1-2 meter) of sediments on incised bedrock. Samples from such strath terraces in Tista valley were taken for feasibility of luminescence dating with respect to bleaching. A poor bleaching indicated by wide dose distribution. However, minimum 10% SAR ages provided a stratigraphically consist inverted age sequences. The luminescence ages suggest that the Darjeeling-Sikkim-Tibet wedge is going through a cycle of various phases of mountain building processes. There were two deformation fronts active between 20–5 ka; one near the Main Boundary Thrust and the other on south of the mountain front. The results suggested that the region close to the Main boundary thrust in Tista valley is neo-tectonically active and out of sequence thrusting occurred due to various phases of mountain building processes. Luminescence SAR ages have indicated a varying incision rates of 3–10 mm/year by river Tista in the studied section.

Overall the present thesis established that reliable ages using Luminescence Dating could be estimated for sediments from wide range of depositional environment. Radiocarbon dating has limited applicability in the region on account of contamination and hence reliable chronology of these sediments was not possible till this work. The present thesis examined the bleaching aspects of luminescence dating and the implication of SAR analysis in sediments from the Himalaya. This study therefore provides a basis for the application of Luminescence Dating and concludes that it can play a significant role in studies related to paleoclimate and tectonic in the Himalayan region.

Acknowledgements

I feel overwhelmed in expressing my gratitude to Prof. Ashok K. Singhvi, under whose supervision this work was carried out. This thesis is the result of his continued support, encouragement and inspiring guidance. His valuable suggestions and critical reviews at all stages of the work had gone a long way in shaping of the work to its present form. His sense of humor was of great support at some difficult times and helped me completing this challenging work on luminescence chronology of Himalayan sediments.

I am extremely grateful to Dr. S.K. Gupta for his guidance, suggestions and review during course of the work carried out for the present work.

It gives me immense pleasure to put on record the guidance and untiring support, I received from Dr. S.J. Patel and Dr. L.S. Chamyal, Department of Geology, M.S. University of Baroda, Vadodara.

I am grateful to Prof. S. Krishnaswami, Prof. R. Ramesh, Prof. S. K. Bhattacharya, Prof. S.V.S. Murty, Prof. M. M. Sarin, Prof. J. N. Goswami, Dr. J.R. Trivedi, Dr. S.K. Singh, Dr. J. S. Ray and Dr. D. Banerjee for their valuable suggestions and critical review during seminars and reviews.

My sincere thanks are due to Dr. B.R. Arora, Director, Wadia Institute of Himalayan Geology, Dehradun for his help, encouragement and moral support during writing of the thesis.

The guidance and encouragement I received from Dr. Malay Mukul, Scientist, CM-MACS, Bangalore and Prof. R.J. Wasson, Charles Darwin University, Australia, during the course of the work including field tour is gratefully acknowledged. I am extremely grateful to Prof. M.D. Shastry, Prof. Andrew Murray, Dr. Mark Bateman and Dr. Mayank Jain for the many useful discussions I had with them.

Financial support in the form of Travel Grants from Department of Science and Technology (DST) and Council of Scientific and Industrial Research (CSIR) is also gratefully acknowledged for supporting a tour to attend the “UK Luminescence and ESR meeting, 2004” held at St. Andrews University, Scotland, UK.

I am extremely grateful to the Director, Physical Research Laboratory for providing infrastructure to carry out the research work. Many thanks are due to staff of the Lab, especially to Workshop, Library, Canteen, Stores and Purchase section. I am thankful to Babu bhai and D.R. Shelat for helping in providing lab material and Nitrogen Gas Cylinders in time to carry out the experimental work.

I am thankful to Anil Shukla, Ravi Bhushan, R. D. Deshpande, R. Mahajan and Dr. M.G. Yadava for their guidance and support to carry out the work. Deepu, Som Sharma, Rama and Bhavsar bhai is highly acknowledged for an enjoyable company during post-lunch tea session.

I am extremely thankful to my senior lab colleagues. Dr. N. Juyal, Dr. P. Srivastava, Dr. P.J. Thomas, Dr. G. Mathew, J.T. Padia and Vachaspati Pandey are highly acknowledged for their critical reviews and thought provoking discussions at all stages of work. Their sweet and brotherly nature for a healthy lab is memorable.

I am thankful to my colleagues Yogesh Nagar, P. Morthekai and Madhav for their help, support and discussions during the course of the work. I enjoyed their joyful company.

I will do injustice to my friends, just by thanks and acknowledging them. Their help, support and motivations cannot be evaluated. Special thanks are due to Bhai sahab–Neeraj Rastogi for his valuable support, help and encouragement throughout the work. His optimistic nature was always helpful to come out from the bad phases of life. I am extremely grateful to Santosh and Anuradha for their moral support and sharing our moments of all the ups and downs of life. Santosh's excellent sense of humor and very original and creative immediate response of any event is memorable. Getting frustrated with Sanjeev is memorable; however, he completed his work on time leaving everybody a bit surprised. Anirban, a cool man behaved like an elder brother in our group and shared our emotions. Sanyal's laugh (after *gussa*) and super fast sound of Sajan is memorable. Manish and Pradyumna Pathak are acknowledged for an enjoyable company especially in TV room. Thanks are due to my neighbor Harish and Deval, Yogesh and Yogita, Soumen and Jhumma for their kind support to my family. I am grateful to Mrs. Pauline and Bhoomi for their emotional support and encouragement during the course of the work. Many thanks are due to Maibam, S.Rajesh, Vinay Rai, Rajesh Agnihotri, Alok Taori, Jitti, Tarun Dalai, Subraoto, Aninda, Sudeshna, Sarika, Shilpy, Harsha, Uma, Jayendra, Tarak, Sanat, Dilip, Virendra, Ravindra, Vinay Choudhary, Satya, Shreyas and Jayesh Das (and Mrs. Das) for a memorable and enjoyable environment in PRL campus. The list is too long to put all of my friends here.

I am also grateful to my friends in Wadia Institute of Himalayan Geology, Dehradun especially Amit, Arun, Deepak, Bhuvan, Shreejit, Dr. Suresh, Jyoti, Anubhooti, Priti, Anusuiya, Sneha, Iqrar, Sandeep, Senthil for their support and an enjoyable company during the thesis writing.

Last but not the least I am grateful and thankful to my mother and my darling wife "Raxita" for their love, affection, unknown sacrifices, help and support. This work would not have been completed without their help and support. I am also thankful to my son 'Shivam' whose smile was enough to feel fresh after work.

Thesis contents

Page

Figures

Page

Chapter 1: Introduction

Chapter 2: Experimental Procedures

Chapter 3: Natural Sensitivity Changes During OSL Measurement

Chapter 4: Limits and Applicability of Standard Growth Curve

Chapter 5: Fluvial sediments in diverse Depositional Settings

Chapter 6: Luminescence Chronology of Fluvial archives: Paleoclimatic and Paleoseismic Implications

Tables

Page

Chapter 1

Introduction

1.1 Introduction

Geomorphology deals with the quantitative understanding of processes and amplitude of erosion and sedimentation on the earth. Geomorphology investigates landforms and the processes that sculpt them. The processes can range from the physical and chemical weathering of rocks to the production of sediments caused by climate and tectonics. In the time domain, these processes can range from an instantaneous short-lived event to a slowly occurring phenomenon spanning few million years (Miall, 1996; Kale, 2001). In general, climatic and tectonic processes are periodic. It therefore, becomes necessary to estimate the recurrence intervals of these events so as to understand and model the nature of the underlying geodynamic processes for a better assessment of risk and hazards associated with such changes. Geodynamic processes that lead to creation, transport, deposition and preservation of sedimentary records are climate and tectonics and proper understandings of their relationship to these forcing functions are keys to geomorphologic science and geological correlations.

The present thesis deals with understanding of the processes and chronology on one such sediment archive – the fluvial sediments to further understand the paleoclimate changes and paleotectonic events. Sedimentary archive of a river system depends on, (i) production; (ii) transfer; (iii) deposition and (iv) preservation, of sediments. These elements are controlled by a variety of factors ranging from the weathering of the source rocks to fluvial discharge and sediment load. Fluvial sediments occur variously as lake sediments, flood plain sediments, terraces, fans and delta, and their potential for paleoclimate and tectonic studies has been well established (Gregory and Benito, 2003). Techniques such as sequence stratigraphic methods, paleomagnetic polarity reversals etc. enable development of a hierarchy of depositional events. However, absolute chronology that enables quantitative estimates of rates of processes and their recurrence intervals has so far been difficult, due to lack of chronometric methods.

Himalaya is a consequence of collision of two converging continental plates viz., the Indian and the Asian plate. In Himalaya, under-thrusting the Indian plate beneath the Asian plate accommodates a part of the plate movement and the rest is accommodated on the surface by folding and thrusting. When compressional stress exceeds the strain limit of these rocks, they fail along the faults producing earthquakes, landslides and landslide induced floods and geomorphic features such as raised terraces and seismites are formed. Chronology of these deposits and their physical parameters provide a means to deduce long-term slip rates and the rates of strain release. Current quantitative estimates of the Himalayan Seismic Hazard are based on Global Positioning System (GPS) data that has been used to compute slips between the Indian and the Asian plates (Bilham et al., 1997; 2001). Though of significance, the GPS data so far spans only a decade, too small duration to assess geodynamic processes. Consequently, a longer-term perspective is needed. This needs securely dated landform features that are caused by tectonic events. The present study is amongst the few contributions to quantitative paleoseismology of Himalaya, which deals with an estimation of the timing of paleotectonic events and will eventually help in the identification of buried faults, estimation of earthquake magnitude and amplitude of slip along the faults and the recurrence interval of past earthquakes. Present structure of the Himalayan orogeny is a consequence of tectonic and climatic processes as well (Phadtare, 2000; Pratt et al., 2002; Juyal, 2004; Hodges et al., 2004; Whipple and Meade, 2004; Burbank, 2005; Leier et al., 2005). The present study attempts to use alluvial fans, slack water deposit and terraces to reconstruct past climate changes and past seismic activities in Himalaya.

Luminescence method provides a direct dating of the depositional event of sediments using their constituent minerals viz. Quartz and feldspar. The method provides the age of deposition of sediments without any ambiguity of sample/strata correlation. The age range (100 a – 500 ka) and the availability of the dating material (i.e. Quartz/feldspar), makes this method applicable to almost all of the mid to late Quaternary deposits. Quartz and feldspar act as natural dosimeters that provide a cumulative record of the radiation exposure from the naturally occurring radioactive elements viz., ^{238}U, ^{232}Th and ^{40}K in sediments. The technique relies on the fact that mineral grains constituting the sediments are exposed to adequate daylight resulting in a photo bleaching of the geological luminescence to a zero or near zero residual value. This event reset the luminescence clock. Typically few tens of seconds of daylight exposure is sufficient to achieve a near total photo bleaching. This criterion is adequately met in case of wind-transported sediments due to the availability of full daylight flux and its short wavelength spectra. However, in the case of fluvial sediments, such a total bleaching may not be reached, due to attenuation of daylight both in respect of its flux and energy spectrum, the water column, its sediment load and turbulence. The daylight spectrum shifts towards the red wavelength when the bleaching cross section drops down by nearly an order of magnitude or more. Thus, even though a short duration of daylight (typically 30-50 seconds of full spectrum) is required for clear daylight photo bleaching, the fluvial sediments may be bleached partially prior to deposition. Methodologically, the present thesis explored the feasibility of luminescence dating for fluvial sediments from a terrain with a high topographic relief implying rapid transportation and deposition of sediment by the fluvial system. A variety of fluvial environments that exists in the Himalayan terrain, were examined. These are–

(i) Flash flood sediment
(ii) Low energy, slack water deposit
(iii) High energy alluvial fan deposit and
(iv) Tectonically uplifted, fluvial terraces.

The basic philosophy was to examine validity of the basic assumption of luminescence dating technique on samples with age controls. In the process new protocols were developed, tested and applied. A brief summary of existing dating methods for fluvial sediments is given below to provide a perspective on the need of luminescence dating.

1.2 Brief description of existing dating method for quaternary sediments

Several dating methods have been employed for the chronology of fluvial sediments. These can be grouped in two categories – (i) relative and (ii) absolute chronometric techniques. In relative chronometric methods, techniques like order of superposition, Paleomagnetism, Amino acid Racemization and other chemical methods are used. The absolute dating techniques include radiocarbon, K-Ar, U-series, ^{210}Pb, radiocarbon, luminescence, cosmic rays produced isotopes etc. A comparison of these methods is provided in Table 1.1.

(i) Paleomagnetism–The present direction of earth's magnetic field changes approximately once a million years from normal to reversal and vice versa. Sediments deposited under free air fall or still water condition preserve the direction of ambient earth's magnetic field known as Depositional Remnant Magnetism (DRM). The continuous gradual change in virtual geomagnetic pole (VGP) is known as secular variation that varies from place to place. The movement of VGP gives a succession of normal (parallel to the present) and reverse (180^{o} out of phase with the present) polarity transitions that are preserved as DRM in the sedimentary rock record. These normal and reverse polarity transitions are chronologically constrained by absolute dating using the dating of volcanic ash layers or index fossils. Thus based on the constant sedimentation rate, successive normal and reverse polarity in the stratigraphy can be assigned absolute ages. The most notable reversal events in the Quaternary era are the Brunhes-Matuyama boundary at 780 ka and the Blake event at 110 ka. (Hailwood, 1989; Aissauoi et al., 1993)

Table 1.1. Age range and material used in various dating techniques for quaternary material. (After Singhvi and Banerjee, 2003)

mETHODS	**aGE rANGE**	**sAMPLES**
1. Paleomagnetism	0.1 Ma – 2 Ma	Sediments
2. Amino-acids	0.1 ka –500 ka	Bones, cells and tooth
3. U Series	100 a – 350 ka	Calcite, bones, corals, shells
4. K-Ar / Ar-Ar	1 ka – >>1 Ma	Volcanic material
5. Fission Track	> 50 ka	Slags and volcanic materials
6. Radiocarbon	1950 AD – 50 ka	Wood, bones, coral, shells, etc
7. Electron Spin Resonance	1 ka –1 Ma	Bones, tooth, coral, volcanic ash
8. Luminescence	100 a – >500 ka	Pottery and sediments

Recently identified, geomagnetic excursion is a brief (<80^o) but significant departure of VGP from the geocentric axial dipole that remains for ~10^3 years. This is an intermediate type of geomagnetic behavior between secular variation and polarity transition (King and Peck, 2001; Sangode et al., 2002). At present the use of excursions and short events to provide stratigraphic control and chronology is promising but requires extensive further study.

(ii) Aminoacid racemization–Amino-acids are found in two forms- ‘L’ (leavo rotator) and ‘D’ (dextro rotator) having same chemical formula but different structural symmetry. Racemization is the process of converting L form to D form. ‘L’ form is dominant in the living tissue that converts into ‘D’ form when the tissue dies and the ratio L/D used as a chronometric tool. The racemization rate depends on the organism type and temperature. Racemization rate is higher in warm condition and consequently undetermined temperature fluctuations lead to systematic error in age estimates. The temperature constraint implies that method has been successful in cool/temperate regions where the average sediment temperatures are low and nearly constant. On the other hand, in the tropics, the method has not found sufficient usage in view of high seasonal changes in temperature. The materials used for the dating are bones, shell and tooth and the age range is 100 a – 500 ka. (Bender, 1974; Bada et al., 1984)

(iii) Radiocarbon dating (^{14}C)–Radiocarbon is probably the most used radiometric dating method to date young sediments (Wohlfarth, 1996). The method depends on the production of ^{14}C from atmosphere. Low energy cosmic ray neutrons interact with ^{14}N to form ^{14}C in the upper atmosphere. ^{14}C so produced, reacts with O_2 to form $^{14}CO_2$, which is chemically similar to $^{12}CO_2$. The CO_2 is fixed in various organic and inorganic reservoirs such as plants, animals (via photosynthesis) and carbonates. When the plant or organisms die, they stop taking ^{14}C from the environment and the ^{14}C present in them decays with a half-life of 5730 years. Measurement of ^{14}C activity in the organic matter enables calculation of the time of cessation of ^{14}C intake. Absence of organic matter in fluvial sequences, uncertainty in the relationship between sample and the strata makes it difficult to use this method. Short half-life of

^{14}C isotope limits its usage only up to ~ 40 ka. Further the technique assumes ^{14}C production was uniform in the past which is not the case as studies on tree rings, corals and varves has demonstrated that ^{14}C production varied in time due to change in cosmic ray fluxes and this calls for calibration of radiocarbon ages (Stuiver et al., 1998). Contamination of the samples by either the 'dead' or the 'modern' carbon from organic and inorganic carbon (carbonates) can alter ages substantially and has been a major impediment in the routine use of the method. Methodologically accelerator mass spectrometry (AMS) technique have now made it possible to achieve high precision ages on small (~ few mg) samples by measuring the concentration of ^{14}C directly without waiting for its decay.

(iv) Cosmogenic radio nuclide dating (^{10}Be and ^{26}Al)–Interaction of Cosmic ray particles such as with rocks and sediments produces radioactive nuclides such as ^{10}Be and ^{26}Al, via reaction such as Quartz and Feldspar provide ideal target material. Due to cosmic ray exposure the concentration of insitu produced ^{10}Be and ^{26}Al increases and can be used as a time marker, provided off course that the production rate of these nuclides could be accurately determined that requires a rigorous understanding of the changes in (a) the cosmic ray flux through time and (b) the irradiation geometry. Though a promising method, in accreting sediment sequences problems due to time dependent changes in shielding makes the cosmic ray age model dependent. Further complications arise due to periods of quiescence/soil formation in sediment accretion, erosion and finite inheritance of radioactivity makes the application difficult (Nishiizumi et al., 1989; Lal, 1991).

(v) Uranium series dating–This is another radiometric dating technique which uses the short lived isotopes of Uranium (U) and Thorium (Th) decay series. Disequilibrium in the Uranium series decay chain has been used extensively to date pure carbonates. The isotope of U remain in solution in seawater where the uranyl ion (UO_2^{2+}) tends to form carbonate complexes {e.g., $UO_2(CO_3)_3^{4-}$}, which allow it to co precipitate with calcium carbonate. As a result, Calcium carbonate minerals such as calcite and aragonite typically contain appreciable concentration of U but lack Th. However, occurrence of pure carbonates in continental setting is rare; furthermore, correction for detritus Thorium is often necessary. The trace element in the carbonate can be used to date material up to about 350 ka old (Ivanovich et al., 1992; Kaufman, 1993).

(vi) K-Ar/Ar-Ar dating–K-Ar dating has been extensively used in geochronology. Potassium has a small radioactive component ^{40}K, which has a half-life of 1.2 billion years. ^{40}K decays by two possible modes, namely ^{40}Ar and ^{40}Ca. Being an inert gas, ^{40}Ar keeps accumulating in the lattice of potassium bearing mineral and does not form any chemical bond. In suitable cases, Ar gas can remain in the lattice over geological time scales. By measuring the concentration of K and Ar, age of the mineral can be computed. This method is suitable only for sedimentary sequences containing volcanic ash layer that ensures the trapping of Ar molecules from the atmosphere only during its formation (Quidelleur et al., 2001). A significant problem with this method is the diffusion of Ar from rocks leading to underestimation of ages. The problem of Argon loss has been overcome by the Ar-Ar method (Faure and Mensing, 2005). First ^{39}K is converted to ^{39}Ar by neutron bombardment to know the ^{40}K as ^{40}K and ^{39}K ratio is fixed in the rock. ^{39}Ar and ^{40}Ar can be measured together in the mass spectrometer. The principle of the Ar-Ar method is therefore the use of ^{39}Ar as a proxy for ^{40}K.

(vii) Fission Track–Fission track (FT) is the radiation-damaged path left by two heavy fragments of uranium-fission. The tracks are formed by the spontaneous fission of ^{238}U with a half-life of 8.2×10^{15} a. The tracks are enlarged by chemical etching to a microscopically visible size of >15 micron length. The tracks accumulate with time, and consequently their number is a measure of the elapsed time, i.e. the age of the material. Although many minerals and glasses contain fossil fission-tracks, only a few of them, mainly zircon, apatite, sphene and various glasses can be used for the quaternary (~10^6 years). This is because the uranium content should be high to produce a sufficient number of fission tracks in the available 10^4 to 10^6 years. The tracks are removed at a blocking temperature and thus reset the clock. Apatite has 90^oC blocking temperature and zircon around 300^oC. Hence it is useful in determining rate of uplift and exhumation of rocks if geothermal gradient is known (Hurford and Green, 1982). The clue for interpreting fission-track ages is the stability of tracks. Fission tracks are unstable, a phenomenon known as fading. Elevated temperatures accelerate the fading process and fading causes shortening of etch able track length. The resulting track loss tends to lower the apparent fission-track age.

(viii) Electron Spin Resonance (ESR)–ESR relates to detection of the concentration of trapped charges due to ionization on absorption of radiation dose from the ambience of the sample to be dated. Thus the trapped charges are proportional to the concentration of ambient radioactivity and time elapsed since the material formed e.g. tooth, bone etc. Some of the trapped charges have a net spin, making them paramagnetic. These act as free magnets, and can be detected by placing the sample under a magnetic field. In the simplest case, these individual magnets can occupy two energy states ($m_s = +1/2$ & $-1/2$) when placed in a magnetic field and the population is higher in lower energy state. It is then possible to cause transition of charges from low-energy state to high-energy state, using appropriate microwave energy. The amount of microwave energy absorbed is proportional to trapped charge concentration and with appropriate calibration using a laboratory Gamma dose, the ESR absorption intensity can be converted into absorbed dose. In ESR dating of bones and tooth, the radiation dosimetry involves some basic assumptions arising due to the uptake of U during burial. In the case of tooth enamel, the post mortem uptake of uranium implies that the present day value of uranium cannot be taken *per se* for dose-rate calculation. Instead, depending on the nature of the sample and the site, the dose is calculated on the basis of either the linear uptake or an early uptake. The dating range of ESR spans 1ka - 1Ma years and is ideally suited to directly date organic remains, provided the dosimetry is established unambiguously (Ikeya, 1993, Mathew et al., 2004). The forgoing makes it clear that as yet no secure method exists for middle to late quaternary fluvial sequences.

Luminescence methods have the potential of providing direct dating of the depositional event of sediments without any ambiguity of sample/strata correlation. The age range (100a -1Ma) and the availability of the dating material (i.e. Quartz/feldspar) that are ubiquitous, make this method applicable to nearly all kind of Quaternary sediments.

1.3 Luminescence Dating- Basic Principles

Luminescence dating is a radiation damage technique, which uses the natural radioactive elements present in the sediment viz. U, Th and K. The minerals used for dating are Quartz and feldspar, which are ubiquitous. The luminescence production in minerals is explained by the band theory of solids. There are three basic steps for luminescence emission. These are–

(i) Production of charges– The passage of ionizing radiations arising from the decay of natural radioactive elements viz. U, Th and K induces ionization in the Quartz and feldspar. The charges are excited from valence band to conduction band after ionization and are free to move in the lattice (Aitken, 1985; 1998) (Fig. 1.1).

(ii) Trapping and storage– Some of these charges get trapped at defects of the crystal. Residence time of these charges range from a few seconds to a few million years and depends on the temperature, energy levels and charge environment of the charge trapping centers.

(iii) Eviction– The stored charges get de-trapped with energy stimulus, either optical or thermal. These travel in the lattice and at suitable site and radiatively recombine to produce luminescence.

If thermal heating does the stimulation of these charges, the process is called Thermally Stimulated Luminescence (TSL or TL). If it is done by light exposure, then the process is termed as Optically Stimulated Luminescence (OSL). Depending upon the wavelength of optical source for stimulation, such as Green Light Stimulated Luminescence (GLSL), Infra red Stimulated Luminescence (IRSL) and Blue-Green Light Stimulation (BGSL) are routinely used. The intensity of luminescence thus produced is proportional to radiation dose and under some assumption can be related to the time of burial of the sediment. In this, the concentrations of the radioactive elements in the sediment can be measured. The dating range over which this technique is used is small enough as compared to half lives of these radioactive elements viz. U, Th and K, implying that as a first approximation, the radiation flux is constant through the burial history. Quartz and feldspar mineral act as sensitive radiation dosimeter of this radiation due to the radioactive viz. U, Th and K in the

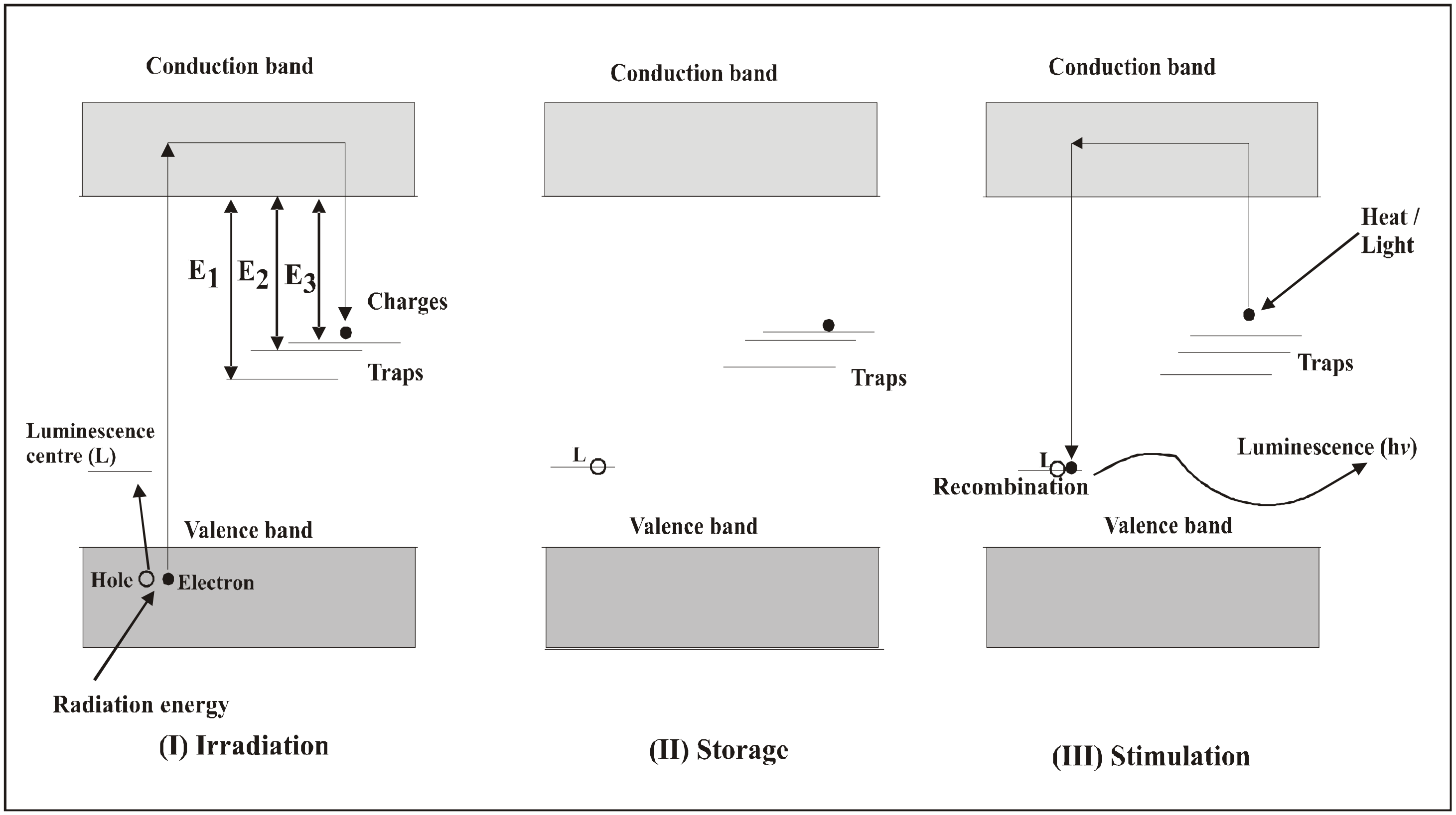

Figure 1.1. Three processes of luminescence production in an insulating solid; (i) absorption of radiation and production of charges; (ii) storage of charges in the defects of the crystal to up to a few Ma and (iii) eviction of charges from the traps on heating/ light exposure and production of luminescence on recombination of these charges. (After Aitken, 1986)

11

sediment. Luminescence method dates the event of last sun exposure/heating of the sediment grains. In view of this luminescence dating of the sediments relies on the fact–

(i) The natural radiation environment of the sediments arising due to the decay of natural radioactive elements viz. ^{238}U, ^{232}Th and ^{40}K along with cosmic rays provides a constant flux of radiation to the natural mineral constituting the sediments.

(ii) These minerals viz. Quartz/feldspar act as sensitive radiation dosimeters to record these radiations with constant sensitivity, in a cumulative manner and preserve this record over geological time.

(iii) The daylight exposure of the sediment/minerals photo-bleaches the geological signal during their transport to a zero or near zero level.

On burial, further exposure to daylight ceases and re-accumulation of charges is initiated due to the ambient radioactivity. This process continues unabated till excavation. The net luminescence acquired in a grain is determined by the rate of irradiation (luminescence production) and the duration of burial.

1.4 Age equation

After burial of a sediment, the naturally occurring minerals e.g. Quartz and feldspar, act as natural dosimeter and absorbs radiation from the radioactive element viz. U, Th and K from the sediment. Thus the luminescence signal in Quartz and feldspar is proportional to the time of burial and the concentration of radioactive elements. This signal acquired after the burial of the sediment can be measured in the laboratory. The age estimation needs two parameters, (i) amount of signal accumulated over burial period (measured as equivalent radiation dose) and (ii) rate of ambience radiation absorbed by the Quartz/feldspar. The unit of amount of energy absorbed is defined as Gray (Gy)(1Gy =1 Joule/kg). The Quartz/feldspar obtained from the natural setting has variable luminescence response at grain level due to, (i) varying amount of impurities (ii) type of defects present and (iii) varying thermal history at source. Therefore, it is important to ascertain the sensitivity of these minerals (response to radiation dose). This can be estimated in the lab by irradiating the Quartz sample using artificial radiation source e.g. ^{90}Sr, then measure the luminescence output to compare with the luminescence received from the naturally irradiated sample. This is termed as Paleodose or accrued dose. Hence Paleodose (P), expressed in Gy, is the amount of laboratory dose given to the mineral to produce same amount of luminescence as the sample, as received.

The second important parameter is to measure the rate of radiation given to the sample in the natural setting. This can be done my measuring the amount of radioactive elements in the sediments. Usually the dose rate is expressed in terms of Gy/ ka.

The age equation is based on the fact that, (i) natural radiation environment is a mixed radiation field comprising alpha, beta and gamma rays and (ii) the luminescence produced by highly ionizing alpha particles (per unit dose) is substantially lower compared to those by weakly ionizing radiation (beta, gamma and cosmic rays) due to number of charges produced in a short track of alpha particle path is much higher than the available traps. Hence most of the charges are wasted with respect to the luminescence production. These factors are accounted for by defining an alpha efficiency parameter a such that,

a = luminescence per unit alpha dose / luminescence per unit beta dose

and by computing the annual dose as a sum of contribution from all the radiation components i.e.

$$\text{Age} = \text{total luminescence} / \sum_{\alpha,\beta,\gamma,c} \{(\text{luminescence} / \text{unit dose}) \times (\text{dose} / \text{year})\}$$

Combining above two relations, the age equation reduces to

$$\text{Age} = \text{Equivalent beta dose (or Paleodose)} / (aD_\alpha + D_\beta + D_\gamma + D_c)$$

Where D_α, D_β, D_γ and Dc represents the dose rate contribution from alpha, beta, gamma and cosmic rays respectively. In dating of coarse-grain Quartz, the alpha dose affected skin (typically 10-15 micron thick) is removed by etching. Hence in dating the coarse grain Quartz, the age equation further reduces to

$$\text{Age} = \text{Equivalent beta dose (or Paleodose)} / (D_\beta + D_\gamma + D_c)$$

The events dated by this method are the event that de-traps the acquired geological luminescence in a sample to the residual level. Hence this method is used to date last heating event of pottery, baked clay, last daylight exposure of the sediment and formation of minerals e.g. gypsum etc.

1.5 Optical bleaching of the sediment

The basic assumption of luminescence dating is the extent of photo bleaching or thermal heating. Typical time for resetting is ~few tens of seconds of cloud free daylight for sediments or few seconds of thermal heating at 500^{o}C in case of pottery. In case of aeolian sediment and sample of archaeological importance (e.g. pottery) this assumption is reasonably met. In the case of fluvial sediment, this may or may not be satisfied due to following reasons,

(i) Attenuation of sun light due to depth of water column and turbidity

(ii) Transport distance of the sediment

(iii) Sediment coagulation by clay

(iv) Inverse dependence of bleaching efficiencies with stimulating wavelength

In view of this bleaching of the sediment grains in fluvial environment is likely to be incomplete and heterogeneous. Kronberg (1983) found that a wide range of wavelength from the solar spectrum bleached the TL of K-feldspar. Significant bleaching occurred in a sample kept at 7 m of clear lake water. Gemmell (1985; 1988) examined the bleaching of fine grain minerals in suspension through laboratory and field experiment. For dense suspension (>1 g/l), a limited reduction in TL was seen depending on flow rate. Godfrey-Smith et al. (1988) showed the photo-luminescence signal of Quartz and feldspar are well bleached by sunlight within a few minutes to few hours, which also progresses during overcast condition, and that the bleaching rate observed was proportional to the light level. Berger and Luternaur (1987) have demonstrated that the intensity at 4 m depth in a turbulent river is ~10^{4} times less than at the surface and severely attenuated below 500 nm and above 690 nm of the wavelength of that light (Fig. 1.2). Ditlefsen (1992) examined bleaching of the sediment in a 75 cm column of water for different concentration of suspended matter. He observed that for dilute suspension (<0.02 g/l), optically stimulated luminescence was reduced by 95% within 20 hrs whereas the TL was reduced only by 25-50%. In the more dense suspension (>0.05 g/l), light level was reduced significantly primarily due to the suspended particles rather than by the turbulence. Fuller (1994) has shown the attenuation of the UV component of the solar spectrum as it passes through water. The attenuation occurs in still water and increases under turbid water conditions, where fine grained particle scatter light.

These results, suggests that heterogeneous and incomplete bleaching is a likely for water-lain (fluvial) sediments. Laboratory experiments suggest that TL signal takes 5-6 hrs to bleach on daylight exposure whereas OSL signal bleaches in a few tens of seconds. Proszynska-Bordas et al. (1992), Murray et al. (1992), and Kamaludin et al. (1993) applied successfully this technique on fluvial sediment. On the other hand Gemmell (1997) & Forman and Ennis (1992) did not find TL dating suitable for dating fluvial sediments.

Similarly OSL dating has been applied to fluvial sediments. Balescu and Lamothe (1994) established chronostratigraphy between ^{14}C, ESR, amino acid, TL and IRSL dates with two exceptions. Murray (1996) concluded that luminescence dating offers a considerable improvement over other techniques including ^{14}C for dating recently transported fluvial sediments. Single Aliquot Regeneration (SAR) technique provided insight into the variability of paleodoses caused by heterogeneous bleaching (Murray and Roberts, 1997). Olley et al. (1998) examined 70 years old flood sediment from the Murrumbidgee River and found that age computed from mean paleodose varied from 400 – 1000 years depending on the grain size with the coarser size being relatively better bleached. The minimum age computed from least 5% of the dose distribution provided consistent age. Thomas et al. (2004) investigated fluvial deposit in Anantpur district, south India, using small aliquots and single grain technique having ^{14}C age control. The average ages were 200 years off from the ^{14}C age of 507 ± 40 years. However, doses calculated from leading edge method (Lepper et al., 2001) gave consistent ages. Zhang et al. (2003) found an overestimation of 200 years in averaged OSL age in a fluvial sediment containing 700 years old potsherd. When they applied the method similar as given by Fuchs and Lang (2001), results were consistent with the expected age. Rittenour et al. (2003) dated three, channel belt deposit from the lower Missisippi valley using luminescence. All the optical ages were in good agreement with geomorphological relationship and the existing radiocarbon age control. Chen et al. (2003) compared to radiocarbon ages with OSL ages from a core of ~200 m thick sediment in the subsiding southwestern coastal plain of Taiwan. He found a good agreement in the optical ages and radiocarbon ages up to

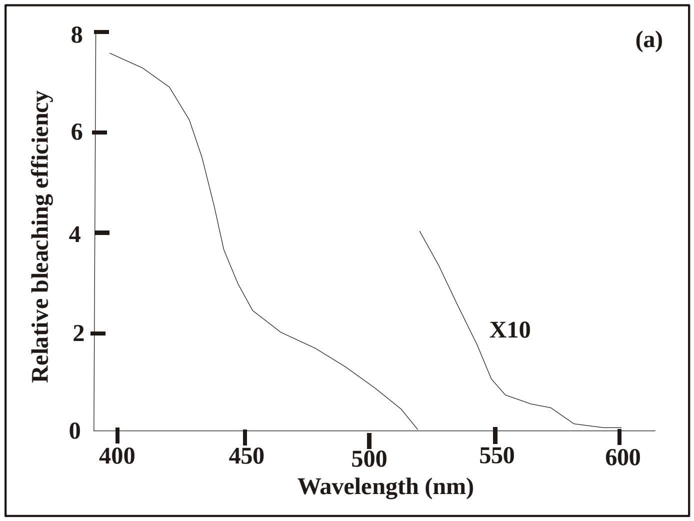

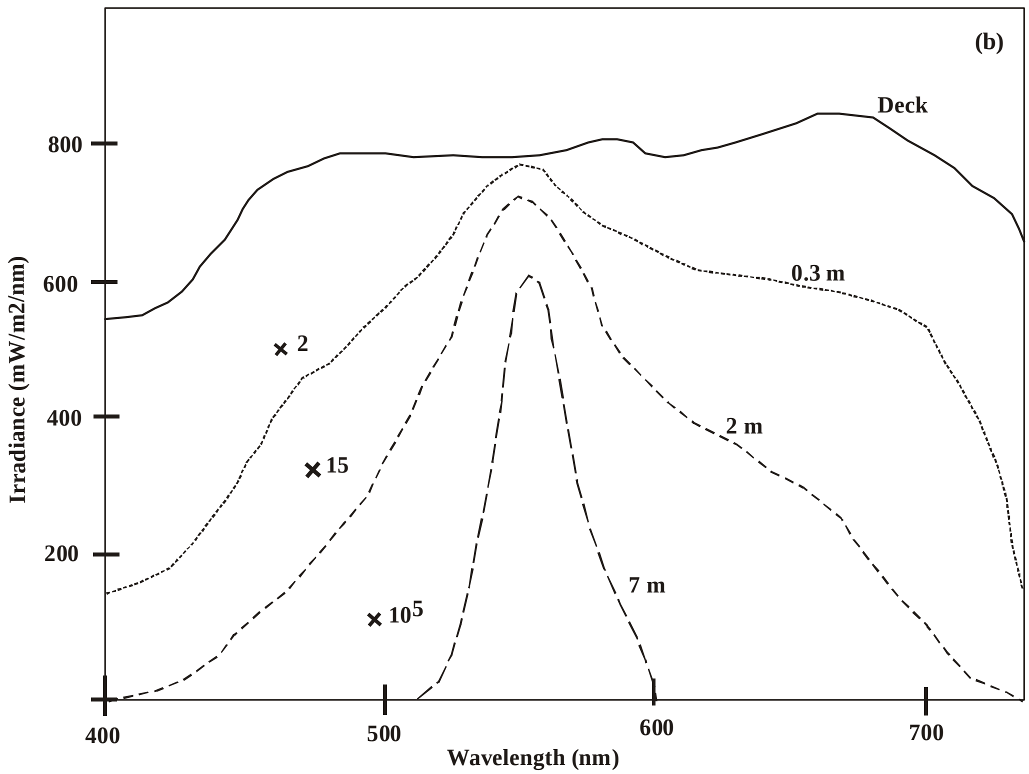

Figure 1.2. (a) Decreased bleaching efficiency with respect to increase in wavelength (after Aitken, 1998). (b) Attenuation of daylight intensity in the water as a fuction of depth. As depth increases, the intensity of daylight decreases rapidly together with the cut off of lower wavelength spectrum. (After Berger, 1990)

14 ka suggesting well bleached sediment. However, modern sediment from the channel deposit gave the ages from few hundred years to 12 ka, which is surprising.

Summarizing, that results from above discussed examples and similarly several more various geomorphological archives have shown that partial bleaching of fluvial sediment still remains a potential problem in the luminescence dating and is the field of active research that needs extensive study.

1.6 Luminescence dating techniques

Initially the luminescence method was applied on pottery and sediments from desert environments that are supposed to be free from any problem of resetting of luminescence clock. Hence the techniques involved in evaluating ages for such samples were applied successfully viz. multiple aliquot additive dose (MAAD) and multiple aliquot regeneration (MAR). These techniques involve a large number of aliquots (typically 30-40) to calculate a single age. This technique assumes that all the aliquots used in the measurement are having equal thermal/bleaching history, which is true for baked pottery or wind blown sediments, but may or may not be true in case of partially bleached sediments and thus can lead to erroneous ages. These techniques are discussed in detail in chapter-2, “Experimental Procedures”, of the thesis.

Huntley et al. (1985) gave the concept of single aliquot analysis. Duller (1991) took the initiative to do some analysis on fine grain using IRSL and applied Single Aliquot Additive Dose (SAAD) method in which OSL readout, irradiation and dose growth curve was constructed on an aliquot, avoiding inter aliquot comparison. In this, OSL readout is done for 0.1 second, which ensures an insignificant loss of signal and then same aliquot was irradiated followed by preheat. OSL is readout again for the same amount of time. This is repeated 4-5 times and a growth curve is constructed between OSL counts and laboratory added beta doses. The intercept of this growth curve on the dose axis gives the paleodose. Significant amount of signal loss was observed in each cycle because of preheat. Hence in the last, this was corrected by repeating measurements for preheat only. Duller (1994a; 1994b) suggested correction procedures for the loss in OSL intensity due to preheat. Stokes (1994) applied this procedure successfully on Quartz from aeolian contexts with good agreement between single aliquot additive dose and multiple aliquot methods. Galloway (1996) and

Murray and Roberts (1997) summarized procedure for SAAD on Feldspar and Quartz respectively.

The luminescence sensitivity can change due to light or heat treatment. This limits the use of SAAD, as there is no provision to correct for sensitivity changes at each stage of irradiation/preheat cycle. Due to significant drop in sensitivity during measurement of natural signal, this method was unsuccessful when applied to samples of river Loire in France (Colls, 1999). Single Aliquot Regeneration (SAR) method developed by Murray and Roberts (1997) provides for OSL sensitivity changes during preheat and measurement. In this method, OSL is readout for 60-100 seconds to record and bleach the natural signal. The same aliquot is then given a small test dose (<10-20% of paleodose) followed by preheat and OSL measurement. This signal is used to correct for any change in sensitivity, which would have occurred during natural OSL measurement. Then on the same aliquot, a cycle of incremental laboratory doses, preheat and OSL measurements is carried out along with test dose measurement at appropriate instance to construct sensitivity corrected growth curve. The sensitivity corrected natural OSL is interpolated onto this growth curve to estimate the paleodose. This method is used widely to date water-lain sediments as well as aeolian sand too. Typically a large number of aliquots (~50-100) are analyzed and a large number of paleodoses are obtained. The distribution of paleodoses then permits the use of optimum paleodose value. This was not possible using multiple aliquot methods. The SAR method has several advantages over multiple aliquot methods–

(a) Inter-aliquot normalization is not required as all the measurements are done on one aliquot.

(b) Small sample size is required which makes it suitable for small amount of sample with low yield of Quartz e.g. pottery and ceramics.

(c) High precision data due to large number of paleodoses from the same sample and these being independent measurements, an standard error on mean is used.

(d) SAR technique gives a range of paleodoses, thus enable estimation for degree of bleaching in a sample. A poorly bleached sample will show a large scatter of doses having high standard deviation of the data.

The most bleached part is the fraction yielding the lowest paleodose. For older samples, the amount of partial bleaching may not be significant proportion of the natural signal. Jain et al. (2004) reviewed the work of OSL dating on fluvial sediments and categorized the sample in two sections, (i) <1 ka old sample; (ii) >1ka old. These authors suggested that the minimum age model is successful in <1 ka old sample and mean age is preferable for the samples >1 ka old, as the residual signal was a small proportion of the natural signal build during extended burial of the samples. However, it may be pointed out that this boundary is only indicative and will change with a variety of factor ranging from the dose rate, the sensitivity and the pre-depositional bleaching.

1.7 Estimation of bleaching using SAR

Li and Wintle, (1992) and Li (1994) suggested a procedure to estimate the extent of bleaching by analyzing a plot of natural luminescence intensities against their respective paleodoses. They argued that in a well-bleached sample, individual aliquots will have identical paleodoses but may show a wide variation in natural intensities because of varying sensitivity of individual grains. However, poorly bleached sample will show a wide variation in both, paleodose and brightness. This is a useful method to graphically represent the extent of bleaching, but does not enable for quantitative analysis.

Clarke (1996) suggested some threshold values to determine the degree of bleaching based on scatter in the paleodoses. In young samples, if the standard deviation (Sd) of all the paleodoses is below an arbitrary number 5, the sample was considered well bleached. It is noteworthy that the scatter in the data due to experimental factors (measurement errors in dose growth curve, beta source heterogeneity and variation in environmental natural dose due to heterogeneity in natural beta dose) can lead to standard deviation of up to 20-30% of the paleodose. For samples >1-2 ka, the scatter on paleodoses decreases as a proportion of the mean paleodose with the age of the sample. In view of this, Clarke (1996) defined some additional parameters (Sn, defined as ratio of standard deviation to the mean of paleodoses) to determine the degree of bleaching. According to that,

When $Sn < 0.05 \Rightarrow$ majority of the grains are well bleached.

If, $0.05 < Sn < 0.1 \Rightarrow$ moderately well bleached

If, $0.1 < Sn < 0.15 \Rightarrow$ moderately poorly bleached

If, $Sn > 0.15 \Rightarrow$ poorly bleached.

On the basis of above if $Sd > 5$ and $Sn > 0.1$, indicates poorly bleaching and if $Sd > 5$ and $Sn < 0.1$ then it means that sample was poorly bleached at time of deposition but it is no more a hurdle for dating due to large burial time.

1.8 Estimating Paleodose from a Dose Distribution

From a measured distribution of SAR paleodoses, the determination of optimum paleodose for age determination is also difficult. Though average paleodose is used extensively to assign true paleodose, it basically compromises on bleaching history and nearly approximates a multiple aliquot analysis. Average value can be used when paleodoses distribution can be approximated to a narrow Gaussian distribution. For a skewed paleodoses distribution, the use of a mean paleodose is likely to yield erroneous results and aliquots with larger paleodose will bias the results.

Murray et al. (1995) examined the dose distribution from 70-year-old fluvial sample. The historical records provided a firm control of age. The dose distribution was not a simple Gaussian suggesting heterogeneous bleaching. The paleodose distributions were highly asymmetric, positively skewed and in only one case, the average De corresponded to the historical ages. Thus in orders to obtain the representative De, three largest paleodoses had to be discarded.

Olley et al. (1999) suggested that, "the more asymmetric the distribution, the greater the probability that the aliquots with the lowest dose more closely represent the true burial dose." It was stated that the asymmetry is because of two discrete subset of grains of different resetting history, however it is not clear that why there should be two discrete groups, because natural sedimentary processes are more likely to produce grains representing a continuum of solar exposures rather than discrete subsets of grains with uniform exposures.

Lepper et al. (2001) hypothesized that experimentally measured dose distribution is the convolution of the distribution arising from natural sedimentary processes and experimental error propagation. He tried to deconvolute the effect of experimental error and distribution arising from sedimentary processes.

Fuchs and Lang (2001) studied fluvial Quartz sediments from Greece on a small number of aliquots (N=10) due to very small amount of Quartz present in the sediment. A dose recovery test was done, which gave a relative standard deviation of 4%, which is the percentage ratio of standard deviation to the mean. This error was considered to be experimental error associated with the measurements. All the paleodoses were ranked in ascending order and standard deviation was calculated starting from the lowest two paleodoses to match it with experimental error of 4%. The number of paleodoses in each step was increased till these matched the experimental error. The relative standard deviation (RSD) defined as percentage ratio of standard deviation to the mean. RSD matches with the experimental error of 4%. Only those aliquots were considered for paleodose estimation whose relative standard deviation is ~ 4%. This approach provided ages in agreement with control/anticipated age.

Olley et al. (1998) suggested an approach utilizing the variation in paleodose in Quartz sediment. He represented the paleodose variation in a histogram constructed from typically small aliquot of 60-100 grains on each aliquot and concluded that the lowest 5-12 % of the paleodoses arranged in ascending order gave the optimum estimate of the true paleodose. He has successfully shown it by applying the technique on a 5 years old flood sample.

Zhang et al. (2003) worked on the fluvial sand from the Yongdinghe alluvial fan near Beijing city and suggested that the scatter in paleodose estimation due to experimental error and varying luminescence properties should be similar to the scatter of the first regenerated OSL as it is measured for a similar dose from each aliquot similar to dose recovery test. This suggested to use the relative standard deviation (RSD) in the first regenerated OSL as a surrogate for experimental error. The procedure given below enables selection of the most bleached aliquots–

1. The RSD of the sensitivity corrected first regeneration OSL is calculated (say RSD1).
2. The aliquots are ranked in ascending order of their sensitivity corrected natural OSL.

3. Beginning with the two aliquots with the lowest natural OSL, the RSD of the natural OSL is calculated by increasing one aliquot each time till it reaches to value when the value is equal to RSD1. Thus the preceding aliquots are considered as relatively well bleached.
4. Finally the average of these are taken as representative dose.

Summarizing, the determination of the most realistic paleodose from dose distribution is still a matter of active research. The dose distribution curve has been variously analyzed. For a narrow Gaussian distribution, the average can be the representative paleodose, however, in case of positively skewed distribution, the lowest values can be considered as true representative of the paleodose. The relative standard deviation (RSD) of the data serves as an indicator of the heterogeneity in paleodoses as it informs on the magnitude of deviation from the mean paleodose.

1.9 Luminescence dating and Himalaya

In India, Luminescence dating was initiated in the context of archaeological samples and later applied to aeolian and fluvial samples from the Thar Desert, southern Desert margin, Ganga plain and Himalaya. (Singhvi et al., 1982; Someshwar et al., 1997; Jain et al., 1999; Kale et al., 2000; Srivastava et al., 2001; Juyal, et al., 2003; Srivastava et al., 2003; Singh et al., 2003; Kar et al., 2004; Chamyal and Juyal, 2005). The mineral grains in Ganga plain sediments travel a distance of a few hundreds of km before entering into the Ganga plain from Himalaya. It can therefore, reasonably be assumed that such sediment in Ganga plain were adequately bleached before their deposition in different fluvial environment and this has been observed (Someshwar et al., 1997).

Himalaya provides a unique system that preserves the record of ancient to modern seismic and climatic regimes. Few studies have been done using luminescence techniques. Banerjee et al. (1999) dated fault gouges at Nainital, central Himalaya and inferred that a major tectonic activity in the region at around 40 ka. They have further suggested that geological luminescence in fault gouge was reset to zero by frictional heating during faulting event. More recently using luminescence dating of relict lake sediments in Garbyang basin in the higher Himalaya for paleoclimatic and paleoseismic studies (Juyal, 2004).

Himalayan comprises rocks of various lithologies, which on weathering provide sediments that are transported primarily by glacial melt and rain water. These sediments have Quartz grains of diverse luminescence properties. The high relief of the region implies rapid transport, but higher altitude of the region enables higher energy component in the daylight. Such a contrasting configuration of processes, one that favours rapid bleaching and the other that impede, made it necessary to examine their relative effects under various depositional settings. This is discussed further in the following section.

1.10 The objectives and scope of the thesis

Besides examining the prospects of dating on sediments from the Himalayan region for paleoseismology and paleoclimatology this thesis also explored new methodological avenues in the application of luminescence.

1.10.1 Methodological aspects

In Optical dating, the single aliquot regeneration method has been the preferred analysis protocol (Murray and Wintle, 2000). The natural signal is plotted on laboratory generated Luminescence–Dose growth curve. The luminescence generated growth curve is plotted such that any sensitivity change due to laboratory illumination and preheat is corrected for. In the thesis we examined two aspects related to the use of this method–

(i) Sensitivity changes during the read out of natural signal– Stokes and Singhvi, (under preparation) suggested that the conventional SAR protocol did not take into account, the sensitivity changes during the read out of natural OSL. This could imply systematic offsets in age estimation. In this thesis that suggestion was examined for a variety of sediments and comparison on sensitivity corrected paleodoses and uncorrected paleodoses were made. In this, it was first demonstrated that the 110^{o}C TL peak was correlated with BGSL signal and then this peak was used as a surrogate for the OSL sensitivity. Results indicate a significant sensitivity changes that can effect the ages significantly, if ignored.

(ii) Optimization of data throughput in SAR–In the dating of a partially bleached samples, a large number (typically 60-100) of aliquots are needed to construct a statistically valid dose distribution. Given that a typical SAR sequence requires 2-3 hours of machine time per aliquot. Analysis of a sample may take up to ~200 hrs (i.e. 7-8 days) of TL/OSL reader time. This limits the data throughput to 3-4 samples/month. To overcome this slow throughput somewhat, Roberts and Duller, (2004) suggested use of the Standard Growth Curve (SGC). In this approach, a fixed number of SAR growth curves of a sample are constructed. These are then merged to form a standard growth curve onto which the natural OSL of numerous aliquots are interpolated, thereby avoiding the need for constructing growth curve for each aliquot. The applicability and limitation of the method was tested further on samples from the above-discussed sequences and a criterion for its applicability was suggested and tested on samples of diverse depositional environment.

1.10.2 Feasibility of sediment dating from Himalayan terrain and their implications to Paleoseismology and Paleoclimatology

Various sedimentary archives in the Himalaya have preserved the signatures of paleoseismic and paleoclimatic events. However, their chronometry has been a problem due to difficulties in reliable application of the radiocarbon method. The applicability of luminescence dating for the sediments of different depositional environment was examined in detail. A brief survey of the geological archives and their bleaching aspects are as under–

(i) Sediment bleaching during flash flood–Flash floods in Himalaya are associated with breaching of landslide induced temporary reservoirs. These last for few hours to few days. Such floods can occur under poor light (overcast sky) condition with high sediment to water ratio. In the present study an attempt was made to investigate the extent of bleaching experienced by the flash flood sediments during 1970’s Alaknanda flood as a function of distance from the origin and grain size. Both peak flood sediments (assorted sand) and winnowing phase of flood sediment (flood plain fine, silty-sand) were collected at 5 localities from Gohna Lake to Rishikesh (~250 km down stream) and analyzed using the standard SAR protocol.

(ii) Slack water deposits–Slack water deposit is found in the tributary streams away from the trunk channel during high floods. Flood water when enters the tributary stream looses its energy. This facilitates the sequential deposition of sand, silt and clay. Alternately it can be suggested that sediment remain in suspension for long time particularly the silt and clay hence well bleached. This aspect was examined in the slack water deposit at Raiwala, near Haridwar in the state of Uttaranchal.

(iii) High sediment load alluvial fan deposit–Alluvial fan is a characteristic feature of mountain fronts where a sudden drop in topographic relief occurs. A stream emanating from the mountain abruptly loses its energy and deposits its load as a fan shaped body. Dimension of alluvial fans varies from few km to hundreds of km in extent. Thus, in order to create such a large sedimentary body it is important to have, (a) high sediment supply and (b) hydraulic energy for transporting the sediment. Large volume of sediments can be generated either by climate (glacial grinding, or physical weathering) or by tectonics (physical break down of rocks). Sediment transport generally is facilitated during the transitional climatic condition (arid to humid). Thus chronology of fan sequences can provide information about past climate and/or tectonic history. However, in view of their transportation under high sediment water ratio, bleaching of sediment was expected to be partial. In the present study, Yamuna-Ganga (mega fan) and piedmont fan sequences were investigated for luminescence characteristic and chronology using SAR protocol on Quartz mineral extract.

(iv)Tectonically uplifted fluvial terraces–Seismicity in Himalaya is associated with major boundary thrusts. Episodic activity along these thrusts is manifested in the development of various geomorphic features. Fluvial terraces are one such feature that responds to the seismicity by way of their vertical offsets and development of unpaired terrace sequences. Unlike seismities that can be generated by the activity along distal thrusts (far field effect), incised terraces are related to the proximal thrusts. In view of this, dating of the incised terraces provides information about the palaeoseismic activity along the thrust. In the lower Tista valley 5 incised terraces are developed in between the South Kalijhora Thrust (SKT) and Andherijhora Thrust (AT). The terrace sequence is differentiated by distinct vertical offsets ranging from 20 m to 2 m suggesting varying activity in the associated thrusts (Mukul, 2000). Present work deals with the luminescence dating of sediments from these terraces and then applied to infer about the seismic activity of the region.

1.11 Chapter wise details

<u>Chapter-1</u>: Introduction– This chapter describes various dating methods for quaternary sediments and the merits of Luminescence dating. Basic principles and methodology of Luminescence dating is discussed in some detail. Various measurement protocols such as the Single aliquot methods, multiple aliquot methods, are briefed. Applicability of the method to fluvial sediments is reviewed. The chapter describes the various geomorphologic archives studied in the thesis.

<u>Chapter-2:</u> Experimental procedures– This chapter describes the various experimental methods and protocols used in the measurement of OSL and age calculation. These include the sample preparation, measurement protocol, analysis and the instruments used. New analysis that includes assessment of spatial heterogeneity of the beta dose from a beta source, the use of Linearly Modulated-OSL (LM-OSL) partial bleach method and the extent of bioturbation and its effect on Luminescence dating in sediments, is described.

<u>Chapter-3:</u> Changes in natural OSL sensitivity and its implications to dating– Stokes and Singhvi (under preparation) recently suggested that the conventional SAR protocol does not take into account the change in Luminescence sensitivity during measurement of natural OSL. This effect occurs during preheat and luminescence readout. In the conventional SAR, the sensitivity is corrected using test dose measurement only after the natural OSL measurement. This implies that the sensitivity change during the read out of natural OSL is not accounted for and can lead to gross systematic errors. In this thesis, this aspect is examined in detail. In order to do so, the SAR protocol has been modified by, (i) demonstrating correlation of 110^{o}C TL peak with the OSL peak and (ii) using the 110^{o}C peak as a surrogate for sensitivity. Results on samples are discussed which indicate systematic offset. Most of the samples have shown sensitivity changes up to 20-30%, however, a few of them have shown up to 50%. This chapter describes the sensitivity changes and its possible repercussions on the samples collected in the Himalaya.

Chapter-4: Limit and applicability of standard growth curve– This chapter describes a methodological advance in the application of the SAR protocol, by suggesting the criteria for applicability of the Standard Growth Curve (SGC) for SAR. Single Aliquot Regeneration (SAR) is a widely used protocol in luminescence dating. However, a practical handicap is that it consumes considerable machine time implying a low data throughput. A practical solution towards increasing the data throughput has been suggested recently by Roberts and Duller (2004). In this merging a fixed number of laboratory generated growth curves generates a Standard Growth Curve (SGC) and the natural signal is read onto that curve to get the paleodose. This chapter describes the applicability of SGC on samples of different depositional environment in Himalayan.

Chapter-5: Fluvial sediments in diverse depositional settings and applicability of luminescence dating– In this section, experimental data on the dose distribution of various samples collected from four geological settings in Himalayan terrain are presented and discussed with reference to their depositional environment. Various parameter that provide an estimate on the extent of bleaching is discussed and general inference on the extent of bleaching in various depositional domains within the fluvial regimes are discussed.

Chapter-6: Luminescence chronology of fluvial archives and its applications to paleoclimatology and paleoseismology– This chapter deals with geological interpretation of the ages obtained on various sediments as discussed above. It includes three sections -(i) Chronology and its implications in reconstructing paleocliamte of Yamuna-Ganga alluvial fan are discussed in detail; (ii) Chronology and paleo-flood record near Raiwala at Hardwar was described. It helped in computing the recurrence interval of a flood in the area; (iii) Chronology of uplifted river terraces in Tista valley with its application on Himalayan evolution in relation to Critical Wedge Taper model.

Chapter-7: Conclusion and Future Outlook- This chapter outlines results obtained from the present study and also describes the future prospect of the work presented in the thesis.

References

Aissauoi, D.M., McNeill, D.F. and Hurley, N.F., (eds.) 1993. Applications of paleomagnetism to sedimentary geology. *Society for sedimentary geology*, special publication, 49, 216 pp.

Aitken, M.J., 1985. *Thermoluminescence dating*. Academic Press, London.

Aitken, M.J., 1998. *An introduction to optical dating*, Oxford University Press, Oxford.

Bada, J. L., Gillespie, R., Gowlett, J. A. J. and Hedges, R. E. M., 1984. Accelerator mass spectrometry radiocarbon ages of amino acid extracts from California palaeoindian skeletons. *Nature*, 312, 442–443.

Balescu, S. and Lamothe, M., 1994. Comparison of TL and IRSL age estimate of feldspar coarse grains from waterlain sediments. *Quaternary Geochronology*, 13, 437–444.

Banerjee, D., Singhvi, A. K., Bagati, T. N., Mohindra, R., 1997. Luminescence chronology of seismites at Sumdo (Spiti valley) near Kaurik-Chango Fault, Northwestern Himalaya. *Current Science*, 73**,** 276–281.

Banerjee, D., Singhvi, A.K., Pande, K., Gogte, V.D. and Chandra B.P., 1999. Towards a direct dating of fault gouges using luminescence dating techniques: methodological aspects. *Current Science*, 77, 256–268.

Bender, M.L., 1974. Reliability of amino acid racemization dating and paleotemperature analysis of bones. *Nature*, 252, 378–381.

Berger, G.W. and Luternauer, J.J., 1987. Preliminary fieldwork for Thermoluminescence dating Studies at the Fraser river delta, British Columbia. *Geological Survey of Canada Paper* 87, 901–904.

Berger, G.W., 1990. Effectiveness of natural zeroing of the Thermoluminescence in sediments. *Journal of Geophysical Research*, 95, 12375–12397.

Bilham, R., Larsen K., Freymueller, & Project Idylhim members, 1997. GPS measurement of present day convergence across the Nepal Himalaya. *Nature*, 386, 61–64.

Bilham, R., Blume, F., Bendick, R. & Gaur, V.K., 1998. Geodetic constraints on the translation and deformation of India, implications for future great Himalayan earthquake. *Current Science*, 74, 213–229.

Bilham, R., Gaur, V.K. and Molnar, P., 2001. Himalayan seismic Hazard. *Science*, 293, 1442–1444.

Burbank, D.W., 2005. Cracking the Himalaya. *Nature*, vol. 434, 963–964.

Chamyal, L.S. and Juyal, N., 2005. Climatic events in Southern Thar Desert Margin and Higher Central Himalaya during the Last Glacial Stage (LGS): Possible linkages. *Himalayan Geology*, 26, 241–252.

Chen, Y.W., Chen, Y.G., Murray, A.S., Liu, T.K. and Lai, T.C., 2003. Luminescence dating of fluvial deposits on the southwestern coastal plain, Taiwan. *Quaternary Science reviews*, 22, 1223–1229.

Clarke, M.L., 1996. IRSL dating of sands: bleaching characteristics at deposition inferred from the use of single aliquots. *Radiation Measurement*, 26, 611–620.

Colls A.E.L., 1999. Optical dating of fluvial sediments from the Loire Valley, France. *M.S. dissertation*, Unversity of Oxford, Oxford, UK.

Ditlefsen, C., 1992. Bleaching of K-feldspar in turbid water suspensions : A comparison of photo and Thermoluminescence signals. *Quaternary Science Reviews*, 11, 33–38.

Duller, G.A.T., 1991, Equivalent dose determination using single aliquots. *Nuclear tracks And Radiation measurement*, 18, 371–378.

Duller, G.A.T., 1994a. Luminescence dating of poorly bleached sediments from Scotland. *Quaternary Science Reviews*, 13, 149–156.

Duller, G.A.T., 1994b, Luminescence dating using single aliquots: new procedures. *Quaternary Geochronology,* 13, 149–156.

Faure, G. and Mensing, T.M., 2005. *Isotopes: Principles and Applications*, John Wiley and sons, 896 pp.

Forman S.L. and Ennis G., 1992. Limitation of thermoluminescence to date waterlain Sediments from glaciated fjord environments of western Spitsbergen, Svalbard. *Quaternary Science Reviews*, 11, 61–70.

Fuller, I.C., 1994, Alluvial response to environmental change : luminescence dating of late quaternary sediment system. *Unpublished Ph.D. thesis*, University of Wales, Aberystwyth, UK.

Fuchs, M. and Lang, A., 2001. Optically Stimulated Luminescence dating of coarse-grain fluvial Quartz using single aliquot protocols on sediments from NE Peloponnese, Greece. *Quaternary Science Reviews*, 20, 783–787.

Galloway, R.B. 1996. Equivalent dose determination using only one sample: alternative analysis of data obtained from infrared stimulation of feldspar. *Radiation Measurement*, 26, 103–106.

Gemmell, A.M.D., 1985. Zeroing of the TL signal of sediment undergoing fluvial Transportation: A laboratory experiment, *Nuclear Tracks*, 10, 695–702.

Gemmell, A.M.D. 1988, Zeroing of the TL signal of sediment undergoing fluvioglacial Transport. An example from Austerdalen, Western Norway. *Quaternary science Reviews*, 7, 339–345.

Gemmell, A.M,D. 1997, Fluctuations in the thermoluminescence signal of suspended sediment In an Alpine glacial meltwater stream. *Quaternary Geochronology*, 16, 281–290.

Godfrey-Smith, D.I., Huntley D.J. and Chen, W.H., 1988. Optical dating studies of Quartz feldspar sediment extracts. *Quaternary Science Reviews*, 7, 373–380.

Gregory, K.J. and Benito, G., (eds.) 2003. *Paleohydrology, Understanding Global Change*. 390 pp., John Wiley and Sons Limited, England.

Hailwood, E.A., 1989. Magnetostratigraphy, 84 pp. Geological Society of London, *special report*, 19.

Hodges, K.V., Cameron, W., Ruhl, K., Schildgen, T. and Whipple, K., 2004. Quaternary deformation, river steepening and heavy precipitation at the front of the higher Himalayan ranges. *Earth and Planetary Sciences Letters,* 7012, 1–11.

Huntley, D.J., Godfrey-Smith, D.I. and Thewalt, M.L.W. 1985, Optical dating of sediments *Nature,* 313, 105–107.

Hurford, A.J. and Green, P.F., 1982. A user's guide to fission track dating calibration. *Earth and Planetary Science Letters*, 59, 343–354.

Ikeya, M.,1993. *New application of electron spin resonance dating, dosimetry and microscopy*, World Science, Singapur, New Jersey, Hong Kong, 520pp.

Ivanovich, M., Latham, A.G. and Ku, T.L., 1992. Uranium-series disequilibrium applications in geochronology. In M. Ivanovich and R.S. Harmon (Eds.), *U series disequilibria; Applications to earth, marine and Environmental Sciences*, 2nd ed., pp. 62-94. Clarendon, Oxford, UK.

Jain, M., Tondon, S.K., Bhatt S.C., Singhvi A.K., Mishra S., 1999. Alluvial and Aeolian sequences along the river Luni, Barmer district: physical stratigraphy and feasibility of luminescence chronology methods. In Vedic Saraswati, Radhakrishna B.P., Merh, S.S. (eds.) *Geological Society of India, memoir*, 42, 273–245.

Jain, M, Murray, A.S., Lars, Botter-Jensen, 2004. Optically Stimulated Luminescence Dating: How significant is incomplete light exposure in fluvial environments? *Quaternaire*, 15, 143–157.

Juyal, N., Kar, A., Rajaguru, S.N. and Singhvi, A.K., 2003. Chronostratigraphic evidence for episodes of desertification since the last glacial epoch in the southern margin of Thar Desert, India. In: A.S. Alsharhan, W.W. Wood, A.S. Goudie, A. Fowler and E.M. Abdellatif (eds.), *Desertification in the Third Millennium*. Swets & Zeitlinger (Balkema) Publishers, The Netherlands, 123–128.

Juyal. N., 2004. Chronology of Dryland sediments in western India and their correlation with the climate changes in Central Himalaya. *Unpublished Ph.D. Thesis* submitted to M.S. University of Baroda.

Kale, V.S., 2001. *Introduction to geomorphology*, Orient Longman Ltd.

Kale,V.S., Singhvi A.K., Mishra P.K. and Banerjee D., 2000. Sedimentary record and luminescence chronology of Late Holocene paleofloods in the Luni river, Thar desert, northwest India. *Catena*, 40, 337–358.

Kar, A., Singhvi, A.K., Juyal, N. and Rajaguru, S.N., 2004. Late Quaternary aeolian sedimentation history of the Thar desert. In: Sharma, Singh and De (eds.). *Geomorphology and Environment*, acb publication, Kolkata, India, 105–122.

Kamaludin, B.H., Nakamura, T., Price D.M., Woodroffe, C.D. & Fuji, S. 1993. Radiocarbon and thermoluminescence dating of the Old Alluvium from a coastal site in Perak, Malaysia. *Sedimentary Geology*, 83, 199–210.

Kaufman, A., 1993. An evaluation of several methods for determining ^{230}Th/U ages in impure carbonates. *Geochimica Cosmochimica Acta*, 57, 2303–2317.

King, J. and Peck, J., 2001. Chapter 4: Use of paleomagnetism in studies of lake sediments. *Tracking environmental change using lake sediments*, 1, Edited by, William M. Last and John P. Smol, Kluwer Academic Publishers.

Kronberg, C. 1983, Preliminary results of age determination by TL of interglacial and Interstadial sediments. *PACT*, 9, 595–605.

Lal, D., 1991. Cosmic ray labeling of erosion surfaces: In situ nuclide production rates and erosion models. *Earth and Planetary Science Letters*, 104, 424–439.

Leier, Andrew L., DeCelles, Peter G. and Pellitier Jon D., 2005. Mountains, monsoons and mega fans. *Geology*, 33(4), 289–292.

Lepper, K., Agersnap, L.N. and McKeever, S.W.S., 2001. Equivalent dose distribution analysis of Holocene eolian and fluvial Quartz sands from central Oklahoma. *Radiation Measurement*, 32, 603–608.

Li, S.H. and Wintle, A.G. 1992, Luminescence sensitivity change due to bleaching of sediment. *Nuclear Tracks Radiation Measurement*, 20, 567–573.

Li, S.H. 1994, Optical dating: insufficiently bleached sediments. *Radiation Measurement* 23, 563–567.

Mathew, G., Gundu Rao, T.K., Sohoni, P.S. and Karanth, R.V., 2004. ESR dating of inter fault gypsum from Katrol hill range Kachchh, Gujarat: implications for neotectonism. *Current Science*, 87, 1269–1274.

Miall, 1996. *The geology of fluvial deposit*, Springer-Verlag.

Mukul, M., 2000. The Geometry and Kinematics of the Main Boundary Thrust and related Neotectonics in the Darjiling Himalayan Fold-and-thrust belt, West Bengal, India. *Journal of Structural Geology* 22, 1261–1283.

Murray, A.S., Wohl E., & East, J. 1992. Thermoluminescence and excess ^{226}Ra decay dating of late quaternary fluvial sands, East Alligator river, Australia. *Quaternary Research*, 37, 29–41.

Murray, A.S., Olley, J.M. and Caitcheon, G.G., 1995. measurement of equivalent doses in Quartz from contemporary water-lain sediments using Optically Stimulated Luminescence. *Quaternary Science Reviews*, 14, 365–371.

Murray, A.S., 1996. Developments in Optically stimulated Luminescence and photo-transferred Thermoluminescence datingof young sediment : Application to a 2000 years sequence of flood deposits. *Geochimica et Cosmochimica Acta*., 60, 565–576.

Murray, A.S., Roberts, R.G. & Wintle, A.G., 1997. Equivalent dose measurement using a single aliquot of Quartz. *Radiation Measurement*, 27, 171–183.

Murray, A.S., Wintle, A.G.,2000. Luminescence dating of Quartz using an improved single aliquot regenerative-dose protocol. *Radiation Measurement*, 32 (1), 57–73.

Nishiizumi, K., Winterer, E.L., Kohn, C.P., Klein, J., Middleton, R., Lal, D. and Arnold, J.R., 1989. Cosmic ray production rates of ^{10}Be and ^{26}Al in Quartz from glacially polished rocks. *Journal of Geophysical Research*, 94, 17907–17915.

Olley, J.M., Caitcheon, G., & Murray A., 1998. The distribution of apparent dose as determined by optically stimulated luminescence in small aliquots of fluvial Quartz: implications for dating young sediments. *Quaternary Science Reviews*, 17, 1033–1040.

Olley, J.M., Caitcheon, G. and Roberts, R.G., 1999. The origin of dose distribution in fluvial sediments and the prospect of dating single grains from fluvial deposits using Optically Stimulated Luminescence. *Radiation Measurement*, 30, 207–217.

Phadtare, R. N. 2000, Sharp Decrease in summer monsoon strength 4000–3500 cal yr B.P. in the central higher himalaya of India based on pollen evidence from alpine peat. *Quaternary Research*, 53, 122–129.

Pratt, B., Burbank, D.W., Heimsath, A. and Ojha, T., 2002. Impulsive alleviation during early Holocene strengthened monsoons, central Nepal Himalaya. *Geology*, 30, 911–914.

Proszynska-Bordas, H., Stanska-Proszynska, W., and Proszynski, M., 1992. TL dating of

River terraces with fossil soils in the Mediterranean region. *Quaternary Sciences Reviews*, 11, 53–60.

Quidelleur, X., Gillot, P.Y., Soler, V. and Lefevre, J.C., 2001. K/Ar dating extended into the last millennium: application to the youngest effusive episode of the Teide volcano (Spain). *Geophysical Research Letters*, 28, 3067–3070.

Rittenour, T., Goble, R. and Blum, M., 2003. An optical age chronology of the late Pleistocene fluvial deposits in the northern lower Mississippi valley. *Quaternary Science reviews*, 22, 1105–1110.

Roberts, H.M., Duller, G.A.T., 2004. Standardized Growth Curves for optical dating of Sediment using multiple-grain aliquots. *Radiation Measurement*, 38, 241–252.

Sangode, S.J., Suresh, N., Bagati, T.N., Bloemendal, J., Kumar, R. and Thakur, V.C., 2002. Discovery of an aborted reversal (geomagnetic excursion) in the late

Pleistocene sediments of Pinjor Dun, NW Himalaya. *Current Science*, 82, 210–215.

Singh, I. B., Manoj K. Jaiswal, A. K. Singhvi and B. K. Singh, 2003, Rapid subsidence of western Ganga plain during late pleistocene : Evidence from optical dating of subsurface samples. *Current Science*, 84, 451–454.

Singhvi, A.K., Sharma Y.P. and Agrawal D.P. 1982. Thermoluminescence dating of sand dune in Rajasthan. *Nature*, 295, 313–315.

Singhvi, A. K., D. Banerjee, K. Pande, V. Gogte, K. S. Valdiya, 1994. Luminescence studies on Neotectonic Events in South-Central Kumaun Himalaya-A Feasibility Study. *Quaternary Science Reviews*, 13**,** 595–600.

Singhvi, A.K. and Banerjee, D., 2003. Luminescence dating in Earth and Planetary science- an appraisal. *Proceedings of the Fourth South Asia Geological Congress, New Delhi, India,(GEOSAS-IV)*, 11–25.

Someshwar Rao, M., Bisaria B.K. and Singhvi A.K., 1997. A feasibility study towards absolute dating of Indo-Gangetic alluvium using thermo-luminescence and Infrared stimulated luminescence techniques. *Current Science*, 72, 663–669.

Srivastava P., Juyal N., Singhvi A.K., Wasson R. J., Bateman M.D., 2001. Luminescence chronology of river adjustment and incision of Quaternary sediments in the Alluvial plain of Sabarmati river, north Gujarat, India. *Geomorphology*, 36, 217–229.

Srivastava P., Singh I.B., Sharma M., Singhvi A.K., 2003. Luminescence chronometry and late Quaternary geomorphic history of the Ganga plain, India. *Paleogeography, Paleoclimatology, Paleoecology*, 197, 15–41.

Stokes, S., 1994. The timing of OSL sensitivity changes in a natural Quartz. *Radiation Measurements*, 23, 601–605.

Stokes, S. and Singhvi, A.K.. Changes in natural OSL sensitivity during Single Aliquot Regeneration procedures and their implications to equivalent dose determination (Under preparation).

Stuiver, M., Reimer, P.J., Bard, E., Beck, J.W., Burr, G.S., Hughen, K.A., Kromer, B., McCormac G., Vander, P.J. and Spurk, M., 1998. IntCal98 radiocarbon age calibration, 24,000–0 cal BP. *Radiocarbon*, 40, 1041–83.

Thomas, P.J., Jain, M., Juyal, N. and Singhvi, A.K., 2004. Comparison of single grain and single aliquot OSL dose estimation in <3000 years old river sediment from south India. *Radiation Measurement*, 39, 457–469.

Whipple, K.X. and Meade, B.J., 2004. Controls on the strength of coupling among climate, erosion and deformation in two-sided, frictional orogenic wedges at steady state. *Journal of Geophysical Research*, 109, 1–24.

Wohlfarth, B., 1996. The chronology of the last termination: a review of radiocarbon-dated, high-resolution terrestrial stratigraphies. Quaternary Science Review, 15, 267–284.

Zhang, J.F., Zhou, L.P. and Yue, S.Y., 2003. Dating fluvial sediments by Optically Stimulated Luminescence: selection of equivalent doses for age calculation. *Quaternary Science Reviews*, 22, 1123–1129.

Chapter-2

Experimental Procedures

This chapter summarizes the various experimental aspects of analysis used in the studies presented in the thesis. Chapter includes a discussion on the following aspects–

(i) Sample preparation
(ii) TL/OSL measurements
(iii) Calibration of irradiation source
(iv) Estimation of paleodose
(v) Annual dose measurement

2.1 Sample preparation

All the sediments were collected in a specially designed cylindrical tube (~20 cm long and 5 cm diameter) made of aluminum or galvanized iron. These tubes were hammered into a vertical face of a cleaned stratigraphic sequence. Inside the laboratory, these tubes were opened under subdued red light conditions and the sediment from outer (light exposed) portion of both the ends of the tube was collected and kept for estimating the concentration of radioactive elements. Samples in the middle portion of the sample pipe was sequentially pretreated with 10% HCl and 30% H_2O_2 to remove carbonates and organic material. Further separation depended on the type and the mean grain size of the sediment. These were, quartz mineral separates (>100 micron) and polyminerallic fine grains (4-11 micron). The sample preparation for fine/coarse-grained sediment is below–

2.1.1 Coarse Grain separation technique

Chemically pretreated coarse-grained sediments were sieved (grain size 90-150 micron). Density separation using Sodium Polytungstate (ρ=2.58 g/cm^3) was carried out to separate quartz and feldspar minerals. The quartz fraction was etched with 40% HF for 80 min to remove the alpha affected skin. 12N HCl treatment for 40-50 minutes immediately followed the HF treatment to convert insoluble fluorides to soluble chlorides. Clean quartz grains extracted were then mounted on stainless steel discs (aliquot) with help of *Silkospray*™ silicon oil and their purity was tested for IRSL to detect possibilities of residual feldspar contamination. Samples with finite IRSL indicated a feldspar contaminant and such samples were re-etched for 10 minutes of HF followed again by 12N HCl.

2.1.2 Fine grain separation technique

Extraction of 4-11 micron grain size fraction involved de-flocculation of the samples with 0.1N sodium oxalate after treatment by HCl and H_2O_2. In general several treatments of Sodium oxalate were needed. At each stage samples were given vigorous ultrasonic treatment. The deflocculated sediment was put in 6 cm high column of acetone and allowed to settle for 1.5 minutes. In this period the grain size fraction of >12 micron settles down. From the suspended sample the grain fraction 4-11 micron were obtained by allowing this size to settle on typically for 15 minutes. This fraction was then dispersed either in acetone or alcohol solution and equal volumes (1 ml) of this suspension were dropped using pipette onto small flat-bottomed glass vials, each containing a polished aluminum disc (~9.65 mm diameter) at their bottom. After drying the solution in an oven (temperature < 45^{o}C) for ~15-16hrs, the discs with thin layer typically a few micron of fine grain were taken out and transferred into sample holders.

2.2 TL/OSL Measurement

The TL/OSL measurements were made on three TL/OSL readers - (i) Daybreak 1100; (ii) Risoe TL/OSL Reader DA-15 and (iii) Risoe TL/OSL with Single grain attachment. All the systems comprised a photon counting system and a digital ramp based temperature control system (Fig.2.1). The luminescence was detected by EMI 9635 QA Photo Multiplier Tube (PMT) attached to a filter pack consisting of BG-39 + U-340 (in case of UV emission and blue stimulation OSL for quartz) or BG-39 + Cs 7-59 (in case of IRSL for feldspar/polyminerallic fine grain). For very bright samples, fused silica neutral density filters were used and the maximum photon counts rate was always kept below $5x10^5$ counts/second to avoid any pulse pile up effects. The signal from the PMT was routed through a computer interface to an IBM-PC. TL measurement was done using a heat ramp rate of 5^oC/second. All measurements of TL/OSL were done in an ultra pure Nitrogen gas atmosphere.The system stimulation window comprises, an array of blue LED's (λ = 470 ± 30 nm) and red LED's (λ = 880 ± 80 nm) for blue and Infra red photon stimulations of the quartz and feldspar respectively. The average power delivered from these LED's ranged from 25-45 mW/cm^2 in total. In Daybreak TL/OSL reader (model 1100) 57 aliquots can be kept at once in the machine but due to absence of inbuilt beta irradiator, it restricts its use for Single Aliquot measurement as it needs 5-6 cycles of irradiation, preheat and OSL measurement on a single aliquot. In Risoe TL-DA 15, one can put 48 aliquots at a time to analyze and due to inbuilt irradiator; all the SAR measurements were done on this system only (Botter et al., 2000; Botter and Murray, 2001)

2.3. Laboratory Irradiation and Calibration of the Beta Dose Source

Beta source dose calibration is an important part of the growth curve construction in luminescence dating. It is necessary to assign the accurate as well as precise value for it. For single aliquot analysis, a set of 6 small aliquots having 90-150 µm of gamma dosed (5 Gy) calibration Quartz (from Risoe National Laboratory, Denmark) were run for SAR during installation of the TL/OSL reader. The mean value of all the Paleodoses was taken as a source dose rate.

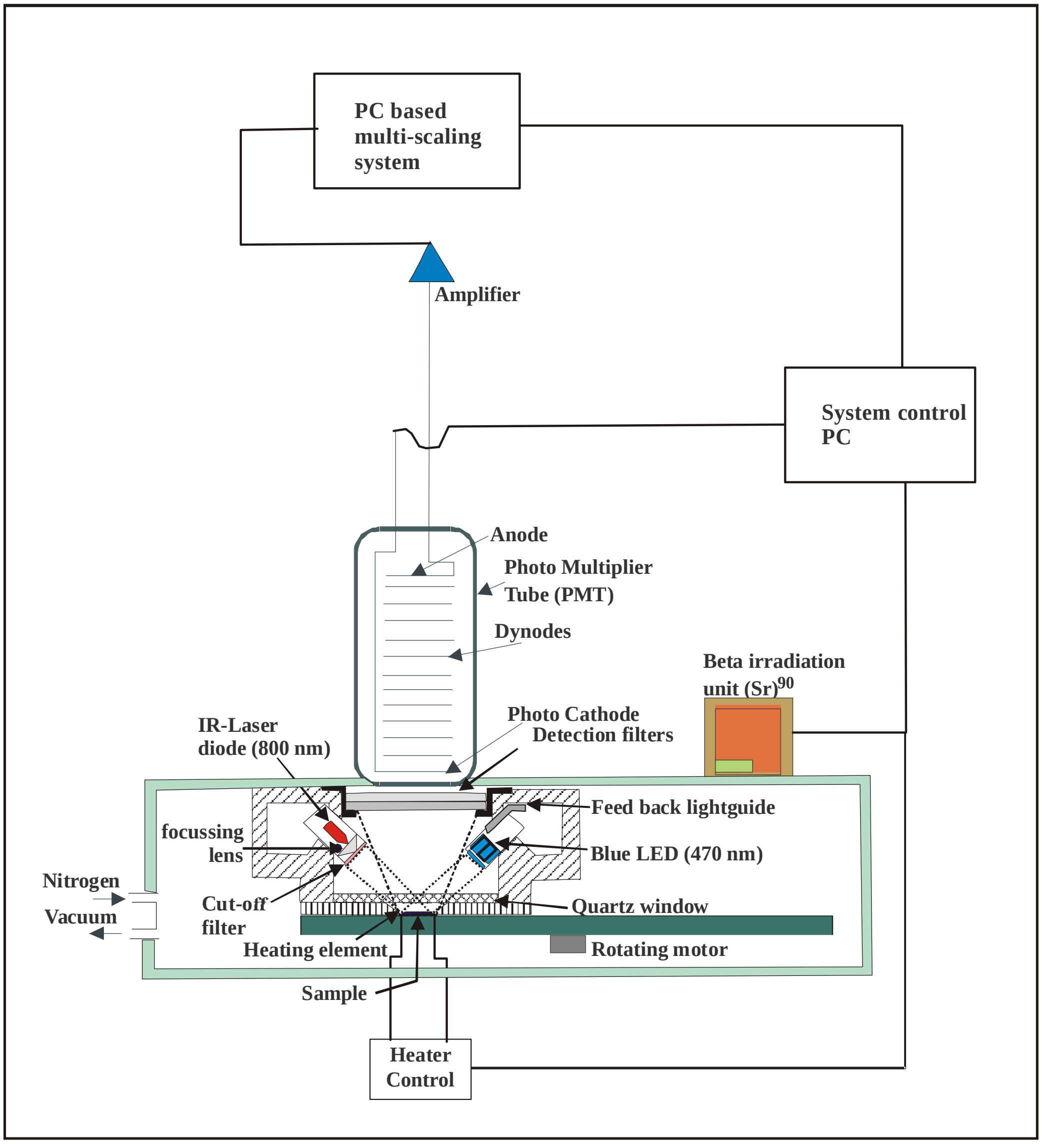

Figure 2.1. Schematic of the instrument used for the TL/OSL measurement. (Modified after Aitken, 1998; Botter Jenson et al., 2000)

Most of the experiments were done on Risoe TL/OSL reader-15, which has inbuilt beta irradiator, making convenient to do all the measurements in a single machine and thus reducing the chances of loss of any grains from aliquots during transportation. The calibration of Risoe TL/OSL reader (model TL DA-15) gave the beta source dose rate to be 7.31 Gy/minute measured in April, 2001.

Beta irradiations on some of the samples were performed by a 20 positions beta irradiator manufactured by Daybreak-Nuclear and medical systems. The source was calibrated for fine (4-11µm) and coarse grain (90-150 µm) samples using CaF_2 from Oxford and Quartz supplied by Risoe National Laboratory, Denmark. An inter-laboratory calibration was made between BARC-Mumbai and Oxford luminescence laboratory sources. The calibration of Daybreak beta irradiator was done on April 2001 that gave a dose rate of 3.65 Gy/minute and 2.44 Gy/minute for Quartz (90-150 µm) and fine grained (4-11 µm) respectively.

The Single Grain TL/OSL reader was calibrated including to check for the homogeneity of the beta dose rate on an aliquot In case of single grain analysis, the paleodose is to be calculated from a grain sitting on one of the 100 holes (300 µm diameter each) arranged in a matrix of 10 x10. Hence it was necessary to do the calibration of each hole containing grain and to ensure about the homogeneity of the beta dose source. To do so, 210-250 µm size grains of gamma dosed calibration Quartz grains were mounted on the single grain disks. Nine disks were analyzed containing 900 (100 x 9) grains. The homogeneity was checked by measuring average paleodose from each successive rectangle containing the grains on the disk (Fig. 2.2). The outermost rim contains 36 grains, second outermost contains 28 grains, middle rim contains 20 grains, second innermost rim contains 12 grains and innermost rim contains only 4 grains. The average paleodose from the each rim is tabulated in Table 2.1. The standard deviation of the data was <5% of the natural. The values of the paleodoses decreases slightly as you move from outermost rim to the innermost rim, however total change in paleodose is < ~7.5 %. These results shows that beta irradiator provide a homogeneous dose rate on the aliquot with ~7.5 % variation.

Table 2.2. Source dose rate distribution in a single grain disk from the outermost rim to the innermost rim. The data are averaged over 9 single grain discs (~100 grains in each disc).

Rim	Dose Rate (Gy/minute)
Outermost	7.0 ± 0.1
Second outermost	7.2 ± 0.1
Middle	7.4 ± 0.2
Second innermost	7.5 ± 0.2
Innermost	7.6 ± 0.4

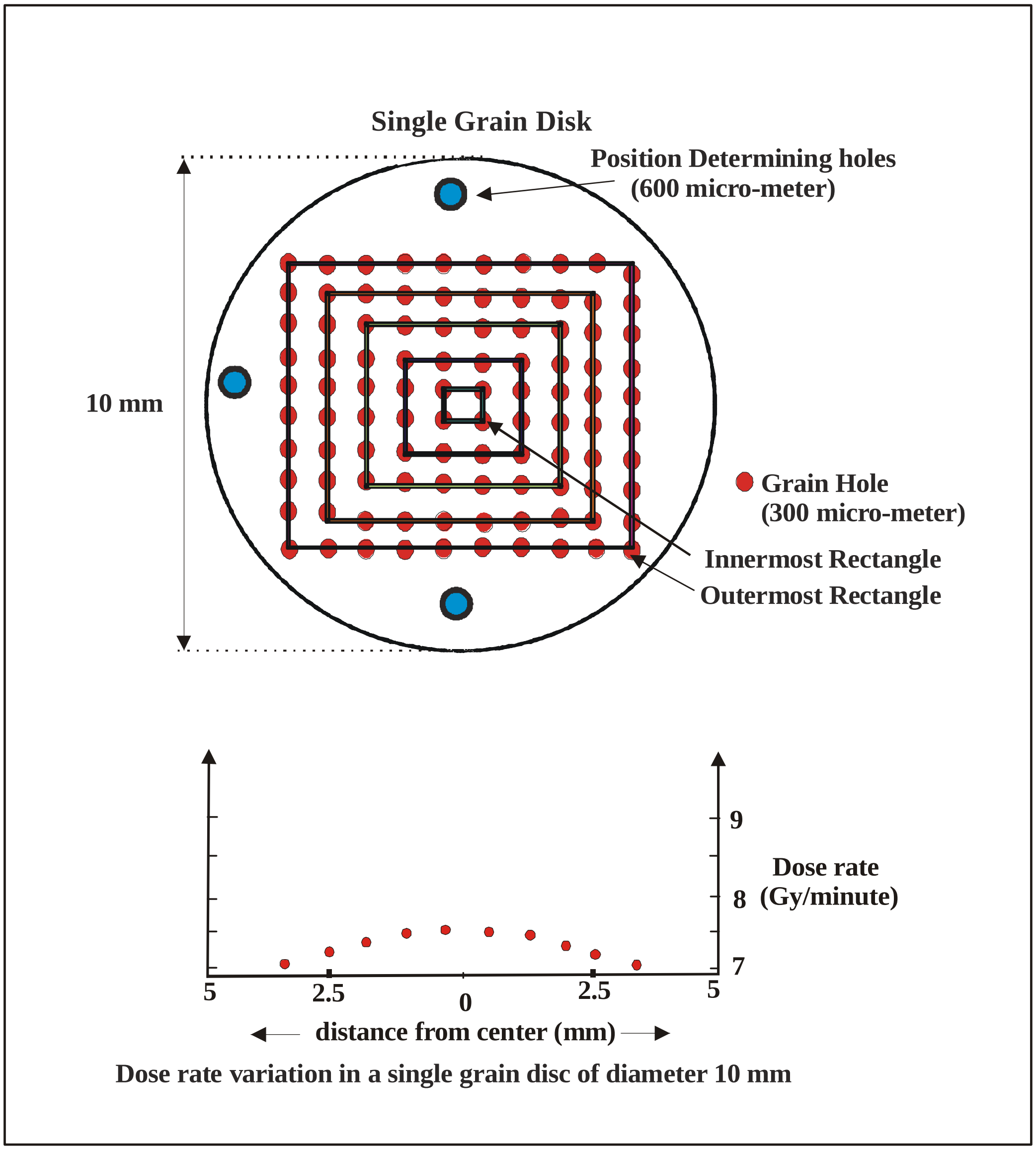

Figure 2.2. Diagram of a single grain disc. The calibration of the dose source was done using 5 Gy gamma dosed calibration quartz. The dose source strength was calculated on each rim of the disc as shown above. The source strength was found highest in the innermost rim i.e. around the center. However, values decreased systematically towards the outer rim with a maximum difference of up to 7.5 %. The error ranges from 1.5% to <5% on the dose rate values from outer to central rim.

2.4 Estimation of paleodoses

Several methods have been developed for the measurement of Palaeodose, which deal with situation of partial or total bleaching, sensitivity change and luminescence dose saturation. Totally bleached samples are most likely in wind-transported sediments (sand dunes etc.) and sediments deposited in stagnant water conditions (e.g. silt or silty-clay). The samples where partial bleaching can occur are proximally transported aeolian or fluvial sediments deposited under condition of large bed load etc. The methods can be placed in two broad categories,

(i) The Multiple aliquot Methods: (a) Multiple aliquot additive method (MAAD)
(b) Multiple aliquot regeneration method (MAR)
(c) Partial bleach method

(ii) The Single aliquot Methods: (a) Single aliquot additive method (SAAD)
(b) Single aliquot regeneration (SAR).

2.4.1 Multiple aliquot methods

This method assumes that at a grain level sample is homogeneous in respect of thermal or bleaching history. Consequently this method has been successfully applied in the case of archaeological pottery, burnt sediments (baked clay) and wind blown sediments (well exposed to the daylight) using both the TL and OSL. The multiple aliquot methods are,

2.4.1.1 Multiple Aliquot Additive Dose (MAAD)

In this method, several aliquots (typically 30-40) are used to determine the paleodose. In this, few aliquots are kept for natural measurement. A few groups of aliquots (~5-6 aliquots in each group) are given additional laboratory beta doses in increasing order (say β_1, β_2, β_3,…) such that $\beta_1<\beta_2<\beta_3<$…… and then their luminescence is read onto TL/OSL reader. The luminescence yield of the aliquots is plotted against applied dose added (β_1, β_2, β_3,…) to aliquots to construct a luminescence vs. dose growth curve (Fig. 2.3). This procedure ensures that the aliquots have identical thermal and radiation history. Extrapolation of this to dose axis provides equivalent laboratory beta

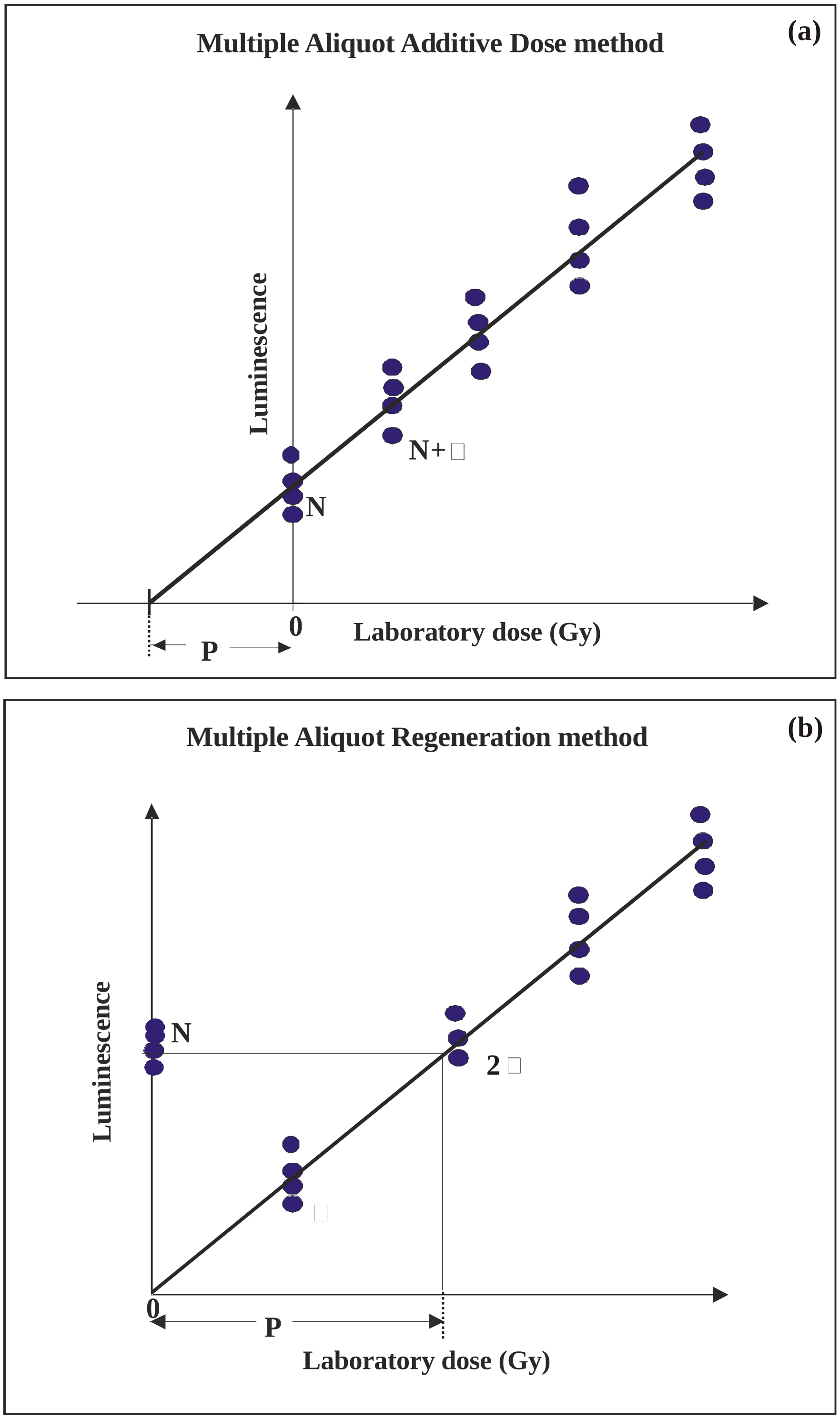

Figure 2.3. Multiple aliquot methods: (a) multiple aliqupt additive dose growth curve constructed between incremental additional lab doses and luminescence counts. Paleodose is calculated by extrapolating the growth curve onto dose axis. (b) multiple aliquot regeneration method in which paleodose is calculated by interpolating natural luminescence counts onto growth curve plotted between luminescence counts and incremental beta doses given to sun bleached aliquots.

dose that is needed to induce in a sample a luminescence equal to the natural luminescence. This is termed variously asequivalent dose or paleodose (Aitken 1985; 1998). This method while ensures against sensitivity changes, requires an apriori assessment of the nature of the growth curve. Based on monte-carlo simulations done by Felix and Singhvi (1997) provide practical recipes for construction of growth curves and extrapolations. As the construction of growth curves involves a large number of aliquots, appropriate normalization is needed. There are several normalization procedures (Aitken, 1985; 1998; Jain et al., 2003) and these are listed below–

(a) Weight normalization

(b) Post OSL residual TL normalization

(c) Zero glow normalization

(d) Natural normalization or short shine normalization

(e) Dose normalization or second glow normalization.

In present study, the samples were normalized using natural normalization (short shine normalization). In this method, the sample aliquots with their natural OSL were stimulated by blue light for 0.3 second and the OSL was measured. This duration and stimulation flux was so adjusted that the depletion of natural OSL was <1% of the total OSL signal. This intensity was used as a measure for luminescent grains and helped normalize to remove inter-aliquot variability in respect to variation in number of luminescent grains and their sensitivities from each aliquot. An assumption in this procedure is that the luminescence sensitivity in the first interval and the rest of the shine down curve are covariant, sensu-stricto. This conditionality was not met in some cases, as also, short shine photon statistics was poor making it difficult to normalize. In such cases, second glow normalization was used. In second glow normalization, after all the OSL measurement the luminescence output for a test dose is measured and used for the normalization.

2.4.1.2 Multiple Aliquot Regeneration (MAR)

In regeneration method, the natural process is replicated. Here except the set of natural, each set of disk is sun bleached and then incrementally irradiated. A regenerated growth curve is then constructed between laboratory doses and the luminescence yield. Paleodose is then evaluated by interpolating natural signal onto the growth curve (Fig. 2.3). This method has an advantage over MAAD of interpolating the natural OSL onto the growth curve rather than extrapolation onto the dose axis that increases the chance of error due to poor fitting of the growth curve. The limitation of this is the change in luminescence sensitivity of the sample may occur during daylight bleaching prior to regeneration.

The nature of luminescence vs. dose growth curve can be complex depending upon the luminescence properties. It can ranges from linear, non linear, exponential and a combination of these. The nature of the growth curve with respect to doses and thus the selection of proper dose protocol are discussed in detail by Felix and Singhvi (1997).

2.4.1.3 The Partial Bleach Method and Linearly Modulated Optically Stimulated Luminescence (LM-OSL)

Partial bleach methods recognize and exploit the fact that the luminescence of a mineral (Quartz/Feldspar) comprises several components with different sensitivity to photo bleaching. Typically the Blue light stimulated luminescence shine down curve of the Quartz comprises three parts viz., (i) the fast component (most sensitive); (ii) the medium component and (iii) the slow component (hard to bleach). In a partially bleached sample, it is expected that only a part of the signal (fast component) was bleached and other components of the signal (medium and slow) were partially reset. (Wintle and Huntley, 1979).

In such samples the measurement of paleodose comprises several sets of aliquots. A normal additive growth curve is constructed (i.e. N, N+β, N+2β,….) as also additional additive dose growth curve using samples which record a short duration daylight exposure after beta dose (i.e. the sequence, N+$\in$sun, N+β+$\in$sun, ….). Luminescence-dose growth curve is constructed for each set of daylight exposure. The intersection of the growth curve of the daylight-exposed set of aliquots with the growth curve of unexposed set of aliquots gives the paleodose. This is called the partial bleach method. A simplified approach of this method was suggested by Singhvi and Lang (1998). In this approach, the portion of Infra Red Stimulated Luminescence shine down curve was analyzed. It was suggested that in a shine down curve, the intensity of the first interval represents an unbleached signal and the later intervals effectively represent equivalents of daylight-bleached samples. Partial bleach growth curves are then constructed as above. Paleodose is estimated from intersection of these growth curves from the unbleached growth curve. This approach is now known as ‘differential partial bleach’ (Fig. 2.4).

Bulur (1996) gave the concept of measuring luminescence output with linearly increasing intensity of stimulation light. Conventional constant stimulation method provides a monotonically decreasing signal (shine down curve) whereas Linearly Modulated OSL provides the opportunity of probing the substructure of a shine down curve in a manner similar to a TL glow curve. This procedure therefore provided new possibility of analysis of different components of a signal. Overlapping OSL components considered to originate from different traps can be separated and characterized. The three components of a shine down under constant stimulation, viz., are fast, medium and slow. LM-OSL enabled identification of an additional component (Bulur and Goksu, 1999; Bulur et al., 2000).

Larsen et al. (2000) used LM-OSL to find out partial bleaching in quartz and feldspar. He took annealed quartz disk, irradiated and bleached for different time duration ranging from 0.2 second to 10,000 seconds followed by LM-OSL measurement. Then by plotting a graph between partially bleached signal and non-bleached signal, he was able to show most rapidly bleachable signal, which is not seen clearly in the constant wave OSL (CW-OSL). The key is that the LM-OSL method separates the various components through differences in the photo-ionization cross-section of the traps. These are not easily detectable with conventional CW-OSL. In the present thesis, a combination of LM-OSL and differential partial bleach method was used to arrive at a most effective way to deal with partially bleached samples. In doing so, the integration times for signal were so computed so as to keep the net flux equal in each interval. A preheat of $240^{o}C$/10 seconds was used.

2.4.2 Single Aliquot methods – Single aliquot Regeneration (SAR)

In this method, aliquots of 5mm diameter of the sample area, were used for analysis which comprises ~500-600 grains of Quartz. Though on methodological grounds it is desirable to work with aliquots of 60-100 grains or less (Olley et al., 1998; 1999),

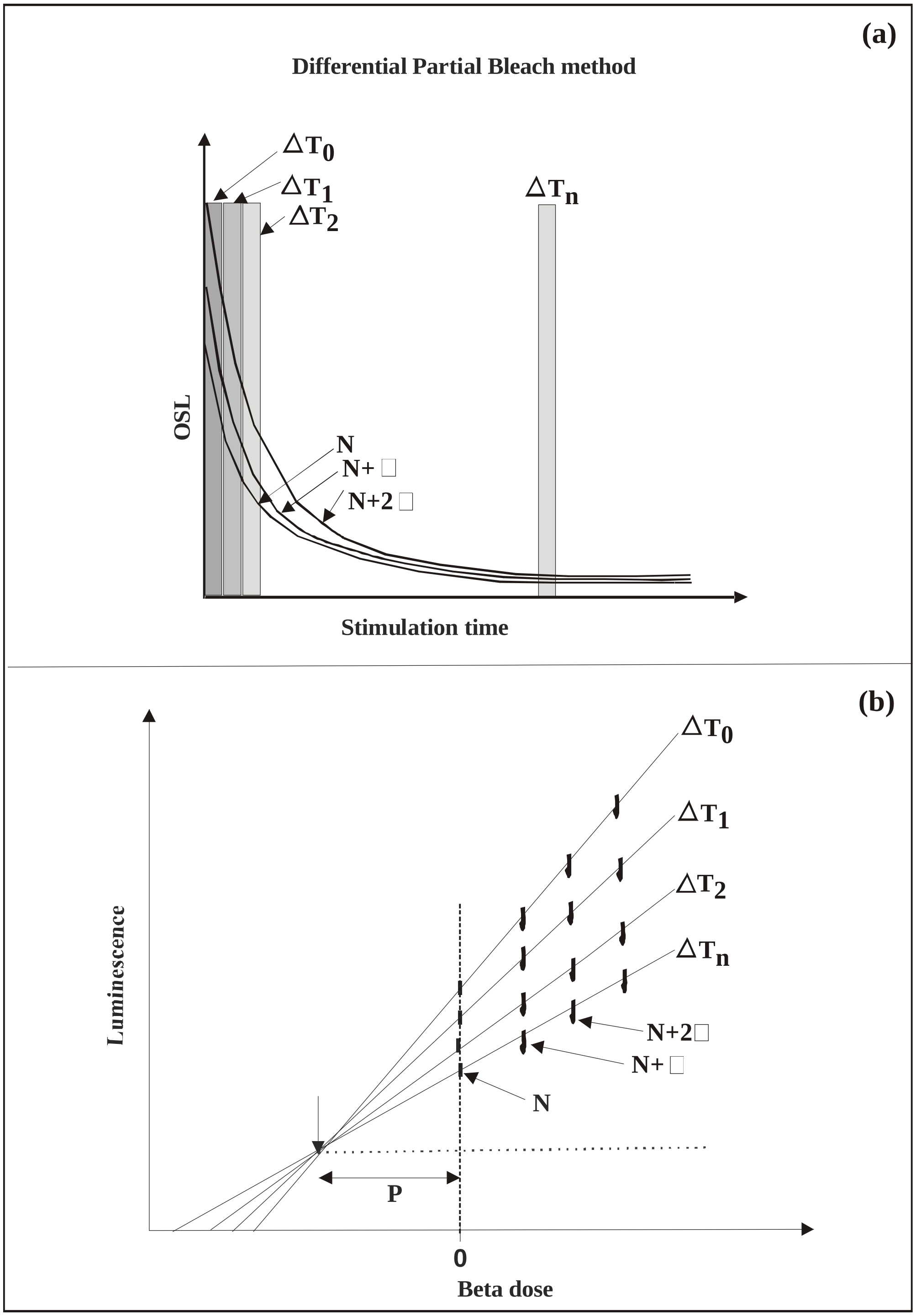

Figure 2.4. The partial bleach method: (a) shine down curve is divided for a fixed time interval and then (b) the luminecence counts from these portion of shine down is plotted against the laboratory doses. The paleodose is the intersection point of these growth curves (modified after Singhvi and Lang, 1998)

poor luminescence sensitivity of Himalayan samples necessitate use of larger number of grains. SAR protocol by Murray and Wintle (2000) was used (Fig. 2.5 and 2.6). In this method, first natural OSL (Ln) is measured after preheat of 240^{o}C/10 seconds. Any changes in luminescence sensitivity during preheat and OSL measurement is corrected by measuring the OSL output (Tn) from a small test beta dose (10-20% of natural dose). The sample is heated to ~160^{o}C prior to measurement of Tn. This preheat termed as cut heat. The ratio L/T provides a sensitivity corrected OSL. After this incremental regenerated laboratory doses R_1, R_2, R_3 respectively are given on same aliquot and OSL L_1, L_2 and L_3 is measured for each regeneration dose along with test dose OSL T_1, T_2, T_3 (Fig. 2.5 and 2.6). The zero dose point is measured in the similar manner but without giving any dose. In last a regeneration point is recycled by giving similar dose to monitor the validity of sensitivity corrections. A typical SAR protocol involves 12 cycles of irradiation, preheat and OSL measurement and can take up to several hours for a single aliquot. A growth curve between dose points (L_1/T_1, L_2/T_2 and L_3/T_3) and laboratory regeneration doses (R_1, R_2 and R_3) is then constructed. The natural signal (Ln/Tn) is read onto that growth curve to get the laboratory equivalent dose i.e. paleodose. In the present study initial 2 seconds of the shine down curve was taken with a background subtraction from the same curve.

2.4.3 Natural Sensitivity Corrected SAR (correction for changes in natural OSL sensitivity)

In a SAR procedure, the sensitivity change during first OSL readout is corrected by the test dose luminescence followed by the natural OSL measurement. The sensitivity after natural OSL readout does not account for possible sensitivity changes during preheat and measurement of the natural signal. Stokes and Singhvi (Under preparation) pointed out that this has been ignored in standard SAR protocol suggested by Murray and Wintle (2000) and can cause systematic errors. They proposed the use of 110^{o}C TL peak that was correlated with OSL signal and a revised protocol was made (Fig. 2.7) (Stoneham and Stokes, 1991; Stokes, 1994a, 1994b). In the present study it was shown that OSL and TL signal correlates for that sample with respect to test dose. Using this, sensitivity corrected SAR procedure was used with encouraging results.

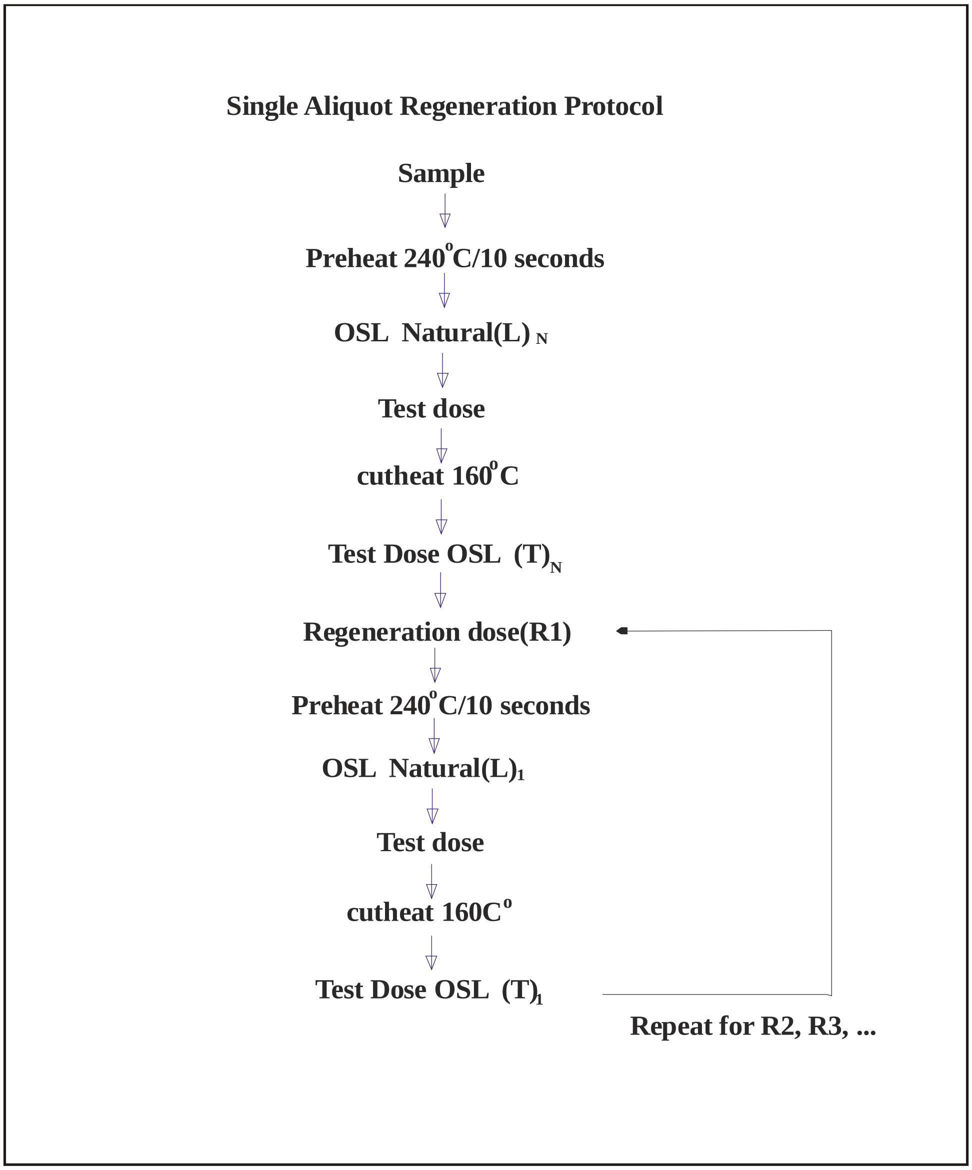

Figure 2.5. The Single Aliquot Regeneration protocol as used in dating fluvial sediment. It involved 6 cycles of irradiation, preheat and OSL measurement along with test dose measurement (after Murray and Wintle, 2000)

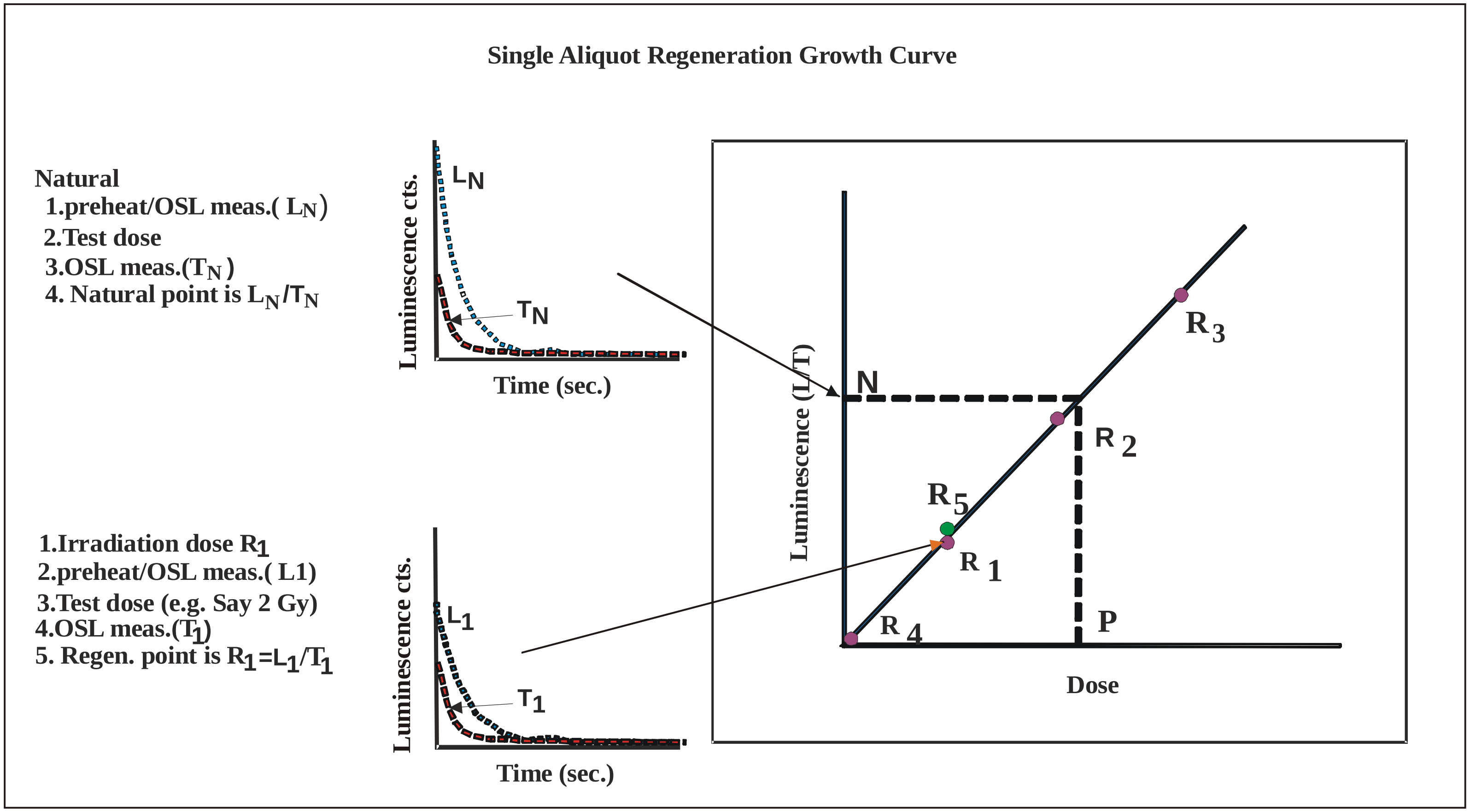

Figure 2. 6. SAR growth curve showing constructed between sensitivity corrected luminescence (L/T) and incremental dose points R1, R2 and R3. The sensitivity corrected natural luminescence (Ln/Tn) is interpolated onto that growth curve for estimating paleodose (after Murray and Wintle, 2000)

NSC-SAR protocol

Sample

↓

Test dose (T1)

↓

TL (110 ^{o}C measurement, TL_1)

↓

Preheat 240^{o} C/10 sec.

↓

Test dose (T1)

↓

TL (110 ^{o}C measurement, TL_2)

↓

OSL Natural(L_N)

↓

TL (110 ^{o}C measurement, TL_3)

↓

Test dose (T1)

↓

TL (110 ^{o}C measurement, TL_4)

↓

Test dose (T1)

↓

Cutheat 160^{o}C

↓

Test Dose OSL (T_N)

↓

Regeneration doses and then same as SAR

Figure 2.7. The natural sensitivity corrected Single Aliquot Regeneration protocol as suggested by Stokes and Singhvi (under preparation). It involved additional steps of irradiation and 110^{o}C TL measurement during natural OSL measurement along with test dose.

In NSC-SAR method, additional steps of test dose and its $110^{o}C$ TL peak measurement have been introduced in the standard SAR protocol to quantify the exact sensitivity changes occurred during preheat and natural OSL measurement. First a test dose (T) is administered to the natural sample followed by $110^{o}C$ TL (TL_1) measurement by heating it up to $160^{o}C$. TL_1 represent the sensitivity of natural sample prior to OSL measurement. Similarly few more measurements are made as depicted in Figure 5. Measurement TL_4 represent the sensitivity of the sample after preheat and OSL measurement. In present method a term "natural correction factor" (ncf) has been introduced that is defined as the ratio of TL_1 and TL_4 and is used to correct for the sensitivity. A plot of the sensitivity corrected regenerated OSL signal with dose enables the construction of an OSL-dose growth curve. In this procedure, natural signal is corrected using test dose signal and ncf for any sensitivity changes and then it is read out on regenerated OSL growth curve (Fig. 2.8)

2.5 Annual Dose Measurement

The annual dose was computed by measuring the elemental concentration of Uranium, Thorium and Potasium. Uranium and Thorium concentrations were measured using thick source ZnS(Ag) alpha counting (Woithe and Prescott, 1995). Potassium concentrations were measured using NaI(Tl) gamma ray spectrometry. The dose rate depends upon the average moisture content of the sediment through its antiquity, cosmic ray variation, alpha efficiency value, grain size and disequilibrium in the radioactive decay chain.

In most of the luminescence dating, a secular equilibrium in the decay chain of U and Th is assumed. This is reasonably met in most cases. Olley et al. (1996) has examined the disequilibrium in fluvial sediments of different age range and found that ^{232}Th decay chain was near to secular equilibrium in almost all kinds of fluvial sediment. This was due to very short half-life of Rn in the decay chain. Disequilibrium in the ^{238}U decay chain is evident in most of the sediment examined; however, the overall effect on dose rate is decreased by 6% for 100 micron grains and 8% for fine grain for the

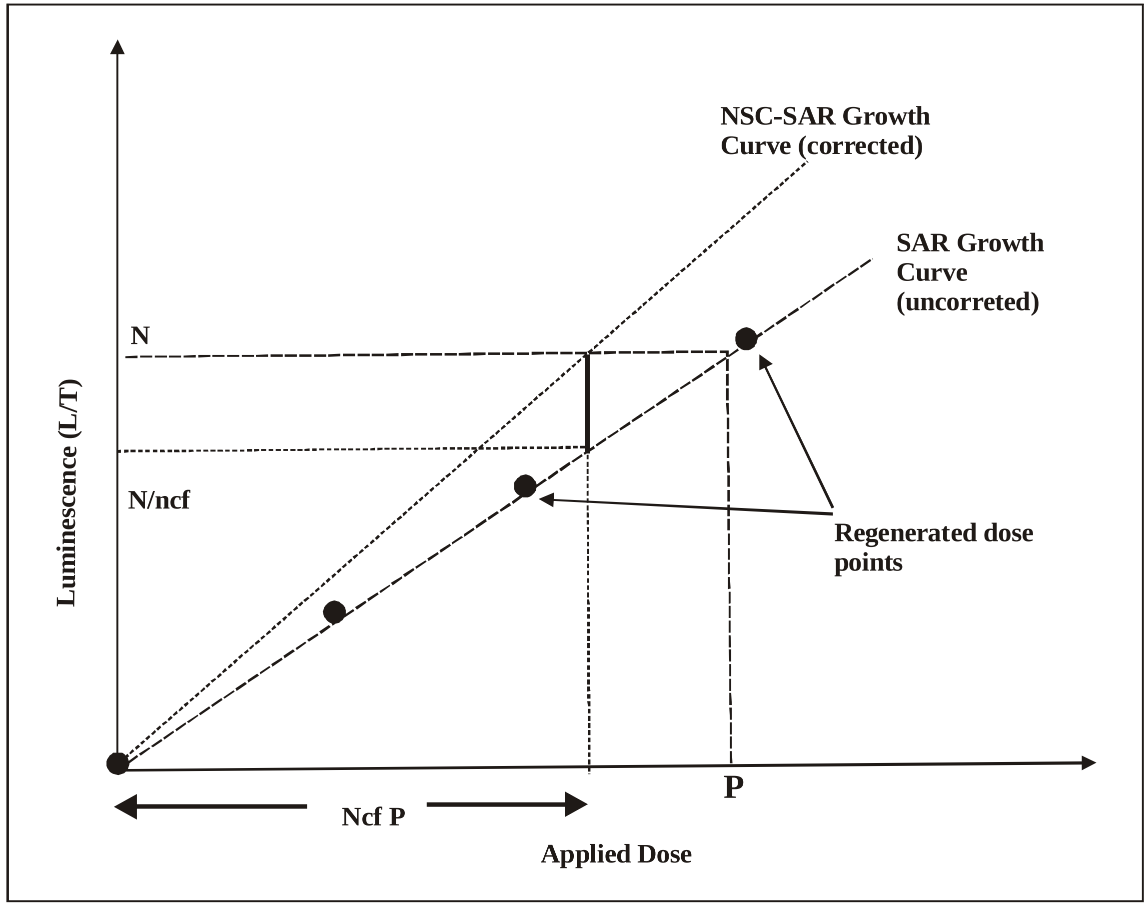

Fig. 2.8. Natural Sensitivity Corrected-SAR (NSC-SAR) growth curve. The natural luminescence is corrected using ncf and then interpolated onto the uncorrected SAR growth curve. The growth curve that will give the ncf corrected paleodose will be the virtual growth curve considered as NSC-SAR growth curve.

sediment comprising 1 ppm ^{238}U, 3 ppm ^{232}Th and 1% K. (Aitken, 1985; Dickson and Wheller, 1992; Krbetschek et al., 1994).

For measuring Uranium and Thorium concentrations, the samples were gently crushed to thickness less than 10 μm, then spread onto a ZnS(Ag) scintillator. For coarse grain, the samples were crushed to powder (<10 μm) and used for estimation of average radioactivity concentration. This is essential for determining beta dose from U and Th concentration. The counting system was calibrated using NBL Uranium standard BL-3 with 1% U and sand 105A with 10.2 ppm U. The counting threshold was set at 83.5 % efficiency to allow the efficiency of counting for the two decay chains to be nearly equal (Aitken, 1985).

Typical background count rate were ~0.2 counts/ks for a counting area of 13.85cm^2 and the typical samples alpha counts rate were ~8-10 counts/ks for the samples. Typically samples were counted over a period of 300 ks and a total count of >1000 was always achieved to obtain a counting error of <3%. All the measurements were made using a DAYBREAK 582 alpha counter.

The estimation of K was made using 3”x3” well type NaI(Tl) scintillator coupled to a standard amplifier and a multi channel analyzer. The energy window was set at 1.46 MeV. The count rate of 7.9 gram of standard (AR grade KCl) is ~60 counts per minute for the same geometry. In the comparison, only the photo peak counts significantly up to the full width at half maxima were used. Typically sample weights were ~15 gm giving a count rate of 5-7 counts/minute for sample compared to a background of 1-1.5 counts/minute. The cosmic ray dose was estimated using the prescription given by Prescott and Stephan (1982). The correction for moisture content was made according to Aitken (1985). After calculating weight percentages of the above-discussed radioactive elements, the dose rate was calculated from Table 2.2 based on the Aitken (1998).

Table 3.2 Calculation of dose rate from known concentrations of radioactive elements. (after Aitken, 1998).

Se. No.	Elements	Concentration (wt %)	Alpha dose (Gy/ka)	Beta dose (Gy/ka)	Gamma dose (Gy/ka)
1	U	1 ppm	0.231	0.145	0.113
2	Th	3 ppm	0.193	0.082	0.143
3	K	1 %	--	0.782	0.243
4	Cosmic	--	--	--	0.18

References

Aitken, M.J., 1985. *Thermoluminescence dating*. Academic Press, London.

Aitken, M.J., 1998. *An introduction to optical dating*, Oxford University Press, Oxford.

Larsen N.A., Bulur, E., and McKeever, S.W.S., 2000. Use of LM-OSL for the detection of partial bleaching in quartz and feldspar, *Radiation Measurement*, 32, 419-425.

Botter Jenson, L., Bulur, E., Duller, G.A.T. and Murray, A.S. 2000. Advances in luminescence instrument system, *Radiation Measurement*, 32, 523-528.

Botter Jenson, L. and Murray, A.S. 2001. Optically stimulated luminescence technique in retrospective dosimetry, *Radiation Physics & Chemistry*, 61, 181-190.

Bulur, E. 1996. An alternative technique for OSL measurement. *Radiation Measurement*, 26, 701-709.

Bulur, E., and Goksu, H.Y., 1999. IR stimulated luminescence from feldspar with linearly

Increasing excitation light intensity. *Radiation Measurement*, 30, 505-512.

Bulur, E., Botter Jenson, L. and Murray, A.S. 2000. Optically stimulated luminescence from Quartz measured using the linear modulation technique. *Radiation Measurement*, 32, 407-411.

Dickson, B.L. and Wheller, G.E. 1992, Uranium series disequilibrium in exploration geology In: Ivanovich, M and Harmon, R.S., *Uranium-series Disequilibrium: Application to Earth, Marine and Environmental Sciences*, 2nd Edn, p. 704–729. Clarendon Press, Oxford.

Felix, C. and Singhvi, A.K.1997. Study of non-linear luminescence-dose growth curve for the estimation of paleodose in luminescence dating: results of Monte Carlo simulations. *Radiation Measurement*, 27(4), 599–609.

Jain, M., Botter-Jenson, L., Singhvi, A.K., 2003. Dose evaluation using Multiple-aliquot quartz OSL: test of methods and a new protocol for improved accuracy and precision. *Radiation Measurement*, 37, 67–80.

Krbetschek, M.R., Reiser, U., Zoller, L. and Heinicke, J. (1994). Radioactive disequilibria in Paleodosimetric dating of sediments. *Radiation measurements*, 23, 485–489.

Murray, A.S., Roberts, R.G. & Wintle, A.G., 1997. Equivalent dose measurement using a single aliquot of Quartz. *Radiation Measurement*, 27, 171–183.

Murray, A.S., Wintle, A.G.,2000. Luminescence dating of quartz using an improved single aliquot regenerative-dose protocol. *Radiation Measurement*, 32 (1), 57–73.

Olley, J M., Murray M and Roberts R.G. 1996, The effects of disequilibria in the Uranium and Thorium decay chains on burial dose rates in fluvial sediments. *Quaternary Science Reviews*, 15, 751–760.

Olley, J.M., Caitcheon, G., & Murray A., 1998. The distribution of apparent dose as determined by optically stimulated luminescence in small aliquots of fluvial quartz: implications for dating young sediments. *Quaternary Science Reviews*, 17, 1033–1040.

Olley, J.M., Caitcheon, G. and Roberts, R.G., 1999. The origin of dose distribution in fluvial sediments and the prospect of dating single grains from fluvial deposits using Optically Stimulated Luminescence. *Radiation Measurement*, 30, 207–217.

Prescott, J.R. and Stephan, L.G., 1982. The contribution of cosmic radiation to the environment dose for Thermoluminescence dating: latitude, altitude and depth dependences. *PACT*, 6, 17–25.

Singhvi, A.K. and Lang, A. 1998. Improvements in infra-red dating of partially bleached sediments- the ‘Differential’ partial bleach technique. *Ancient TL*, 16, 63–71.

Stoneham, D. and Stokes, S., 1991. An investigation of the relationship between the 110^{o}C TL peak and optically stimulated luminescence in sedimentary quartz. *Nuclear Tracks and Radiation Measurement*, 18, 119–123.

Stokes, S., 1994a. Optical Dating of Selected late quaternary aeolian sediments from the southwestern United States. *Unpublished D.Phil thesis*, Oxford University, Oxford.

Stokes, S., 1994b. The timing of OSL sensitivity changes in a natural quartz. *Radiation Measurements*, 23, 601–605.

Woithe, J.M. and Prescott J.R., 1995. Efficiencies of phosphor screens used in Thick Source Alpha particle counting. *Ancient TL*, 13, 10–14.

Wintle, A.G. and Huntley, D.J., 1979. Thermoluminescence dating of a deep sea sediment core. *Nature*, 279, 710-712.

Changes in natural OSL sensitivity: Implications to Dating

3.1 Introduction

Single Aliquot Regeneration (SAR) protocol is used widely in almost all kind of sediments viz. aeolian, colluviums and water-lain. In recent times, development of SAR procedure has been paid attention in an exhaustive manner. A SAR measurement involves several steps of irradiation, preheat and luminescence measurement on an aliquot to estimate paleodose (Murray, et al., 1997; Murray and Roberts, 1997; Murray and Wintle, 2000; 2003). Preheat and luminescence measurement however can cause changes in the sensitivity (luminescence/absorbed dose-mass) of the sample. In a typical SAR measurement, this change is monitored and corrected for using an OSL output of a small test dose given after natural and regenerated OSL measurements. The robustness of such sensitivity changes is monitored again through a dose recycling point introduced in the SAR procedure.

It has been shown that 110^{o}C TL peak was linearly correlated with OSL response (Stoneham and Stokes, 1991, Stokes, 1994a, 1994b). The 110^{o}C TL peak's mean life is only few hours, which means that traps are unpopulated in a natural sample relating to 110^{o}C temperature. Hence this peak can be used as a surrogate for sensitivity.

While incremental OSL and 110°C TL responses to test dose measured subsequent to the regenerative cycles of doses and OSL measurements are capable of fully quantifying sensitivity changes during construction of the regenerated growth curve, there remains some uncertainty as to whether the measurement of 110°C TL or OSL following stimulation of the natural OSL faithfully describes the behavior of the sample prior to stimulation and preheating. The studies have shown that the most serious sensitivity changes occurred as a result of the erasure of the natural signal (Stoneham and Stokes, 1991; Stokes 1994a, 1994b). Such changes can lead to systematic offset from true paleodoses depending upon the luminescence behavior. Present work examined sensitivity change of a sample during natural OSL measurement in a SAR procedure on quartz extract from Himalayan sediments and suggests the possible corrections to minimize the effect of such sensitivity changes, however, focus of the study is to report the sensitivity changes and its effect on age estimation.

In the present study, the sensitivity of the 110°C TL peak was measured of a small test dose before and after OSL measurement to monitor any sensitivity changes that would have occurred during OSL measurement. Changes in sensitivity during the preheat and measurement of natural OSL have not been considered in a SAR protocol and this could imply systematic offsets in ages (Stokes and Singhvi, under preparation). In view of that, these authors have examined some samples from various archives and have shown that initial (natural) sensitivity varied significantly. The change in sensitivity ranged from an increase by up to 27% and a decrease by up to 30%. A natural sensitivity corrected SAR (NSC-SAR) procedure was proposed by these authors. NSC-SAR protocol has been discussed in detail in chapter-2 of the thesis), which monitors any sensitivity change during natural OSL measurement and in the process makes a SAR protocol, truly robust.

3.2 Experimental details and methods involved

The Quartz fraction from samples was extracted using the method discussed in detail in chapter 2. Small aliquots of 5mm diameter were used for analysis. For constructing growth curve, initial 2 seconds (from 100 seconds of OSL measurement) of a typical shine down curve was taken with a background subtraction from the same curve.

In present method, additional steps of test dose and its 110^{o}C TL peak measurement was done apart from standard SAR measurement. The first test dose measurement (T_1) represents the sensitivity of natural sample prior to any OSL measurement. Measurement (T_4) represent the sensitivity of the sample after its preheat and OSL measurement. In present method a term "natural correction factor" (ncf) has been introduced (Stokes and Singhvi, under preparation) which has been defined as the ratio of T_1 and T_4. Ideally ncf =1, if there is no change in sensitivity and ncf >1 indicates drop in the sensitivity and vice versa.

In the standard SAR method, a growth curve is constructed by giving laboratory beta doses to the aliquot followed by preheat and OSL measurement (Murray & Wintle 2000). The luminescence yield at each dose point is corrected for sensitivity change by measuring the OSL yield for a test dose. A plot of the sensitivity corrected regenerated OSL signal with dose enables the construction of a OSL-dose growth curve and sensitivity corrected natural luminescence intensity is interpolated onto this curve to obtain the equivalent dose, P. In this procedure, natural signal is corrected using test dose signal and ncf for any sensitivity changes and then it is read out on regenerated OSL growth curve (Fig. 2.7 and 2.8, chapter 2). We have compared the Paleodoses separately to see its effect on the minimum 10% and average of a dose distribution obtained after running SAR.

In this method, the ratio of two TL signals is used to correct the sensitivity changes occurred in the OSL output of the natural signal. The corrections would be applicable only if (i) the TL signals correlates linearly with the OSL signal and (ii) the intercept of the line of correlation is zero. Correlation of the TL and OSL signal was examined by using a few aliquots were taken from some samples and cleaned for any natural signal present in it using blue light stimulation. After that, each disk was given a series of beta doses (ranging from 1.2 – 6Gy) followed by a TL measurement (temp. up to 160^{o}C) followed by OSL measurement. A graph was plotted for each disk for TL against OSL (Fig. 3.1). The method was applied to several samples of different parts in Himalaya. For this samples from various locations were collected. These are discussed in detail in Chapter 5 of the thesis.

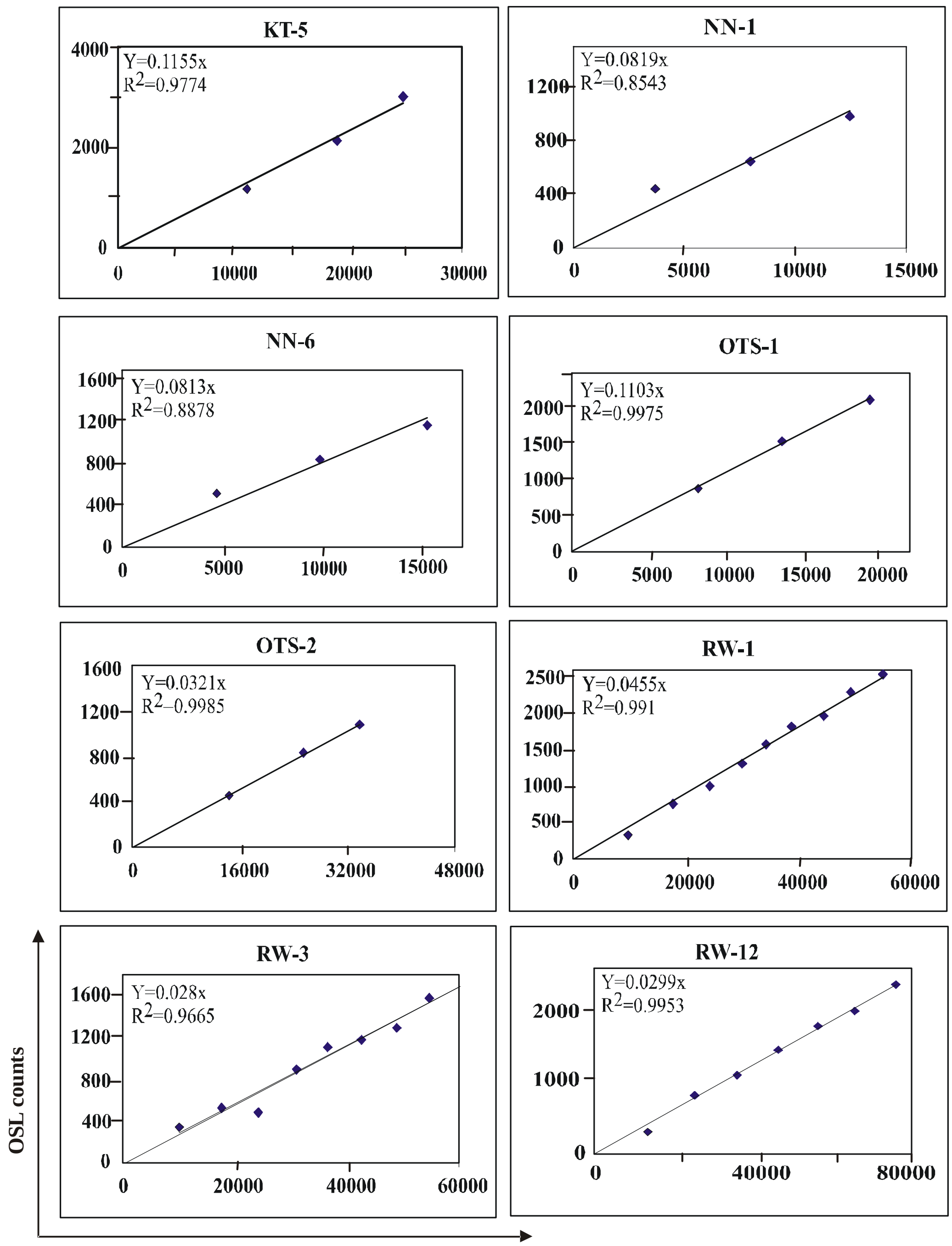

Figure 3.1. Correlation of 110^{O}C TL counts and OSL counts. Dose points starts with 1.2 Gy and rest are in multiple of that. (Regression line has been forced to pass through origin)

3.3 Results and Discussions

Total 14 samples were examined. It was observed that the regression line of TL and OSL is showing a good correlation having high values of regression coefficient (R^2>0.85) (Fig. 3.1). These lines were forced to pass through origin considering that in ideal cases TL and OSL should be equal for zero doses. The sensitivity was checked in the new protocol to observe the effect of both of preheat and OSL separately. To observe this, ratio of T_1 and T_2 was taken to represent any changes in sensitivity due to preheat only (Fig. 3.2). It is clear from the graph that the sensitivity changes is the cumulative effect of preheats as well as OSL measurement too. In the present study, the ncf was taken as the representative of cumulative effect of preheat and OSL measurement. The paleodose was computed with and without corrections and compared. In the extreme cases, ncf varied up to 50% however; typical ncf values ranged from 15 – 25%. The histograms (Fig. 3.3) show the corrected and uncorrected values of P's computed keeping the bin width identical. Gaussian curves were fitted for these distributions of doses and the full width at half maximum (FWHM) of the curve was computed to observe any effect after applying ncf correction. It is clear from the few graphs that FWHM of the Gaussian curve decreased from 20 – 40% after corrections for natural sensitivity changes. It is clear from the histograms and the Gaussian curves that the paleodose distribution improved after ncf sensitivity correction. The average of ncf corrected Paleodoses indicated a significant offset (~7 – 38%) in the ages from the uncorrected ages using the conventional SAR protocol (Table 3.1). As seen from a significant reduction in the FWHM of Gaussian curve of paleodose distribution after ncf corrections, it is evident that sensitivity changes is responsible in some samples for dose heterogeneity which would have been attributed to partial bleaching. This is important in partially bleached sediments of a young sample (1-2 ka) where least values or minimum age model is preferred (Jain et al, 2004). Hence it is recommended that this correction should be used for SAR paleodose estimation.

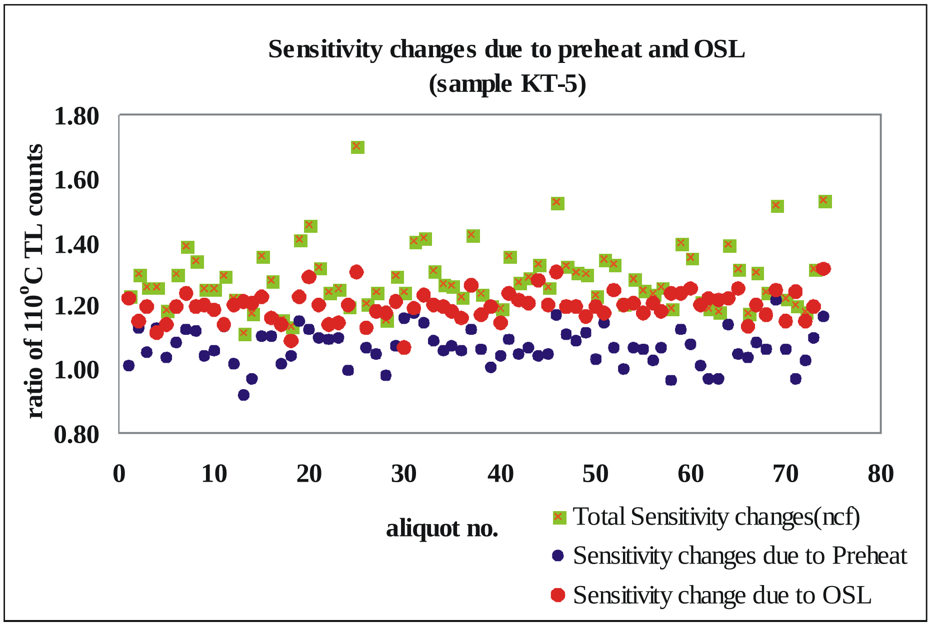

Figure 3.2. Sensitivity changes due to preheat and OSL stimulation alone.

Table 3.1. Effect of natural sensitivity changes on the average paleodose. % Change has been calculated by taking ratio of difference between the corrected and uncorrected paleodose to the uncorrected paleodose.

Sample	Paleodose (average)(Gy)		% Change
	Without sensitivity correction	After sensitivity correction	
NN-1	46 ± 11	37.6 ± 11	18
NN-5	29 ± 6	25 ± 6	14
NN-6	25.7 ± 7.3	23.4 ± 7.7	9
KT-5	11 ± 4	7 ± 4	36
KT-6	8 ± 3	6 ± 3	25
OTS-1	30.4 ± 9.2	28.2 ± 9.7	7
OTS-2	5.7 ± 1.6	4.9 ± 1.5	14
OTS-3	27 ± 7	21.9 ± 5.5	18
OTS-4	27 ± 14	19.8 ± 9.2	26
OTS-5	2.3 ± 0.6	2.1 ± 0.5	9
RW-1	22.8 ± 9.8	18.7 ± 8.5	18
RW-2	7.8 ± 4	6.3 ± 2.6	10
RW-3	12 ± 5	9 ± 4	19
RW-4	28.5 ± 11	22.5 ± 8	21

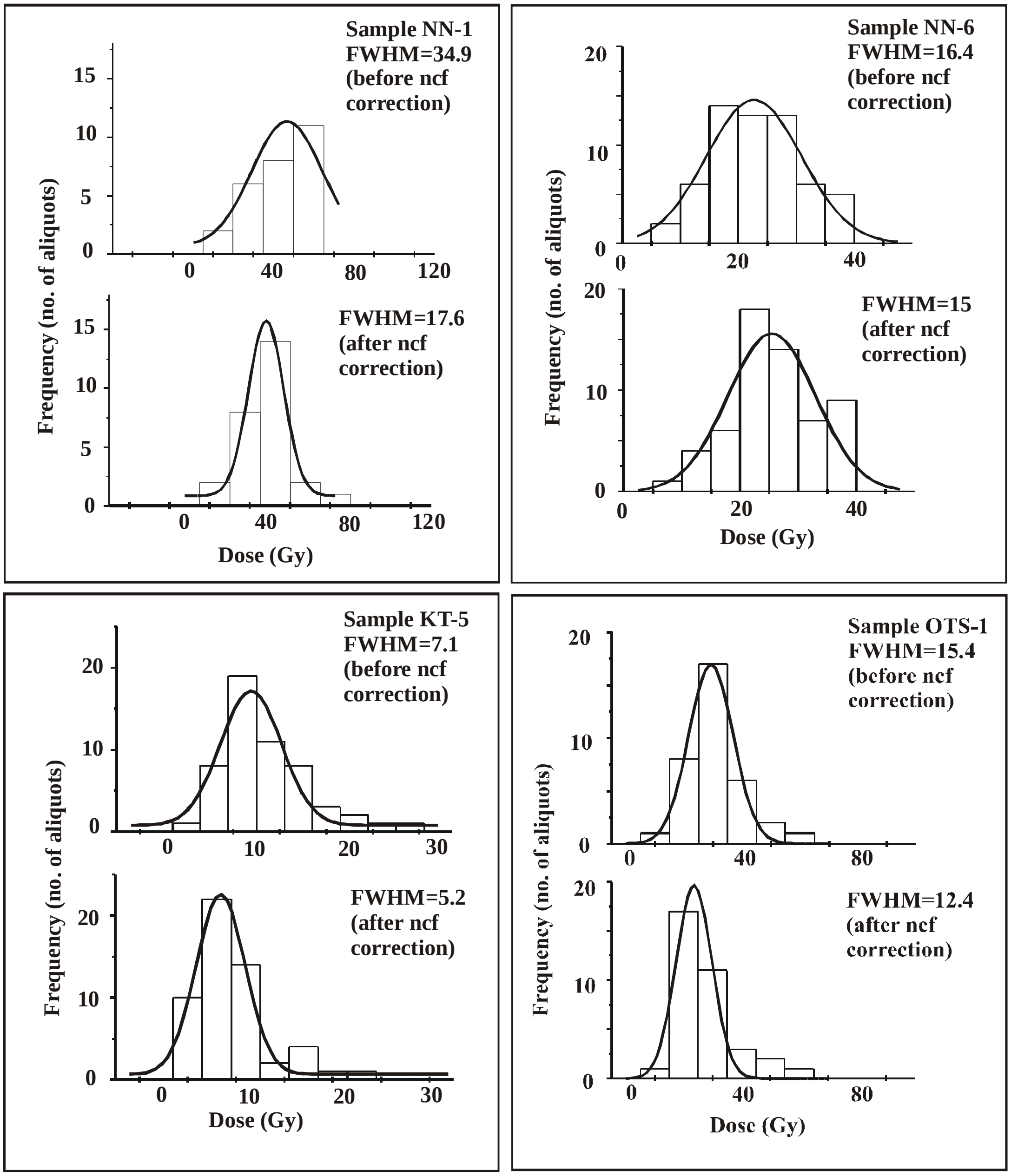

Figure 3.3. The effect of ncf correction on the shape of the dose distribution curve is seen by the decreased FWHM of the curve after correction.

References

Jain, M, Murray, A.S., Lars, Botter-Jensen, 2004. Optically Stimulated Luminescence Dating: How significant is incomplete light exposure in fluvial environments? *Quaternaire*, 15, 143–157.

Murray, A.S. and Roberts, R.G., 1997. Determining the burial time of single grains of quartz using optically stimulated luminescence. Earth and Planetary Science Letters, 152, 163–180.

Murray, A.S., Roberts, R.G. and Wintle, A.G., 1997. Equivalent dose measurement using a single aliquot of Quartz. *Radiation Measurement*, 27, 171–183.

Murray, A.S. and Wintle, A.G.,2000. Luminescence dating of quartz using an improved single aliquot regenerative-dose protocol. *Radiation Measurement*, 32, 57–73.

Murray, A.S. and Wintle, A.G., 2003. The single aliquot regenerative dose protocol: potential for improvements in reliability. *Radiation Measurement*, 37, 377–381.

Stoneham, D. and Stokes, S., 1991. An investigation of the relationship between the 110°C TL peak and optically stimulated luminescence in sedimentary quartz. *Nuclear Tracks and Radiation Measurement*, 18, 119–123.

Stokes, S., 1994a. Optical Dating of Selected late quaternary aeolian sediments from the southwestern United States. *Unpublished D.Phil thesis*, Oxford University, Oxford.

Stokes, S., 1994b. The timing of OSL sensitivity changes in a natural quartz. *Radiation Measurements*, 23, 601–605.

Stokes, S. and Singhvi, A.K.. Changes in natural OSL sensitivity during Single Aliquot Regeneration procedures and their implications to equivalent dose determination (Under preparation).

Chapter-4

Limits and applicability of Standardized Growth Curve

4.1 Introduction

A typical Single Aliquot Regeneration (SAR) method employs a 5-point cycle of measurements in which each cycle involves sequential steps of irradiation, preheat and OSL measurement (Murray and Wintle, 2000; 2003). Typically a SAR run implies ~50-100 minutes or more of OSL reader time per disc depending upon the age of the sample and the beta dose rate of the reader. In case of well-bleached aeolian samples, a tight cluster in single aliquot paleodoses (P) distribution is generally expected (assuming there is no adverse effect on account of beta dose heterogeneity) (Clarke, 1996; Olley et. al, 1998). This implies that a measurement of ~30 discs may be sufficient for a high precision (<5%) estimates of paleodose. However, in the case of partially and in homogeneously bleached sediments (fluvial sedimens), a larger data set of paleodoses (typically ~60-100) have to be analyzed for most appropriate paleodose estimation using a variety of approaches (Thomas et al., 2005). This implies at least 4-5 days of reader time per sample, making the data throughput rather small. To reduce the time needed for generating a set of paleodoses sufficient for a statistically reliable analysis, the use of "standardized growth curve (SGC)" in evaluating paleodose was recently suggested with encouraging results on aeolian quartz and polymінerallic fine-grains, (Roberts and Duller, 2004). We examined this aspect further to determine the applicability of the SGC-SAR on coarse-grained quartz from fluvial and aeolian sediments. Based on these, practical criterion that enable a decision on a reliable use of SGC in routine application was developed.

In a fluvial system, partial bleaching is anticipated. For young sediment, the use of minimum paleodoses is suggested rather than taking average of all paleodoses (Olley et.al., 98; Jain et.al. 2004). However, this aspect was not discussed in Roberts and Duller (2004). It discussed only for average paleodose. Present work examines this part in detail to see the effect on minimum paleodoses (here average of least 10% of the doses obtained) of a dose distribution in fluvial system with special reference to Himalayan sediments.

4.2 Concept and Methodology

In the standard SAR method, a growth curve is constructed by giving laboratory beta doses to the aliquot followed by preheat and OSL measurement (Murray & Wintle 2000). The luminescence yield at each dose point is corrected for sensitivity change by measuring the OSL yield for a test dose. A plot of the sensitivity corrected regenerated OSL signal with dose enables the construction of a growth curve and sensitivity corrected natural luminescence intensity is interpolated onto this curve to obtain the equivalent dose or paleodose. In construction of SGC, a limited set of regenerated growth curves are merged to construct a master growth curve, termed Standard Growth Curve (SGC). On this curve, sensitivity corrected natural intensity of other aliquots is read. However, what should be the appropriate number of growth curves required was not discussed in Roberts and Duller (2004). In present work, this aspect was examined to provide a more practical recipe for the application of SGC. A suite of fluvial samples from three different geological archives in Himalaya was examined for the present study. The location and stratigraphic description of all these samples are discussed in detail in Chapter-5 of the thesis.

4.3 Standard Growth curve (SGC)

4.3.1. Construction of SGC

The SGC of a sample was obtained by merging the SAR growth curve of 20 aliquots. Recuperation in these samples was <3% and because of this the SAR growth curves were forced through the origin. Figure 4.1 provides typical growth curves of some samples. The growth curves of samples in general fitted a linear or polynomial and the regression coefficients (R^2) ranged from 0.57-0.93. The paleodose of remaining aliquots of the sample was obtained by interpolating the sensitivity corrected natural luminescence onto the SGC. Both the minimum 10 % and the mean of all the paleodoses values were calculated and tabulated (Table 4.1). In general, mean values of paleodoses from SAR methods and SGC were comparable within errors; however, the minimum paleodoses values differed in a range of 2-40 %. This difference was less for the samples characterized by higher regression coefficient of the SGC growth curves (i.e. $R^2 > 0.9$).

A plot of the P_{SGC} *vs*. P_{SAR} is shown in Fig. 4.2. In an ideal case, the plot of P_{SGC} against P_{SAR} should fall on the line of slope 1. The trend line of the data does not fall on line of slope 1 and the regression coefficient ranges from 0.27 to 0.91, suggesting that although mean P_{SGC} values were comparable to P_{SAR} values, it was difficult to compare a particular subset of data (e.g. least 10% data) of the two P values because of variability.

4.3.2. Minimum aliquots needed for SGC

Another aspect that we examined was, the appropriate number of growth curves that should be used to form a standard growth curve (SGC). Towards this SGC were constructed using 5, 10 and 20 regenerated growth curves of each sample (Table 4.1). The average P was calculated of all disc from SGC and compared with the SAR P. Sample RW-1, RW-2, RW-4, RW-11, RW-12, OTS-1, OTS-2, OTS-5, OTS-4 & KT-5 have average SGC P (constructed from 10 and 20 aliquots) close to the SAR P compared

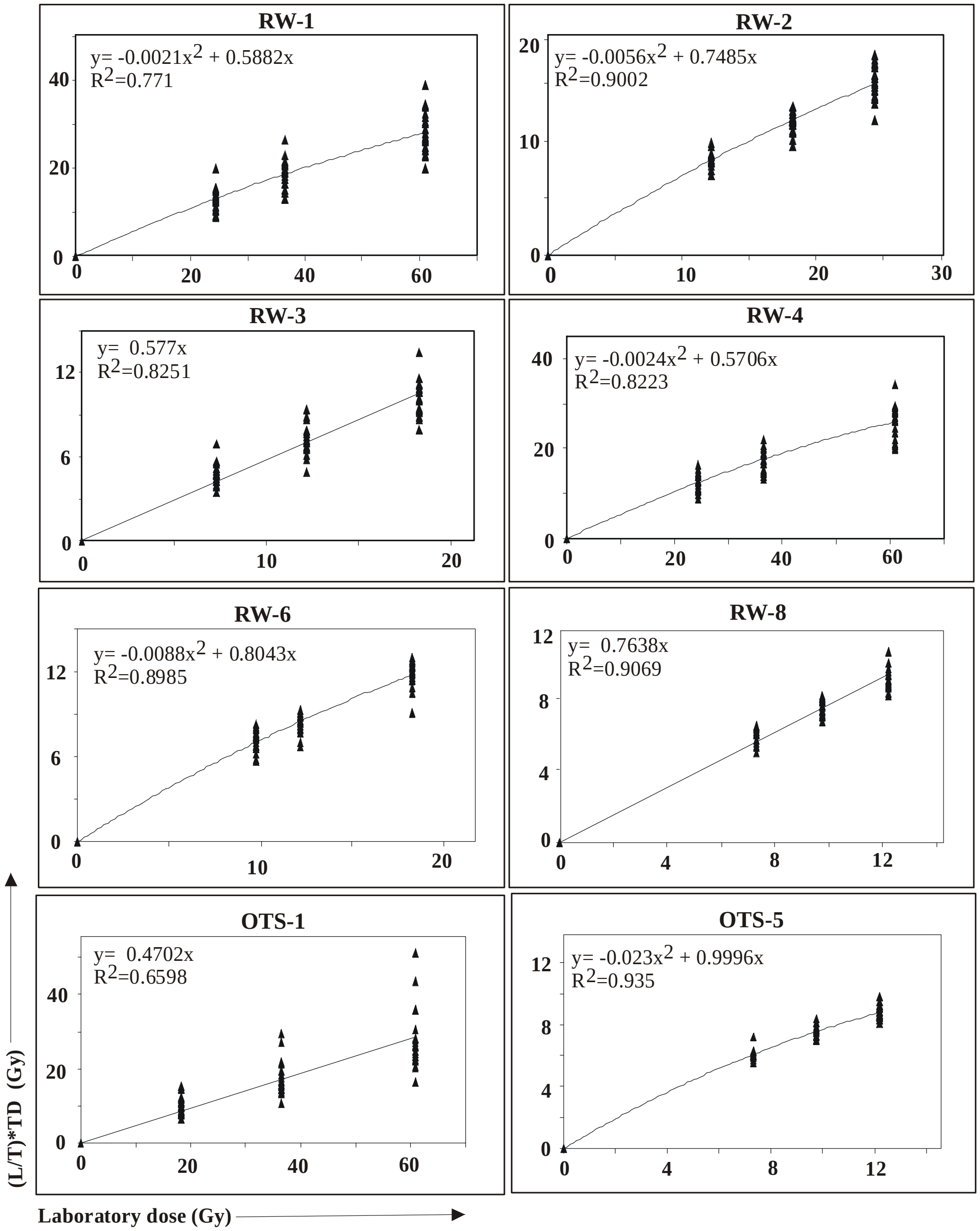

Fig. 4.1. Standard Growth Curve of samples from various locations in Himalaya. The 20 data points are merged for each dose point to construct a master growth curve termed as Standard Growth Curve

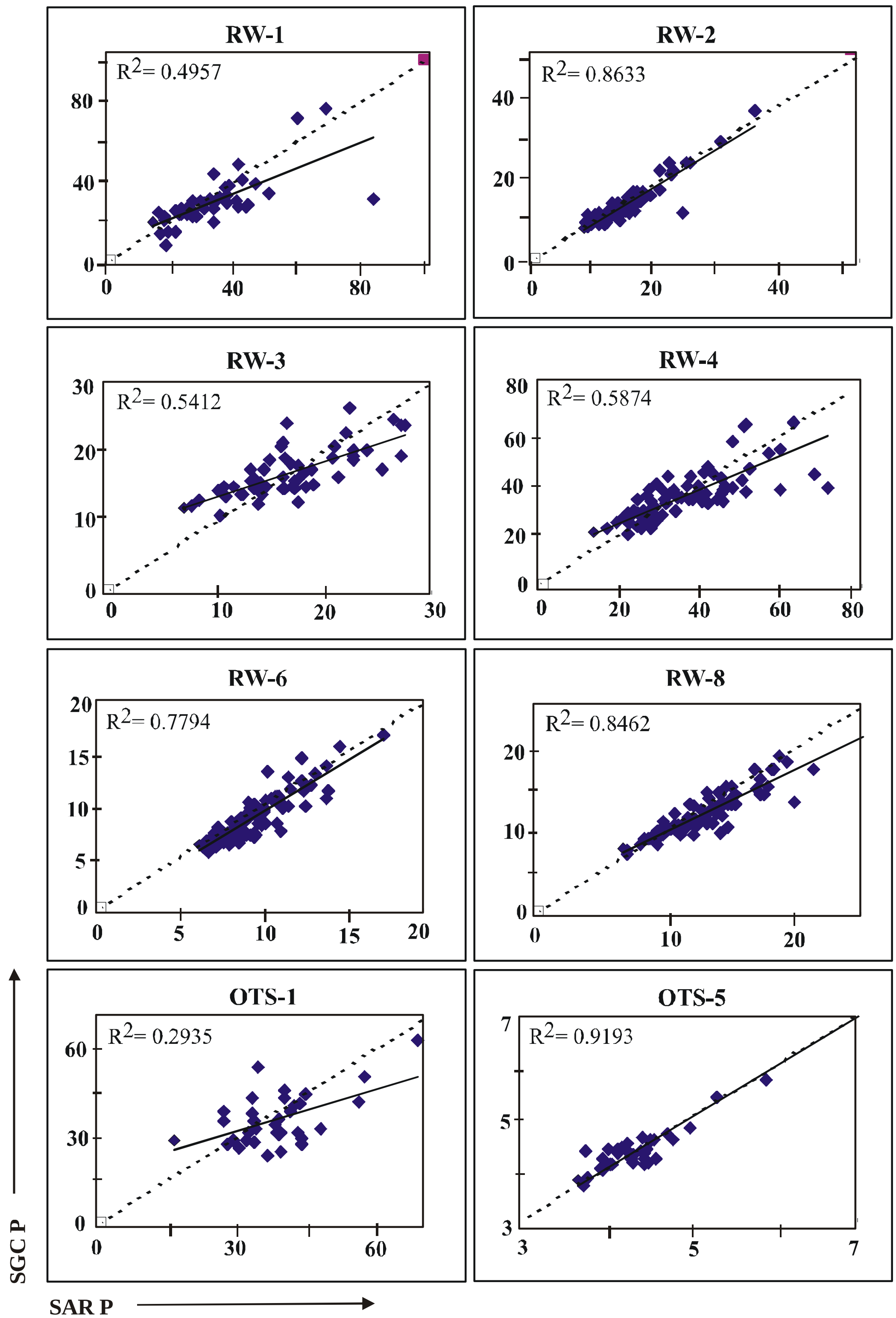

Fig. 4.2. A comparison between paleodoses calculated by SGC and their corresponding paleodose calculated using SAR. Dotted line represents the line of slope 1 and the solid line is the best fit line of these points representing the scatter in the data.

with the SGC P constructed from 5 aliquots only, however they are same within error limits. So we can construct a SGC from 5 aliquots or more, however it will be more reliable to have a large number of aliquots (10-20) to represent more appropriately the overall intrinsic variability of the luminescence sensitivity of the sample. In our study 20 aliquots were used to construct the SGC.

4.3.3. Universal SGC for an entire stratigrahic sequence

Roberts and Duller, 2004, examined a possible application of the SGC to a complete stratigraphic sequence with samples having identical depositional environment. However, it may be difficult to apply this on the samples examined from Himalayan rocks because of variability in luminescence properties leading to the variable fitting parameters (linear and polynomial in the same stratigraphic sequence), defining a fit of the SGC in the present scenario.

4.4 Results and Summary

During the construction of SGC, it was observed that scatter in growth curve for 20 aliquots were variable and the R^2 ranged from 0.57-0.94 (Fig. 1). It was also seen that growth curves of samples with regression coefficients ≥ 0.9 (RW-2, RW-6, RW-8 & OTS-5) in a 20 aliquot SGC exhibited a good concordance between P_{SAR} and P_{SGC} values (Fig. 2). These samples shows less than 8% difference in their minimum 10 % P's compared from SGC and SAR seperately. Based on this, it can be suggested that a regression coefficient of >90% in a growth curve would be a minimum condition for a successful application of SGC on the dating of young fluvial sediment where minimum values are important due to partial bleaching, however in an old sample where partial bleaching is masked by the amount of signal build up during time of burial, it can be applied to any set of sample. The present study shows that,

(i) The SGC analysis can be applied to any set of sample, where the regression coefficient of a SGC based on 20 aliquots is >90%. Application to samples with lower regression coefficients is likely to be less accurate if one wish to apply this on very young fluvial sediments where minimum P's has to be accounted for Paleodose calculation.

(ii) Chances of success of SGC will be more for homogenized sediments of similar characteristics.

Table 4.4. Variation in mean De computed by varying no. of aliquots selected randomly.

Serial No.	Sample	SAR P mean (Gy)	SGC(constructed from 5 aliquots) mean P (Gy)	SGC(constructed from 10 aliquots) mean P (Gy)	SGC(constructed from 20 aliquots) mean P (Gy)
1	RW-1	31.8 ± 14	33.7 ± 13.7	30 ± 12.8	29 ± 12.3
2	RW-2	12.9 ± 4.6	13.8 ± 5.1	13 ± 4.7	12.5 ± 4.7
3	RW-3	17 ± 5.2	17.2 ± 3.6	17.2 ± 3.6	17.3 ± 3.6
4	RW-4	35.2 ± 12.5	34.9 ± 10.9	34.7 ± 11	35 ± 11
5	RW-6	9.5 ± 2.1	9.1 ± 2.4	8.9 ± 2.2	8.9 ± 2.2
6	RW-8	12.9 ± 4.2	12.3 ± 3.4	12.3 ± 3.4	12.2 ± 3.4
7	RW-11	12.9 ± 4.2	13.7 ± 4.2	13.8 ± 4.4	12.9 ± 3.8
8	RW-12	7.6 ± 1.8	8 ± 1.6	8 ± 1.6	7.8 ± 1.6
9	OTS-1	37.7 ± 9.8	31.1 ± 7.6	33.8 ± 8.3	35.6 ± 8.7
10	OTS-2	8.1 ± 1.6	8.5 ± 1.9	8.2 ± 1.8	8.4 ± 1.8
11	OTS-4	31 ± 13	33 ± 15.8	30.5 ± 11.4	29.7 ± 11.3
12	OTS-5	4.4 ± 0.7	4.6 ± 0.8	4.5 ± 0.8	4.4 ± 0.7
13	KT-5	17.5 ± 5.3	19.9 ± 6.2	18.2 ± 5.8	18.6 ± 6.3
14	KT-6	13.7 ± 3.5	15 ± 4	15.6 ± 4.2	14.3 ± 3.8

Table 2. Curve fitting and regression coefficients of SGC and the effect on mean and least 10% of the paleodose

Serial No.	Sample	Curve Fitting	R^2 of SGC	SAR P (least 10%) (Gy)	SGC P (least 10%) (Gy)	% change = ((SGC P-SAR P)/SGC P)*100	SAR P (mean) (Gy)	SGC P (mean) (Gy)	% change = ((SGC P-SAR P)/SGC P)*100
1	RW-1	Poly.	0.77	15.6 ± 1.4	19.7 ± 4.1	20.8	31.8 ± 14	29 ± 12.3	9.7
2	RW-2	Poly.	0.90	8.2 ± 0.5	8.9 ± 0.9	7.9	12.9 ± 4.6	12.5 ± 4.7	3.2
3	RW-3	Linear	0.82	8.7 ± 1.6	12.7 ± 1.4	31.5	17 ± 5.2	17.3 ± 3.6	1.7
4	RW-4	Poly.	0.82	19.5 ± 3.1	24.2 ± 3.1	19.4	35.2 ± 12.5	35 ± 11	-0.6
5	RW-6	Poly.	0.90	6.7 ± 0.3	6.4 ± 0.6	-4.7	9.5 ± 2.1	8.9 ± 2.2	-6.7
6	RW-8	Linear	0.91	7.9 ± 1	8.5 ± 0.9	7.1	12.9 ± 4.2	12.2 ± 3.4	-5.7
7	RW-11	Poly.	0.86	7.8 ± 0.5	9.6 ± 1	18.8	12.9 ± 4.2	12.9 ± 3.8	0
8	RW-12	Linear	0.78	5.3 ± 0.3	6.8 ± 0.4	22.1	7.6 ± 1.8	7.8 ± 1.6	2.6
9	OTS-1	Linear	0.66	23.8 ± 5.3	35.1 ± 4.7	32.2	37.7 ± 9.8	35.6 ± 8.7	-5.9
10	OTS-2	Linear	0.57	5.8 ± 0.5	6.1 ± 1	4.9	8.1 ± 1.6	8.4 ± 1.8	3.6
11	OTS-4	Poly.	0.68	14 ± 2.2	16.2 ± 1.2	13.6	31 ± 13	29.7 ± 11.3	-4.4
12	OTS-5	Poly.	0.94	3.7 ± 0.1	3.9 ± 0.3	5.1	4.4 ± 0.7	4.4 ± 0.7	0.2
13	KT-5	Poly.	0.79	11.7 ± 0.8	14.8 ± 2	20.9	17.5 ± 5.3	18.6 ± 6.3	5.9
14	KT-6	Linear	0.82	9.4 ± 0.5	11 ± 1.6	14.5	13.7 ± 3.5	14.3 ± 3.8	4.2

References

Murray, A.S., Wintle, A.G.,2000. Luminescence dating of quartz using an improved single aliquot regenerative-dose protocol. *Radiation Measurement*, 32, 57–73.

Murray, A.S. and Wintle, A.G., 2003. The single aliquot regenerative dose protocol: potential for improvements in reliability. *Radiation Measurement*, 37, 377–381.

Thomas, P.J., Jain, M., Juyal, N. and Singhvi, A.K., 2005. Comparison of single-grain and small-aliquot OSL dose estimates in <3000 years old river sediments from South India. *Radiation Measurement*, 39, 457–469.

Jain, M, Murray, A.S. and Lars, Botter-Jensen, 2004. Optically Stimulated Luminescence Dating: How significant is incomplete light exposure in fluvial environments? *Quaternaire*, 15, 143–157.

Clarke, M.L., 1996. IRSL dating of sands: bleaching characteristics at deposition inferred from the use of single aliquots. *Radiation Measurement*, 26, 611–620.

Olley, J.M., Caitcheon, G., & Murray A., 1998. The distribution of apparent dose as determined by optically stimulated luminescence in small aliquots of fluvial quartz: implications for dating young sediments. *Quaternary Science Reviews*, 17, 1033–1040.

Roberts, H.M., Duller, G.A.T., 2004. Standardized Growth Curves for optical dating of Sediment using multiple-grain aliquots. *Radiation Measurement*, 38, 241–252.

Chapter 5

Fluvial sediments in diverse depositional settings: Applicability of Luminescence dating

This chapter deals with the various geomorphological archives studied for the feasibility of luminescence dating with respect to daylight exposure. It discusses the processes of sediment depositions in these archives and sampling strategies. Finally the results are presented; however, implications of these results with respect to paleoclimatic reconstruction and neo-tectonic studies are discussed in chapter 6 of the thesis.

Daylight exposure of sediment during the transportation leads to the resetting of geological luminescence. However, in case of fluvial sediments bleaching may be partial or heterogeneous due to the attenuation of daylight by water column (Fig. 1.2, chapter 1), depth of sediment transport and turbidity (Berger and Luternauer, 1987). In such case, luminescence ages could be overestimated from the real age. In the conventional Multiple Aliquot Additive Dose (MAAD) method, palaeodose estimation is based on a measurement of 35 – 40 aliquots with the assumption that all the aliquots have witnessed identical bleaching, thermal and radiation history. Fluvial sediments are transported under different environmental conditions (bed load, high turbidity flow, sheet wash, suspension load etc). Considering this, the above assumption may not be true for fluvial sediments. In many cases large scatter in the dose verses luminescence output was attributed to heterogeneous bleaching at grain level (Clarke, 1996; Li, 1994). Recent development of Single Aliquot Regeneration (SAR) method (Murray and Wintle, 2000) and the Single grain method permits some estimate of heterogeneous bleaching. SAR methods provide opportunity to select the palaeodose corresponding to the minimum paleodose from a set of aliquots that is supposed to be the most bleached.

High topographic relief, glaciers and intense southwest monsoon imply high erosion and sediment fluxes to the Himalaya drainage systems that eventually contribute to high sediment flux into the Bay of Bengal (Goodbred and Kuehl, 2000). The present study was limited to the southern topographic front and the foothill region of Himalaya (the pediment plain) and aimed to understand the spatial and temporal variation in sedimentation. Broadly, two major processes that contribute sediment to the Himalayan rivers are, (i) the glacial outwash and (ii) monsoon induced sediment input (landslides and colluvium). These processes are dominant source of sediment, particularly during the summer monsoon, which contributes ~80% of the precipitation in the Himalayan region (Hasnain, 1999). Since majority of the sediments is transported during monsoon time this would imply poor-bleaching environment due to high-energy transport turbidity, enhanced and variable sunlight flux. Hence for reliable age estimation on such fluvial sediments, it was essential to ensure that geological luminescence was erased to a residual level prior to their burial. This aspects was examined for following sedimentary archives. From bleaching process point of view, these depositional environments imply variable intensity and duration of daylight. The archives used were–

1. Flash flood and incised terrace sediments (T_1).
2. Low energy slack water deposit.
3. High energy alluvial fan deposit
4. Tectonically uplifted fluvial terraces.

5.1 Flash flood deposits

5.1.1 Introduction

Ganga is a major river (>1000 km in length) in north India, drains through a vast alluvial plain before reaching the Bay of Bengal. Himalaya provide most of the Ganga plain sediments. Floods are common during the summer caused both by the monsoon and glacial melt. During this period, the upper catchments of the Ganga River viz. the Bhagirathi River and the Alaknanda River witness frequent landslides that at times lead to the temporary blockage (natural dam) of the rivers. Breaching of such dams cause flash floods that inundundate the lower valley and results in transportation of huge quantity of sediments. The peak of a flood event last for couple of hours to a day whereas its recessional phase can last for few days to a week. Majority of the sediment flux occurs during the peak flood condition and decreases rapidly with the time, thereafter.

Recent meteorological observations suggest that frequencies of flash flood incidences in Himalaya are increasing. Two schools of thought exist towards explaining this increase. The first school suggests that inherent fragility of the terrain is responsible for increase in flood frequencies. The second school suggests that large-scale deforestation during the last century made the higher Himalayan catchments vulnerable during the monsoon (Ives and Messerli, 1989). This debate so far has been inconclusive due to absence of long-term data on the past frequency of flash flood in Himalaya. Studies have shown that the Tethyan and higher Himalayan crystalline are areas of high erosion due to high topographic relief and widespread glacial activity. Compared to this, the lesser Himalaya is a zone of low relief and thickly forested (Valdiya, 1998).

In view of the controversies regarding the genesis of such events, an attempt was made to construct long term record of flash flood events in the Alaknanda basin. Towards this, the youngest incised terrace (T_1) located ~ 6 m above the present day Alaknanda River was studied.

5.1.2 1970's Alaknanda flood

In the upper Alaknanda valley a lake called the Gohna Tal (lake) was created on 22nd September 1893, when around 150-200 million cubic meters of dolomite, shale and quartzite boulders blocked the course of a river Birehi Ganga, a tributary of

Alaknanda River. Gohna Lake was 270 m high, 3 km wide at the base and around 600 m wide at the summit. On 20th July 1970 the southern mountain front (south of high Himalayan crystalline) witnessed unprecedented rain in Alaknanda basin. A majority of the tributary streams of the Alaknanda originates from this region. The width of the lake was to ~700 m and the water depth reduced to ~10 m. This reduction in the lake dimension was attributed to excessive silting during the preceding years (Pal, 1986). Excessive surface runoff during the cloud bursts paved way for slope instability in the tributary valleys of the Alaknanda. The landslide debris assisted in the formation of temporary dams on the tributary streams. Their sequential breaching led to flash flood in the lower Alaknanda valley (Pal, 1986; Weidinger, 1998). The break of Gohna Lake added to the fury of the flood (Weidinger, 1998). Thus, combined effect of the breaching of Gohna Lake and numerous temporary dams on the tributary streams of the Alaknanda River implied unprecedented sediment supply transport. The sediment aggraded in wide valleys along the Alaknanda River e.g. at the confluence of the Birehi Ganga River and the Alaknanda River, around Kaleshwar, Srinagar, Bagwan, Rishikesh (IDPL) and Haridwar (the upper Ganga canal). This peak flood event lasted for around 24 hours during which flood sediments traveled a distance of around 250 km (Birehi Ganga to Haridwar). The 1970's flood deposits can be seen even today in the entire stretch of Birehi to Haridwar (Weidinger, 1998). They are distinct in appearance in the sense that the sediment are dominated by 5-10 m thick grayish dolomite rich sand and pebbles, either abutting the river banks or resting unconformably on the youngest terrace (T_1). A reconstruction of duration of the recession phase based on eyewitness accounts indicates that the flood lasted for over a week.

5.1. 3 Field stratigraphy and sampling details

In view of ascertaining the extent of pre depositional bleaching during flash flood, samples for luminescence dating were collected as function of distance from the source of the flood. Further, in order to understand the bleaching as a function of grain size (mode of transport), both the peak flood sediments and that deposited during the recessional phase (flood plain) were collected. However, the later was found only at Kaleshwar. In addition to this, youngest terrace (T_1) at Srinagar was documented for sedimentology and stratigraphy to reconstruct the past flood history of the Alaknanda basin. This terrace was also sampled for luminescence dating in order to constrain different flood event. Below is the geomorphological and stratigraphic detail of the locations sampled for luminescence study (Fig.5.1 and 5.2).

(i) **Birehi-Alaknanda confluence–**A 6 m thick flash flood deposit of 1970 flood was located 100 m above the confluence (30^{O} 24'N and 79 ^{O} 23' E). The deposit comprises assorted boulders, pebbles and occasional sand lenses. Maximum boulder size was ~3 m along the long axis. Dolomite, quartzite and slate were the dominant lithology. An iron griddle of a bridge that was washed during the 1970 flood was found embedded in the sediment. Sample for luminescence study (MVW-9) was collected from sand lens that was located 1.5 m below the surface (Fig. 5.3)

(ii) **Kaleshwar–**A relatively wide valley around Kaleshwar (30^{O} 70'N and 79 ^{O} 15' E) was plugged with the flood sediments that are spread over a distance of 100 m from the present day river channel. In the exposed section thickness of the deposit varied from 2 – 6 m. From bottom upwards the sequence comprised a 4 m thick coarse pebbly angular sand with false bedding rest over the gravel. This is overlain by 20-50 cm thick impersistent channel gravel. About 30 cm thick laminated sandy-silt lay above this. Towards the top, 1.1 m thick massive silty clay marked the termination of flood sediment. Two samples (KL-1 and KL-2) were collected from the underlying coarse pebbly sand and one sample (KL-3) was collected from the silty horizon (Fig. 5.1)

(iii) **Srinagar–**Two localities on either side of the Alaknanda river were sampled for luminescence study (30^{O} 13'N and 78 ^{O} 46' E). On the left bank, ~ 2 m thick 1970 flood sediment was located above the youngest fluvial terrace T_1 around Keshav Rai temple. The terrace sediment was dominated by coarse to medium textured light grey sand with no discernable bedding and rested unconformably on the underlying surface T_1. Sample OTS-4 was collected from the 1970 flood sediment (Fig. 5.1 and 5.2).

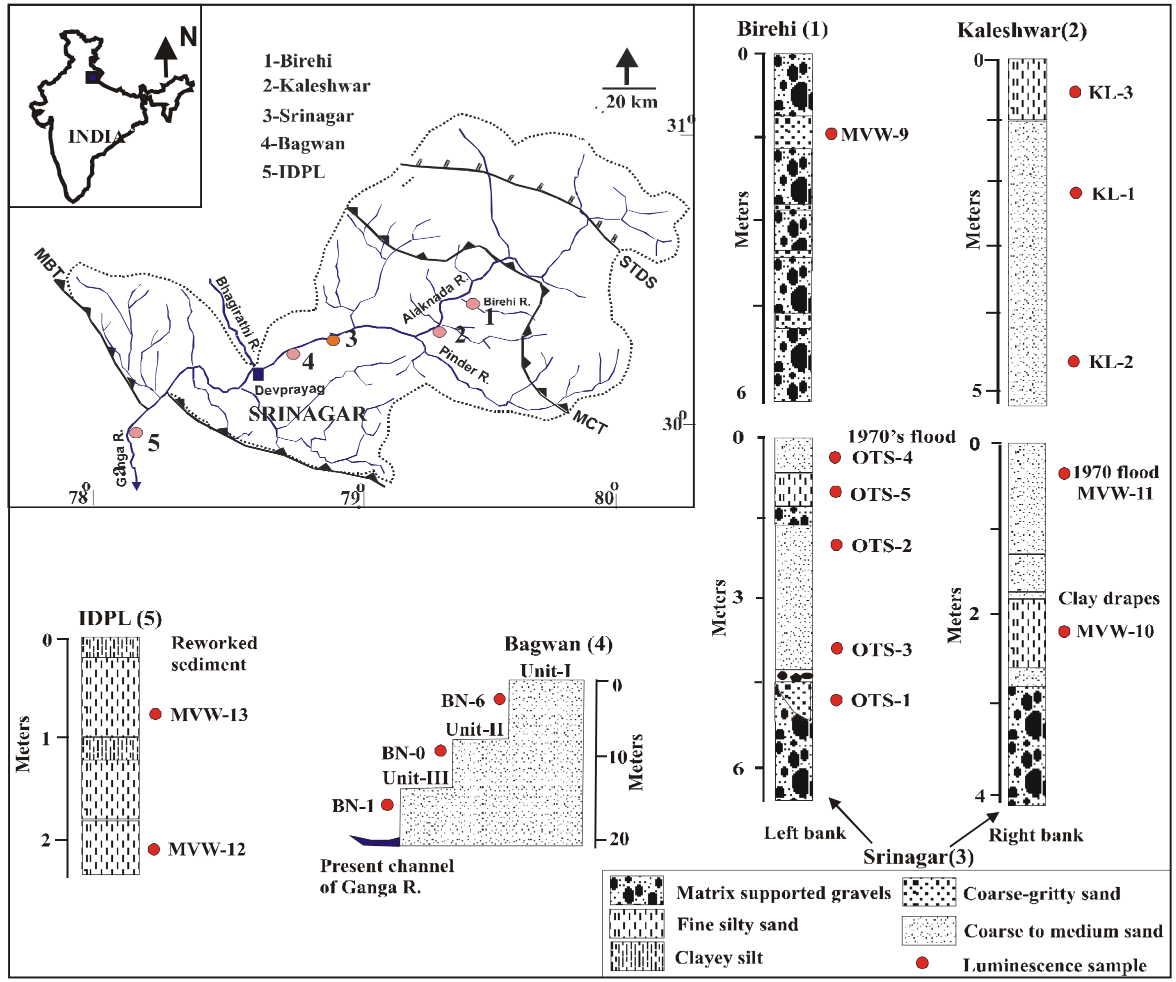

Fig. 5.1. The sample locations (indicated by numbers 1, 2, 3, 4 and 5 on area map) and stratigraphy of the 1970's flash flood deposit.

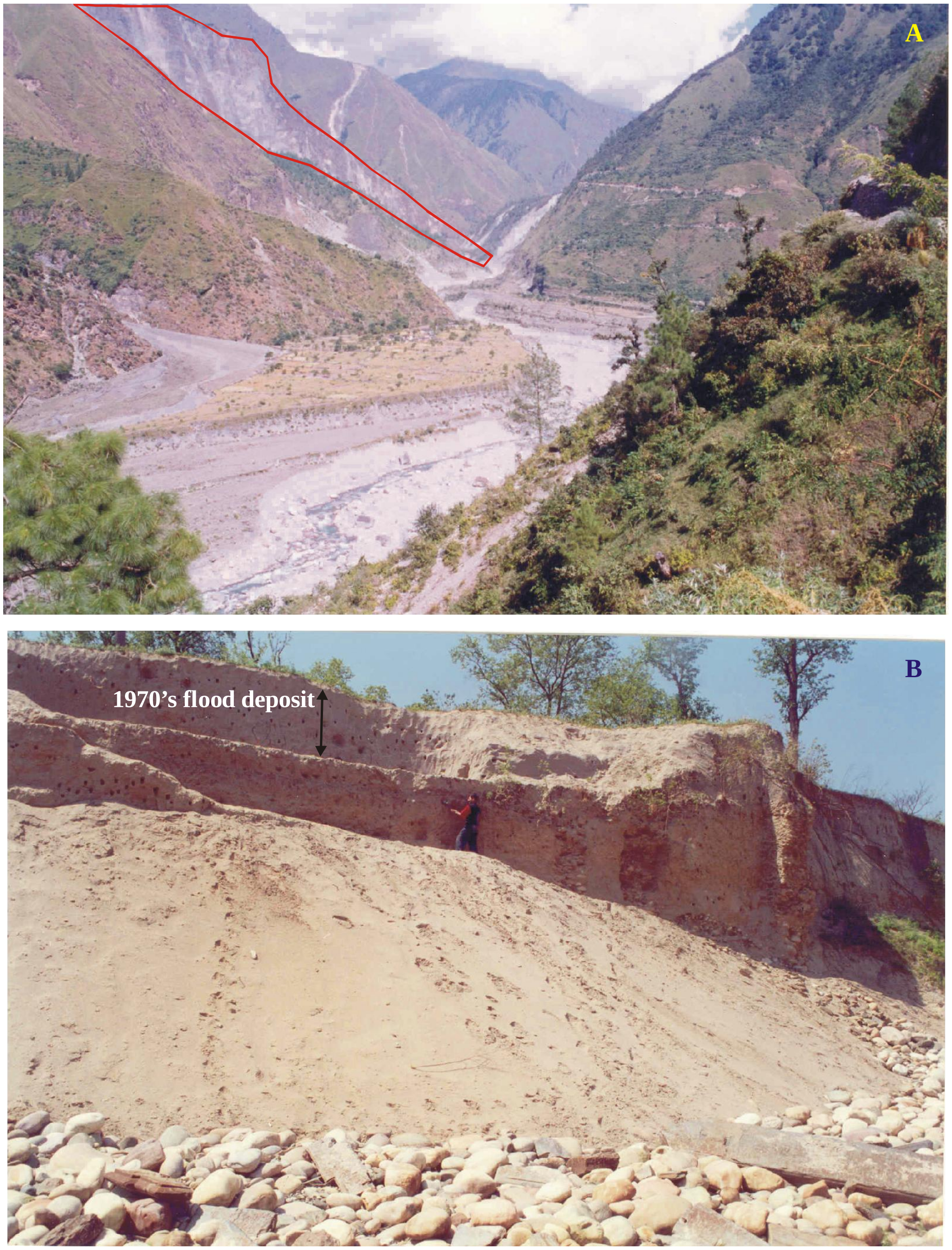

Figure 5.2. (A) The area shown by red line is the part of the mountain slipped during damming of the Birehi Ganga river on 22nd September, 1894. That dam was breached in the year of 1970 and thus created worst flash flood of the century. (B) The area at Srinagar where sediment of this flood was deposited as shown by arrows.

On the opposite flank of the Alaknanda River, a wide ~ 4 m thick scroll bar deposited during the 1970 flood was also excavated for sedimentological and luminescence studies. These sediments were deposited on a 160 cm thick channel gravel. From bottom upwards, 75 cm thick mottled, medium to fine sand with burrows was capped by clay drapes. This was overlain by a massive 40 cm thick coarse to medium gray sand. Coarse to medium gray laminated sand capped this. The sequence terminated with the deposition of 80 cm thick massive coarse to medium gray sand. Two samples one 30 cm below the upper most horizons (MVW-11) and another 18 cm below the 75 cm thick sand horizon (MVW-10) were collected (Fig. 5.1).

(iv) **Bagwan–** Three flood units probably representing flash flood pulses were identified close to a tributary stream meeting the Alaknanda river at Bagwan (30^{O} 13'N and 78 ^{O} 14' E). The oldest Unit-I lies approximately 20 m above the present flood plain and is dominated by massive, medium to coarse grey sand. A weaker flood Unit-II follows this, whereas the lowermost Unit-III lies close to the present day flood plain. Only this unit preserved well-developed laminae with occasional clay drapes. Plastic pieces at the lower part of Unit-III were found. Each unit was sampled for luminescence study. Sample BN-6 was collected from Unit-I, BN-0 from Unit-II and BN-1 from Unit-III (Fig. 5.1).

(v) **Industrial Development Pharmaceutical Limited (IDPL), Rishikesh–** This section lies on a wide undulating flood plain of the Ganga River ~ 5 km downstream of Rishikesh at IDPL (30^{O} 04'N and 78 ^{O} 16' E). The sequence (bottom unexposed) begins with a 70 cm thick brownish fine sandy-silt contained potsherd. This is overlain by a 20 cm thick dark brown weakly weathered clayey-silt. Following this, a 40 cm thick micaceous silty-sand was observed. Finally a 40 cm thick clayey-silt marks the termination of the sedimentation. Two samples one each from the bottom most horizon (MVW-12) and from the micaceous silty sand (MVW-13) were collected for luminescence dating (Fig. 5.1).

(vi) **Youngest Terrace (T_1):** A 625 cm thick fluvial sequence is exposed on the left bank of the Alaknanda River near Keshav Rai temple. From bottom upwards the sequence began with poorly sorted, gravelly boulders (195 cm thick). This is overlain by 390 cm thick pale yellow, well-sorted medium to fine sand. Towards the top of this horizon, swelling and pinching pebbles embedded in sandy matrix could be seen. This horizon was overlain by 40 cm thick silty-clay with occasional rounded to angular gravel. Additionally this horizon shows evidence of human activity that is preserved in the form of charred bones and dispersed charcoal specks. The 1970 flood sediments finally overlie this.

The sedimentary characteristic and textural attributes of the sediment suggests that except for the bottom most gravel, the overlying horizons were deposited as flood plain sediments during events of high floods in the Alaknanda River. For the luminescence study four samples (OTS-1, OTS-2, OTS-3 and OTS-5) were collected from this sequence (Fig. 5.1)

5.1.4 Results and Discussion

All the samples were analyzed using the SAR protocol of Murray and Wintle (2000). In order to evaluate the bleaching heterogeneity of the sediments both average and least 10% of the dose distribution in palaeodose were used (Table 5.1). In addition to this, grain size analyses was also carried out as a function of distance in order to see if there is any grain size dependency in bleaching (Fig. 5.3).

The paleodose distribution of the first sample (MVW-9) that was proximal to the source of the 1970 flood (Birehi-Alaknanda confluence) had a large scatter (relative standard deviation > 38%) as shown by wide paleodose distribution (Fig. 5.4). This sample was dominated by very coarse (>250 μm) sand (>91% by weight). The average palaeodose (mean of all aliquot) was 26 Gy whereas the least 10% palaeodose was 9 Gy. This implies that sediment transportation occurred under poor light condition or the floodwater turbidity attenuated the day light flux. Considering that the flood originated from the Birehi Ganga River (~15 km upstream) during the midnight, poor light condition appears to be the likely possibility of insufficient bleaching of sediment. Further 50 km down stream from the Birehi Ganga-Alaknanda confluence, two samples were analyzed at Kaleshwar. Sample no. KL-1 was dominated by coarse sand (87%) yielded mean palaeodose 24 Gy whereas the least 10% was 9 Gy.

Table 5.1. Paleodose of Flash flood sediments from various locations and flood plain deposit from Srinagar terrace T_1 analyzed using SAR.

Sample No.	Location	Distance from origin of flood (km)	Paleodose (Gy)	
			Least 10%	Mean
MVW-9	Birehi	0	9 ± 2	26 ± 10
KL-1	Kaleshwar	50	9 ± 1	24 ± 13
KL-3	Kaleshwar	50	1 ± 0.3	3.3 ± 2.6
OTS-1	Srinagar	150	20 ± 1	31 ± 9
OTS-2	Srinagar	150	3.4 ± 0.5	5.7 ± 1.6
OTS-3	Srinagar	150	18 ± 0.5	27 ± 7
OTS-4	Srinagar	150	9 ± 3	27 ± 14
OTS-5	Srinagar	150	1.7 ± 0.1	2.3 ± 0.6
MVW-10	Srinagar	150	0.8 ± 0.2	2.7 ± 1.3
MVW-11	Srinagar	150	23 ± 4	32 ± 6
BN-0	Bagwan	200	5 ± 0.2	14 ± 8
BN-1	Bagwan	200	11 ± 3	29 ± 10
BN-6	Bagwan	200	18 ± 5	45 ± 15
MVW-12	IDPL	250	7 ± 1	15 ± 5
MVW-13	IDPL	250	8 ± 1	20 ± 7

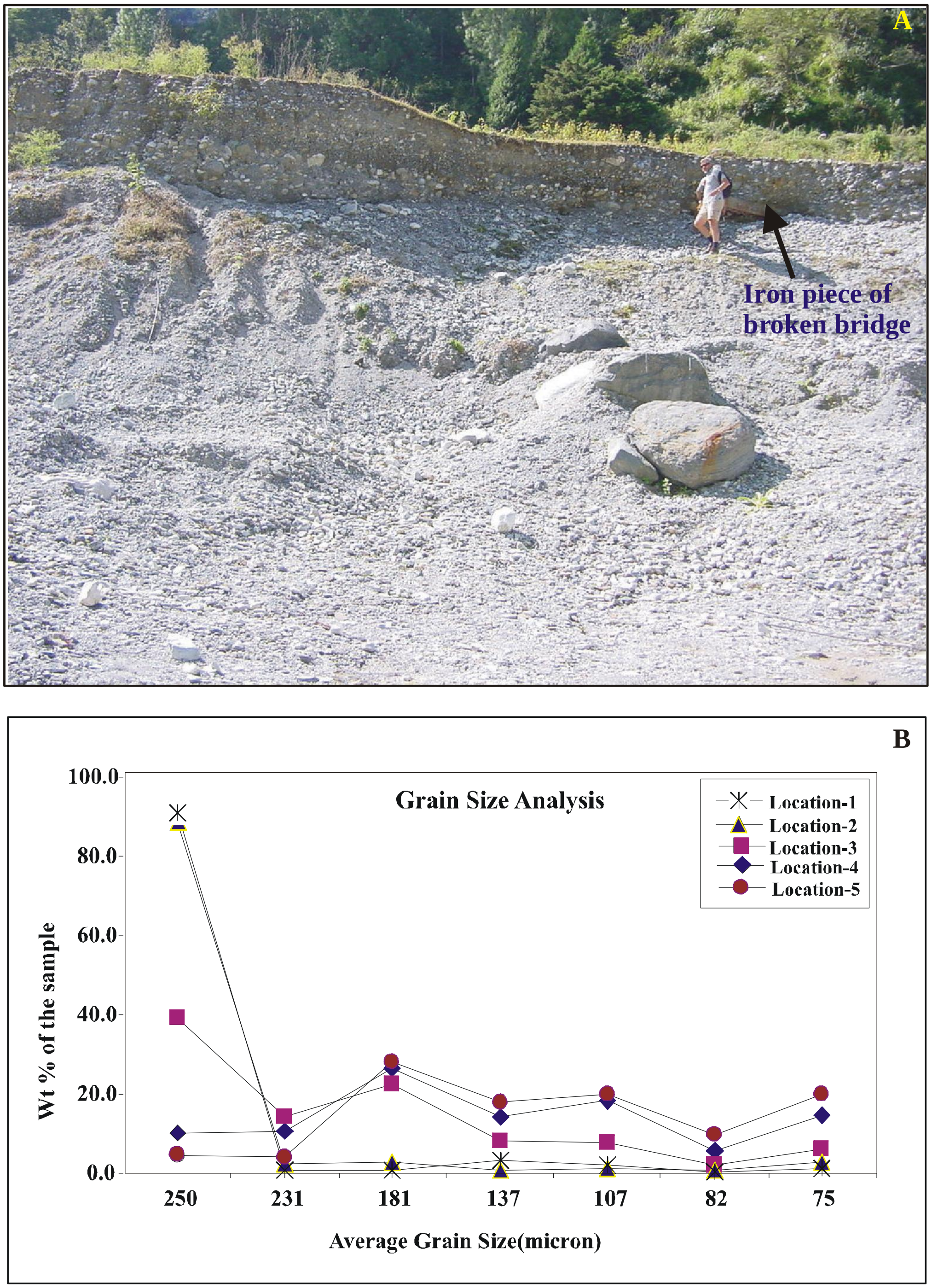

Fig. 5.3. (A) 1979's flood deposit at Birehi comprising matrix supported gravels. A piece of iron bridge was found buried in the sediment. (B) Variation in grain size of the 1970's flood sediment with respect to distance of transport. The coarse fraction of the sediment decreases with distance of travel.

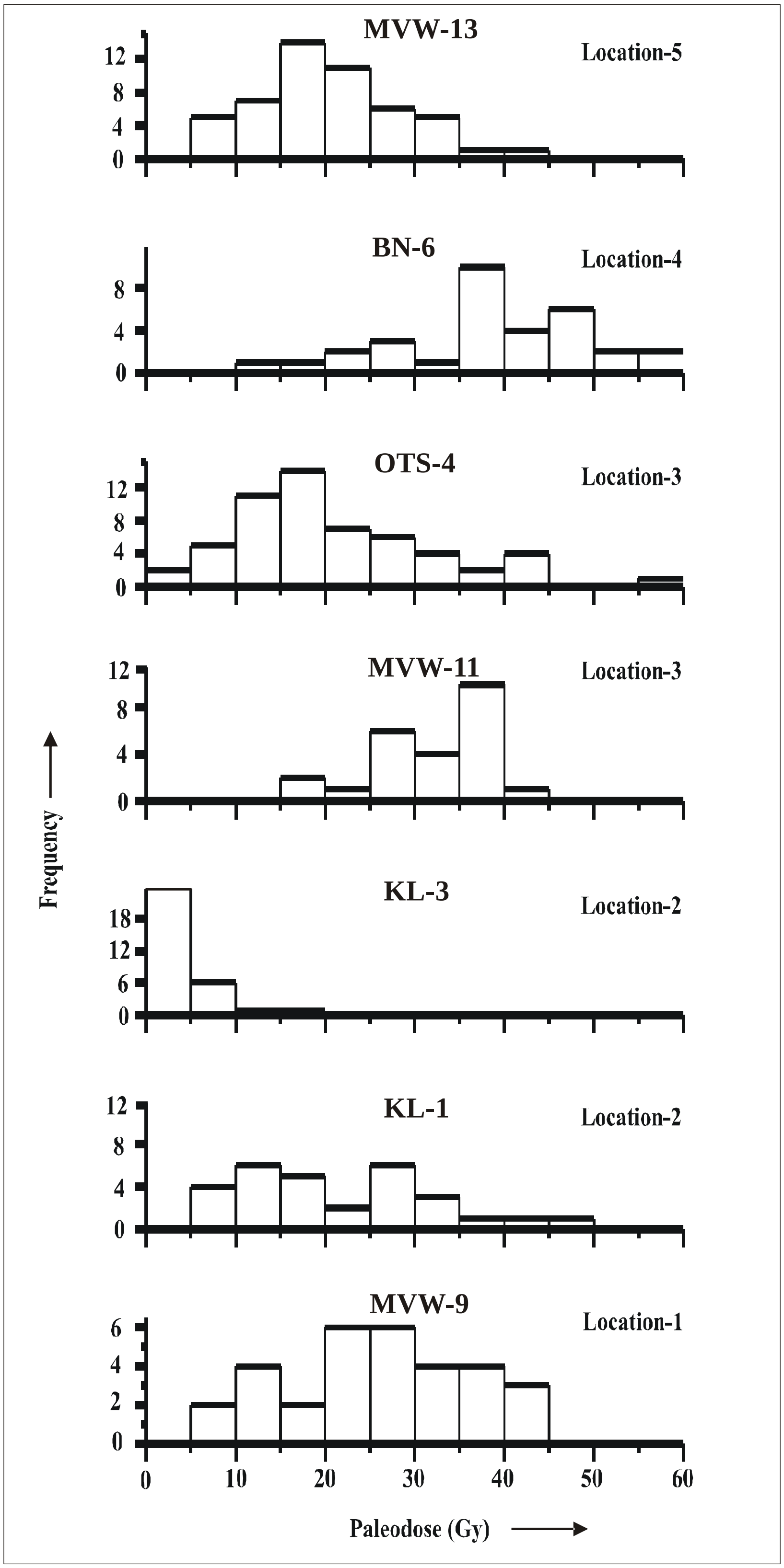

Fig. 5.3. Dose distribution of 1970’s flood sediment

3) overlying the coarse sand was 3.3 Gy and the least 10% was 1 Gy. The lower palaeodose of KL-3 is attributed to the deposition during the recessional phase of flood. Thus, sediment prior to deposition remained in suspension hence facilitating pre-depositional bleaching. Further downstream at Srinagar, 150 km from the Birehi Ganga-Alaknanda confluence, four samples were analyzed from the left and the right flanks of Alaknanda River near Keshav Rai temple. Sample OTS-4 collected from the 1970 flood deposit whereas OTS-5 collected from the tope of Terrace T_1 was silty sand (flood plain deposition). The average palaeodose of OTS-4 was 27 Gy and the least 10% was 9 Gy. The average palaeodose of OTS-5 was 2.3 Gy and the least 10% was 1.7 Gy. Samples from stratigraphically equivalent sequence on the right flank indicated that the average palaeodose of the bottom flood plain sample (MVW-10) was 2.7 Gy and the least 10% was 0.8 Gy. The average palaeodose of the overlying 1970 flood sample (MVW-11) was 32 Gy and the least 10% was 23 Gy. These data indicate samples below the 1970 flood deposits (OTS-5 and MVW-10) were exposed to daylight flux before deposition, a reasonable assumption considering their deposition on flood plain environment.

Bagwan is located 200 km down stream from Birehi Ganga. A total of three samples from Unit-I (BN-6) and Unit-II (BN-0) and Unit-III (BN-1) were analyzed. BN-6 was deposited during the peak flood condition and BN-0 was deposited during the recessional phase of the flood. Compared to this, BN-1 was a recent flood event. The average palaeodose of 1970 peak flood sediment (BN-6) was 45 Gy and the least 10% was 18 Gy. For sample BN-0 the average palaeodose was 14 Gy and least 10% was 4.8 Gy. Whereas for recent flood deposit (BN-1) the average palaeodose was 29 Gy and least 10% was 11 Gy.

The farthest sampling site was near Rishikesh at IDPL about 250 km from Birehi Ganga. At this location two samples were analyzed from a 170 cm thick sequence. The lower MVW-12 was pre 1970 deposit whereas MVW-13 was deposited during the 1970's flood. The average palaeodose of MVW-12 was 15 Gy and the least 10% was 7 Gy. Compared to this the 1970 flood deposit (MVW-13) gave an average palaeodose of 20 Gy and the least 10% was 8 Gy.

The above study suggested that pre-depositional bleaching of sediments in high gradient Himalayan rivers during flash flood are inadequately bleached. There was no systematic increase in bleaching as a function of distance was observed. However, comparing the two extreme samples one collected at Birehi-Alakanada confluence and another at the farthest point (IDPL), a marginal decrease (~35%) in the palaeodose was observed. Considering that the 1970 flood occurred only 35 years ago, the palaeodose of the most bleached sample (MVW-13) at IDPL had significant unbleached component. The study thus indicate that in high energy fluvial environment like Himalaya, during flash flood event, even a distance of 250 km was inadequate for resetting the geological luminescence to a residual value. A part of this was possibly due to flood initiation during the night and it traveled that distance in an overcast sky condition.

It appears that bleaching of flash flood sediment is influenced by the grain size. This study indicates that sediment transported in suspension experienced relatively high bleaching (> 85%) compared to the high turbid coarse fraction. Thus beside the distance, the mode of transport is important. In the present case the flood plain sediment (KL-3) that was deposited 50 km from the origin had 80-90% reduction in palaeodose compared to its counter part that was deposited during peak flood event. This indicates high bleaching probability for sediments that are deposited on flood plain.

Compared to the 1970 flash flood samples, the terrace T_1 sediments (flood plain aggradation) show less variability between the average and least 10% palaeodose suggests bleaching was nearly homogeneous and total. In the terrace T_1, the difference between the average and the least 10% palaeodoses varied between 36 % (OTS-1) and 26% (OTS-5).

The study suggests that during the flood events, it is the mode of transportation besides the distance that decides the extent of predepositional bleaching of acquired luminescence. Suspended load has experience a higher and somewhat unattenuated daylight exposure compared to coarse-grained bed load sediment that only sees a highly attenuated daylight spectrum.

5.2 Low energy slack water deposit

5.2.1 Introduction

Low energy slack water deposits are fine-grained sand and silts that settle out of suspension in protected areas of reduced flow velocity during high magnitude floods. Deposition occurs in areas like back-flooded tributaries, eddy zones or along the irregularities in the channel margin (Baker et al., 1988). These deposits occur at the mouth of east flowing Moti Chur river that meets the Ganga river at Raiwala. At the studied location, the river channel is about 200 m wide and 5 m deep giving rise to large width to depth ration of ~40 (Fig. 5.5). In view of this, the large magnitude floods in the Ganga river that exceed the channel capacity spill over the Moti Chur river. The flood sediments in such geomorphological situation get enough time to remain in suspension before settling. This ensures grading of different grain size. Since longer time is involved in slack water sedimentation, it can be assumed that pre-depositional bleaching of such sediment is adequate.

A typical slack water deposit corresponding to one flood event would constitute the bottom sand followed by silt and invariably capped by clay drape (Kale et al, 2000). In other words they can be called as the fining upward sequences similar to the over bank facies. The vertical stacking of such units would imply that each flood event was magnitude higher then the preceding one. Hydrologists use these records to reconstruct the paleo flood history of a river much beyond the historical record, which is limited to few decades or so. However, in order to reconstruct the spatial and temporal variability of palaeoflood events, it is important to obtain reliable age estimates on them. In the recent years some progress has been made using the luminescence dating technique that was limited to the western and central Indian rivers (Kale et al, 2000; 2003) and no study exists from the high energy fluvial system of Himalaya. High topographic relief of this region implies poor preservation potential for slack water deposits. As a result, so far no classical slack water sequences have been reported. However, in the low energy environment caused by the sudden change in gradient (alluvial plain), enhances the chances for the preservation of slack water deposit increases. That is because during floods, the excess water either spill over on to the flood plain or enters into the a tributary stream that meets the major river. Such a location was identified near at Raiwala, here the Ganga River has wide flood plain and a tributary stream called Motichur meets it from the Siwalik hills.

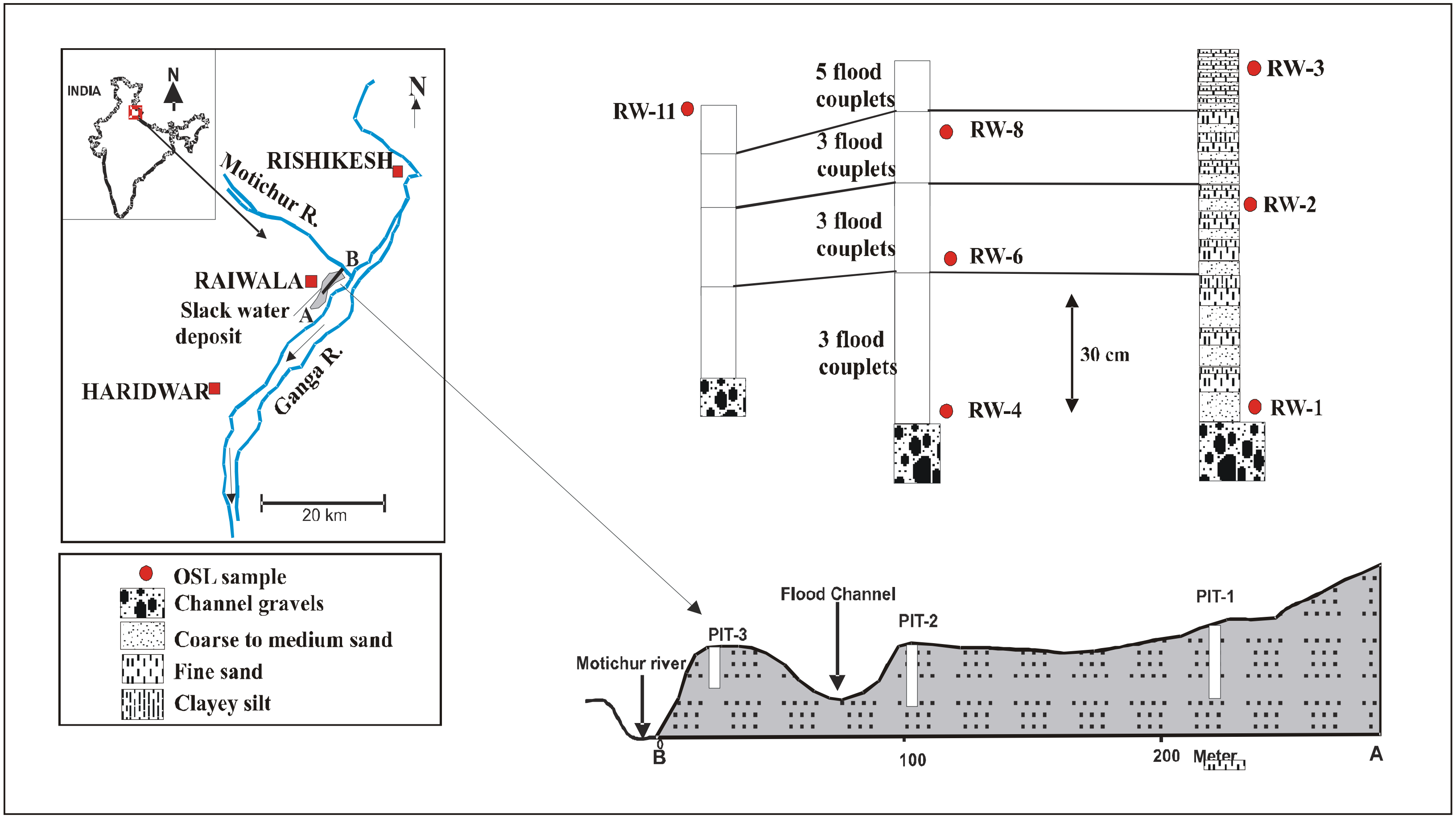

Fig. 5.5. Location and stratigraphy of the section studied for slack water deposits near the confluence of Ganga R. and Motichur stream. In total, 14 flood couplets were identified and correlated from three Pits-1,2 and 3 as shown in figure.

5.2.2 Field stratigraphy and sampling details

On the right bank of the Ganga river slack water deposits were located. These deposits occur in a tributary river Motichur that meets the Ganga at right angle (Fig. 5.5). Presently the Ganga river flows ~200 m east from the studied area. In order to reconstruct the palaeoflood stratigraphy, three pits at some interval (as shown in fig. 5.5) were excavated laterally. This was done to ascertain the lateral continuity of the flood deposits and a composite lithostratigraphy of the palaeoflood succession was made. The flood deposits were underlain by channel gravel. Each flood unit begins with medium to coarse sand followed by silty-sand and capped by clayey-silt. Together they constituted a single flood couplet. A total of 14 such flood couplets were identified suggesting each successive flood event was higher than the preceding one. The thickness of the flood sequences exposed in four-dug pit varied from 75 cm to 120 cm with individual flood couplet thickness ranged from 5 cm to 20 cm. Out of the 14 flood couplets the lower 5 couplets were thicker (15-20cm). For luminescence dating, 7 samples were collected from three pits numbered as P1 (sample RW-1, 2 and 3), P2 (sample RW-4, 6 and 8) and P3 (sample RW-11). P3 was the closest from the tributary channel (30 m), followed by P2 (100 m) and P1 (200 m). In order to estimate the extent of bleaching on modern fluvial sand, a surface sample (RW-12) was collected from the bank of the Motichur stream (Fig. 5.5)

5.2.3 Results and Discussion

Samples were analyzed using the multiple aliquot partial bleach regeneration and the SAR protocol. It was observed that the except for sample RW-1 and RW-2, all other palaeodoses obtained using the partial bleach technique were underestimated compared to the mean SAR palaeodoses. The paleodose using partial bleach for the sample RW-2 is unusually high that had been attributed to large scatter in the data. Barring few samples as shown in Table 5.2, the partial bleached palaeodose were close to the least 10% palaeodoses obtained using the SAR technique. However, the mean palaeodoses obtained by SAR were overestimated by a factor of ~2. Further compared to the mean palaeodoses the least 10% have shown stratigraphic consistency. Thus suggests that samples were heterogeneously bleached even in a low energy fluvial environment as suggested from a

Table 5.2. Paleodose using partial bleach method, mean paleodose and average of least 10% obtained through SAR in the slack water deposit at Raiwala, Haridwar.

Sample no. (Pit-no.)	Depth From Top (cm)	Paleodose De (Gy)		
		Partial Bleach	Mean	Least 10%
RW-3 (P1)	20	6.5 ± 1.8	9 ± 4	3 ± 1
RW-2 (P1)	95	26 ± 12	6.3 ± 2.6	2.7 ± 0.5
RW-1 (P1)	165	23 ± 7	19 ± 9	8.2 ± 1.6
RW-8 (P2)	0	2.8 ± 0.7	7.4 ± 2.6	3.5 ± 0.8
RW-6 (P2)	42	1.5 ± 0.6	5 ± 1	2.5 ± 0.3
RW-4 (P2)	118	20 ± 7	22 ± 8	11 ± 2
RW-11 (P4)	20	1.4 ± 0.7	6.5 ± 3	2.5 ± 0.4
RW-12 (0 age)	–	0.5 ± 0.8	3.5 ± 1.4	1.5 ± 0.3

wider dose distribution too (Fig. 5.6). In view of this, the stratigraphically consistent palaeodoses obtained using the least 10% were used for the age estimation.

5.3 High energy alluvial fan deposit

5.3.1 Introduction

Fluvial mega fans forms where river exist the topographic front of a mountain and migrate laterally in adjacent basin leading to the deposition of large fan shaped bodies (DeCelles and Cavazza, 1999). Mega fans are large geomorphic features (10^3 - 10^5 km^2, low gradient (0.1^0 – 0.01^0) with distinct lateral gradation in the sediment texture (DeCelles and Cavazza, 1999; Horton and DeCelles, 2001). Sedimentation began with the deposition of coarse boulders and pebbles at the fan apex (proximal end), and the finer sediments are carried towards the distal end farthest from the fan apex (Gabler et al., 1997). Process-wise, it can be suggested that fluvial mega fans are important in the dispersal and deposition of sediments in the tectonically active areas (Leier, et al., 2005).

Based on the global distribution of mega fans, Leier et al., (2005) inferred that these features are confined to 15^0 - 35^0 latitude on northern and southern hemisphere and are absent in tropical climate. This would imply that climate play important role even if the tectonic and geomorphological condition were favorable. Thus, their occurrences in sedimentary record can be used to reconstruct the past climatic condition (Leier, et al., 2005).

In the northwestern Ganga plain, mega alluvial and piedmont fans are distinctive geomorphic features. These large size, low relief sedimentary bodies are identified as Yamuna - Ganga Mega Fan (YG-MF), Sarda Mega Fan, Gandak Mega Fan and Kosi Mega Fan. Lateral extent of these features range from few tens to hundreds of kilometer. In order to create such a large body, it is essential that there should be enough sediment supply and stream power to transport sediment from mountain to the alluvial plain. Leier et al., (2005) examined 202 rivers using satellite imageries, topographic maps and digital elevation model suggested that fluvial mega fan development occurs where rivers discharge is modulated by seasonality. These authors suggest a minimum river discharge of ~20m^3/s for the development of mega fan. In our case, the typical discharge of Ganga

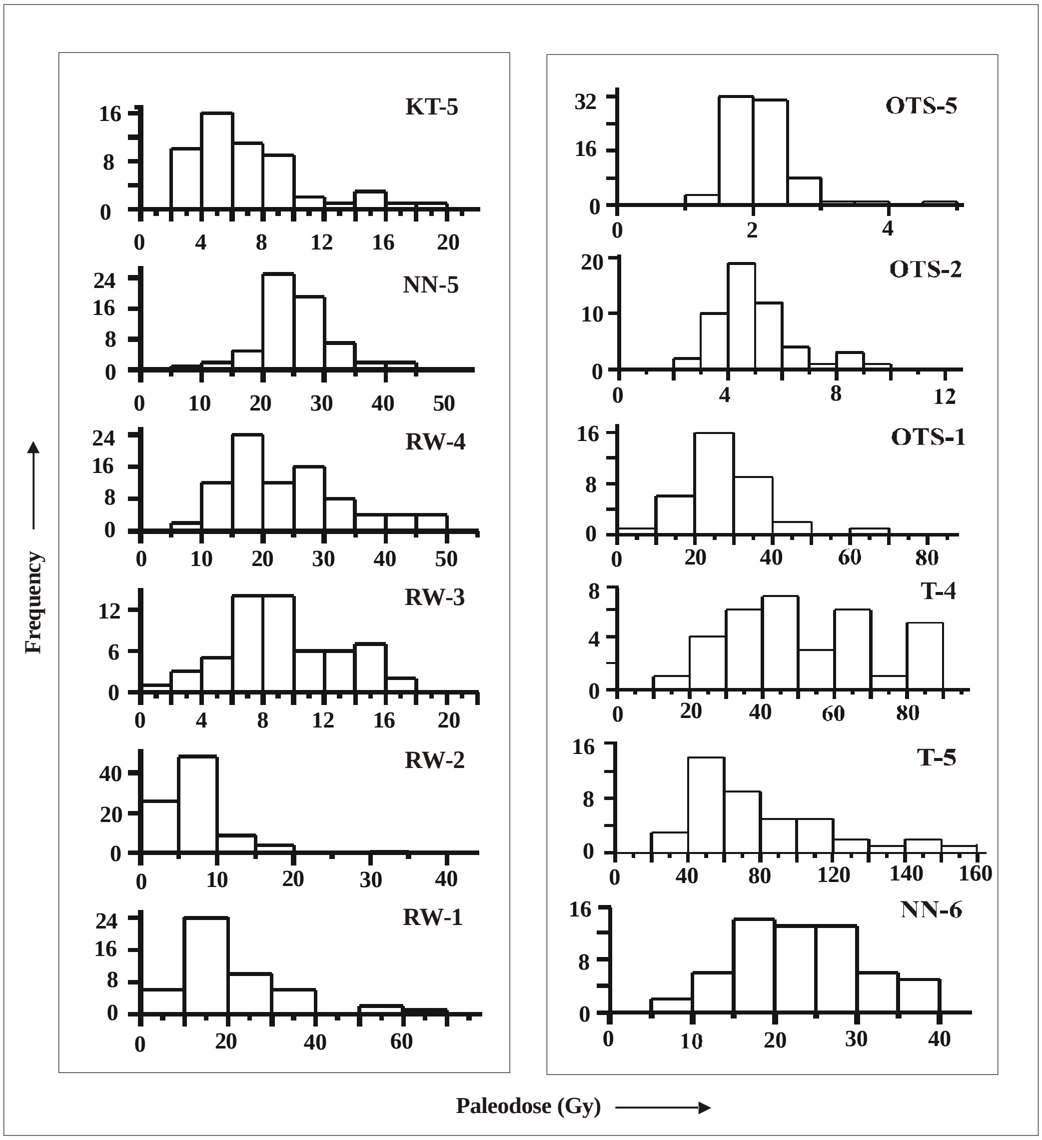

Fig. 5.6. Paleodose distribution of sediment samples from various locations in Himalaya

River is between 20-40 m^3/s during the monsoon (July-October) and for rest of the year it reduces to around less than 5 m^3/s rest of the year (Goodbred Jr., 2003). Thus, the terrain is conducive for the development of mega fans of course e.g. sediment supply, slope and accommodation space are prerequisite.

Usually piedmont alluvial fans are characteristic features of arid landscape, however, such features have been reported from the sub-humid Ganga basin (Shukla et al., 2001). Pediments are broad, gently sloping areas formed by fluvial erosion and usually covered with scattered detritus. Thickness of the detritus increases towards the down slope of the pediment where it is covered with compound alluvial fan deposits (Press and Siever, 1986). In the western Ganga plain, 25 – 30 km wide pediment alluvial fans covers the mega fan surface and occurs adjacent to the Siwalik mountain front (Fig. 5.7). Coalescing of smaller fans (3 – 20 km wide and 10 – 30 km long) has given rise to the piedmont fans and their proximity to the mountain front implies gravelly sediments (Shukla et al., 2001).

Singh (1996) suggested that megafan aggradation in Ganga plain occurred during the time of the initiation of humid climate preceded by an arid phase when huge amount of sediment from the Himalaya were transported into the Ganga plain. During arid periods, reduced vegetation cover facilitates sub aerial exposure of the sediment for weathering. With the initiation of humid condition this weathered material is transported and deposited in areas where the relief changes abruptly. Such areas are located at the mountain fronts. This could have been the case for the development of fans at the foothill of the Himalaya (Shukla et al., 2001). Recently, Goodbred Jr., (2003) has suggested the transitional climatic condition in the Ganga plain favored mega fan aggradation. Considering the above processes, fan sedimentation can be used as a surrogate climatic marker for arid-humid transition. Similalrly, the formation of the younger piedmont alluvial fans has been attributed to reduced sediment supply and subdued tectonic activity in the Himalaya during the latest Pleistocene-Holocene phase (Singh et al., 1997).

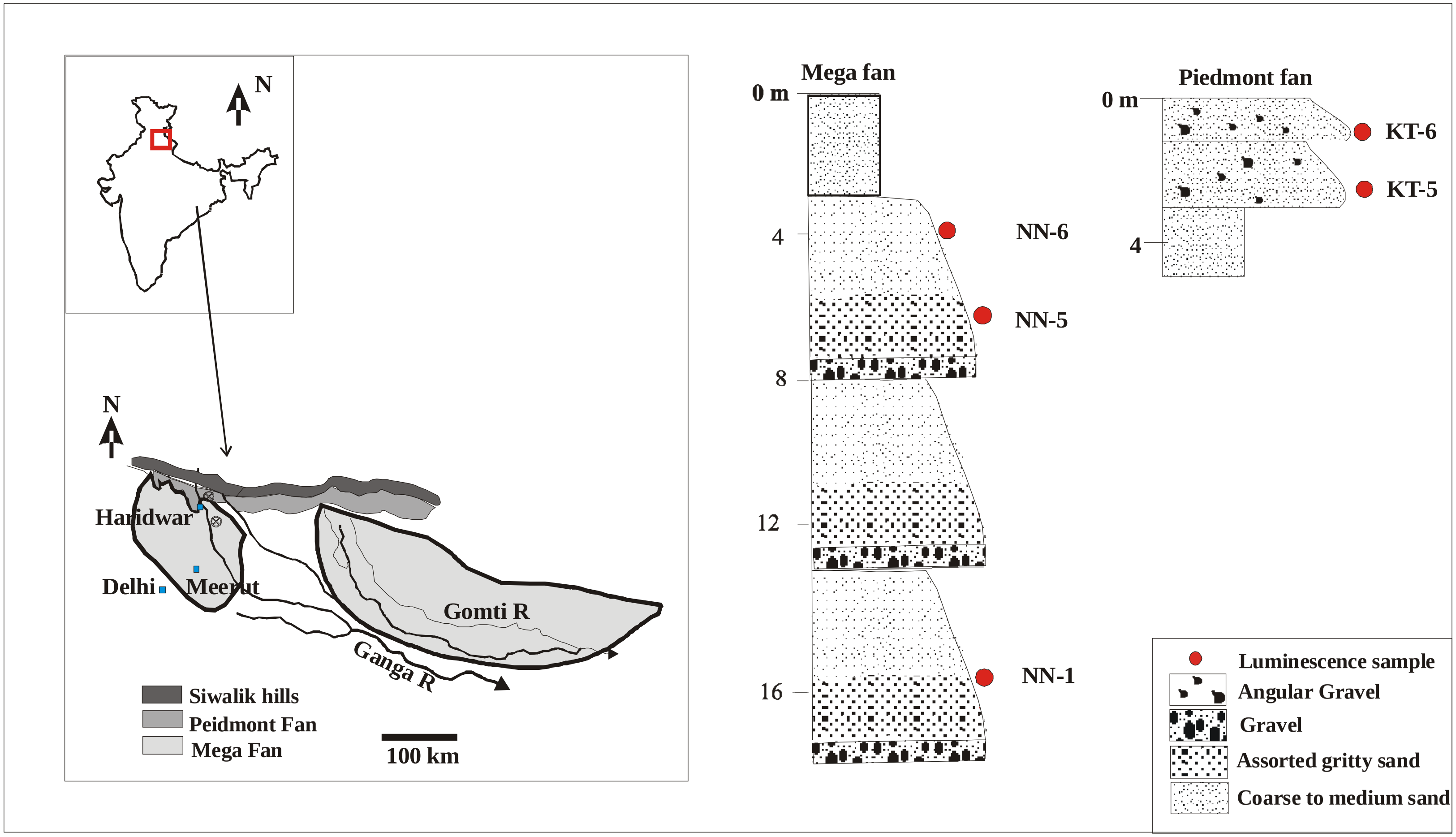

Fig. 5.7. Location and stratigraphy of the samples from Yamuna Ganga mega and piedmont fan. Three fining upward episodes of sedimentation in the mega fan were identified. (After Srivastava et al., 2003)

5.3.2 Study area and climate

The N-S trending, 150 km long and 100 km wide Ganga mega-fan is located in the western Ganga plain (Fig. 5.7). Due to the incision by the Ganga river, 15 – 20 m thick alluvial fan sediments are exposed and can be observed from the northern Siwalik foot hill (Haridwar) to the south of Delhi. Based on their geomorphological occurrences, the mega fan can be divided into two parts (i) the western upland interfluves area (Doab) and (ii) the eastern Ganga- Ramganga upland interfluves (Ruhelkhand bangar;) (Dasgupta, 1975). Innumerable, abandoned channels can be seen in satellite imagery on the fan surface that are truncates at the margins of the Ganga river valley. Present day Ganga river valley that runs N-S is 10-20 km wide and comprises two distinct geomorphic surfaces (i) the active flood plain (T_0) and an elevated river valley terrace (T_1). There is evidence to support that the Ganga River has laterally shifted within its valley in response to tectonics. This is manifested in the development of stepwise tilted T_1 surface (Singh, 1996).

Based on geomorphic and sedimentologic studies, Shukla et al., (2001) have divided the Ganga mega fan into four zones from the northern foothills to the south. These are the gravelly braided streams (Zone-I); sandy braid plain (Zone-II); anastomosing channel plain (Zone-III) and meandering channels with broad interfluves (Zone-IV).

5.3.3 Field stratigraphy and sampling details

Present study dealt with the luminescence characterization and chronology of the mega and pediment alluvial fan that were exposed at Nagal. Details of the sections investigated are given below.

(i) Mega fan sequence – The mega fan sequence studied was located near Nagal town, 30 km, SSE of Haridwar in the district of Uttaranchal (29^{o}54’N, 78^{o}12’E). Incision by the Ganga river has exposed a 18 m thick section on its left bank. According to Srivastava et al., (2003), the lower 15 m of the sequence three episodes of mega fan aggradation can be observed. Each episode began with the deposition of dispersed gravels at the base and terminates with the deposition of fining upward cross-bedded sand (Fig. 5.7). In the upper 3 m a marked change in nature of sedimentation was observed. Sediments in this part are dominantly clayey. The top 3 m is made up of fine muddy sediments, which are devoid of any physical structures. Shukla et al., (2001) on the basis of architectural element argued that the lower cross-bedded units are braided channel deposits and are directly related to fan sedimentation. Whereas, the top muddy unit is a result of sedimentation by sheet flows and gullies occurred after the fan surface was incised and abandoned by the active sedimentation of the major rivers. Therefore the lower 15 m of the sequence only marks the phase of active fan formation and rest 3 m is the result of surface modification of abandoned fan surface.

In order to understand the bleaching characteristic of fan sediments and chronology of mega fan aggradation, five samples collected from the exposed 18 m section (Fig. 5.7).

(ii) Piedmont fan sequence – Near Sabalgarh, piedmont alluvial fan has been incised by the Kotwali river and has exposed 5 m thick sediment succession (Fig. 5.7). Stratigraphy of the section begins with 2 m thick mottled clay at the base. This is overlain by 3 m thick matrix supported angular to sub angular gravel (~20 cm) with sharp erosional contact. Lithoclast analyses of the gravel suggest that they were transported from schistose provenance. The present day lithology of the gravels that are lying on the riverbed has source in the northern Siwalik mountain (Srivastava, et al. 2003). This implies that during the piedmont alluvial fan aggradation, significant amount of lesser Himalayan sediment were transported to the study area. For luminescence study one sample was collected from the mottled clay and two samples from the gravelly horizon (Fig. 5.7).

3.4. Results and discussion

In order to reconstruct the past climatic condition based on alluvial fan stratigraphy, it is important to constrain the events of fan aggradation. Few studies pertaining to the chronology of the alluvial fans in the Ganga plain were attempted by Srivastava et al., (2003). However, the ages were based on the MAAD technique, which could be somewhat overestimated, i.e. process wise for fan sedimentation, MAAD ages would imply average for poorly and well-bleached grains. Thus, there is a possibility that the earlier estimates could be the overestimate of the real age.

In view of this, the present study made an attempt to ascertain the extent of pre-depositional bleaching experienced by the fan sediments before estimating the depositional ages. Towards this, six samples from mega and piedmont alluvial fan were analyzed using MAAD and SAR techniques. MAAD technique was employed on all the eight samples. The results obtained indicate that the MAAD paleodoses are higher (16% - 88%) compared to mean SAR paleodoses (Table 5.3). This indicates that alluvial fan sediments have experienced heterogeneous bleaching during the transport. This was further indicated by the differences in palaeodoses computed using the mean and the least 10% (Table 5.3) of the paleodoses. Based on these results, it can be suggested that alluvial fan sediments suffer from variable bleaching condition during the transportation.

5.4 Incised fluvial terraces

5.4.1 Introduction

Collision of the Indian plate with that of Eurasia around 55 Ma ago led to the initiation of Himalayan orogeny. Continued compress following the collision was manifested sequential evolution of major boundary thrusts from north to south. The first one to form was the Main Central Thrust (MCT) followed by the Main Boundary Thrust (MBT) and the youngest one was the Main Frontal Thrust (MFT). It was suggested that with the evolution of these thrusts, sesimicity also progressed southward. Therefore, conventional modal of seismicity in Himalaya suggests that MFT is the most active domain (Gansser, 1964; Wesnousky et al., 1999; Senthil et al., 2001; Thakur et. al., 2004). However, recent evidences including the present work indicate that this may not be true and the older thrusts probably are still active (Wobus et al., 2005; Mukul, 2000; Mukul et al., 2005). Recent studies have shown presence of out of sequence thrusting in the Himalayan region, antiquity of these structures are still uncertain, but certainly they are younger than the MFT. In order to understand the seismicity in Himalaya, fluvial terrace sequences in North-Eastern Himalaya were investigated for sedimentological and chronometric studies. These sequences are developed in the Tista river basin near

Table 5.3. Paleodoses of the samples collected from mega fan and piedmont fan sections

Serial No.	Sample No.	Paleodose (Gy)		
		MAAD	SAR	
			Least 10%	Mean
1	NN-1	87 ± 5	18 ± 6	38 ± 11
2	NN-5	91 ± 2	15 ± 3	25 ± 6
3	NN-6	–	10 ± 2	25 ± 8
6	KT-5	13 ± 2	2.6 ± 0.3	7 ± 4
7	KT-6	7 ± 1	2.2 ± 0.8	6 ± 3

Kalimpong (27^o 4'N, 88^o 29' E). Several workers (Adams 1980; Burnett and Schumm 1983; Nakata, 1989; Schumm, 1986; Valdiya, 1998) have recognized that morphology of river terraces can be used as a surrogate for active tectonics. During the differential movement along the riverbed, rivers incise to acquire the ambient base level and forms terraces. The terraces are nothing but the ancient riverbeds. In a tectonically active river basin, the presence of a sequence of incised terraces indicates multiplicity of seismic events. Due to the differential movement, such terraces are usually unpaired in nature. Considering that the Global Positioning System (GPS) data that determine rate of convergence is limited to less than a decade, tectonically evolved fluvial landforms can provide supplement information on constant shortening over longer time scale (10^3 to 10^5 years). In view of this, fluvial terraces in the lower Tista valley were investigated for long-term reconstruction of palaeoseismic history of the region. This work was based on a detailed structural framework provided by Mukul (2000).

5.4.2 Geomorphology, tectonic setting and sample location

The study area is bounded by the MBT (north) and South Kalijhora Thrust (SKT) (south). Tista River originates in northern Sikkim (Trans Himalayan) and flows southward towards the foothill. It runs approximately N-S, parallel to the transport direction of the foreland thrusts (Fig. 5.8 and 5.9). The MBT is exposed in the Kalikhola section, south of the Kalijhora town (Acharya, 1994) and manifested by the juxtaposition of Gondwana rocks against the Lower Siwaliks. In the field, MBT appears as folded and crumpled zone. This is attributed to the activity associated with the SKT, 500 m south of the MBT (Mukul, 2000). Due to the activity along the SKT, the lower Siwalik rocks have been thrusted up and lie with a tectonic contact with the middle Siwaliks. Additional surface expression of SKT is seen along the east bank of the Tista River. These are the duplexes consisting of three horses developed on the hanging wall of the middle Siwalik sandstone. Further 1.5 km south of the SKT, Andheri Jhora thrust (AJT) was located. The Main Frontal Thrust (MFT) is located 30 km south of AJT. Five such terraces with distinct vertical offsets have been recognized on the west bank of the Tista River. These terraces developed on the hanging wall of AJT and are exposed on the western bank of the Tista river. The unpaired nature of the terraces (confined to the western bank), differentiated by distinct vertical offsets (20 – 5 m) and presence of duplexes underlying these terraces together indicate their formation due to episodic tectonic activity along the AJT and their associated imbricate faults (Mukul, 2000). Further south of AJT two raised surfaces were located ~1 km and ~21 km from the mountain front. These features are attributed to the presence of blind thrust (Fig. 5.9).

The physical characteristic of the terraces (poor sediment cover and incised Siwalik basement) is suggestive of degradational type strath terraces. This is a likely possibility considering the concentration of thrusts sheets in a narrow zone. In such tectonomorphic situations, the rivers occupied riverbeds for limited time due to episodic tectonic surges. In view of this, chronology of the fluvial terraces would in principle with providing estimate on the rate of incision from T_5 to T_0. Further, an estimation based on the luminescence ages can be utilized for calculating the rate of convergence much beyond the historical record.

However, before estimating the ages of different terraces, it is important to understand the bleaching history of the sediment. In tectonically active and monsoon dominated region like lower Tista valley, heterogeneous bleaching of fluvial sediment is a likely possibility.

5.4.3 Results and discussion

Considering the uncertainty associated with the bleaching of fluvial sediment; all the samples (4 from terraces and 2 from the raised surfaces) were investigated for the extent of predepositional bleaching. Further all the samples were analyzed using the conventional MAAD protocol. It was observed that except two samples, the MAAD paleodose averaging numerous grains (10^6) in 40-50 aliquots was significantly higher compared to the SAR average paleodose that is attributed to the large scatter in data due to heterogeneous bleaching. The dose distribution histograms of SAR palaeodose are shown in figure 5.6. The wide dose distribution of the samples indicates heterogeneous bleaching. In view of this, the least 10% paleodose of SAR was used for final age computation (Table 5.4).

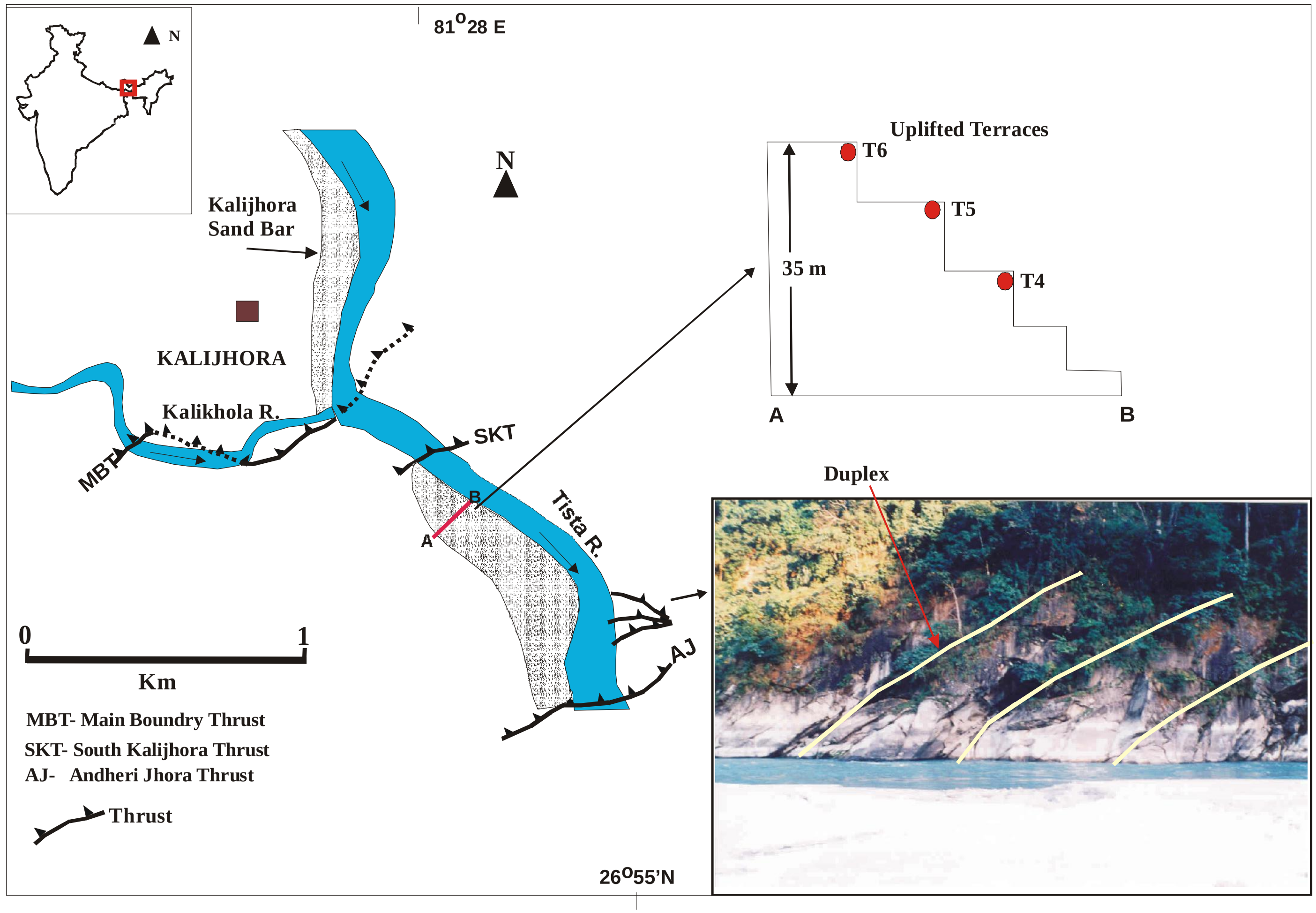

Fig. 5.8 a total of five terraces were identified in the section A-B as shown in the figure in the vicinity of South Kalijhora Thrust. These terraces were formed due to tectonic activity in the duplexes as shown (after Mukul, 2000)

Table 5.4. Paleodoses of terrace sediments obtained through MAAD and SAR analysis

Serial No.	Sample No.	Paleodoses		
		MAAD	SAR	
			Least 10%	Average
1	T-6	184 ± 68	40 ± 2	80 ± 39
2	T-5	180 ± 39	22 ± 2	73 ± 31
3	T-4	68 ± 28	7 ± 0.4	43 ± 23
4	T-0	0.6 ± 1.3	0.2 ± 0.6	2.5 ± 2.2
5	PRLT-3	128 ± 43	77 ± 5	145 ± 48
6	PRLT-5	26 ± 2	28 ± 1	58 ± 24

.

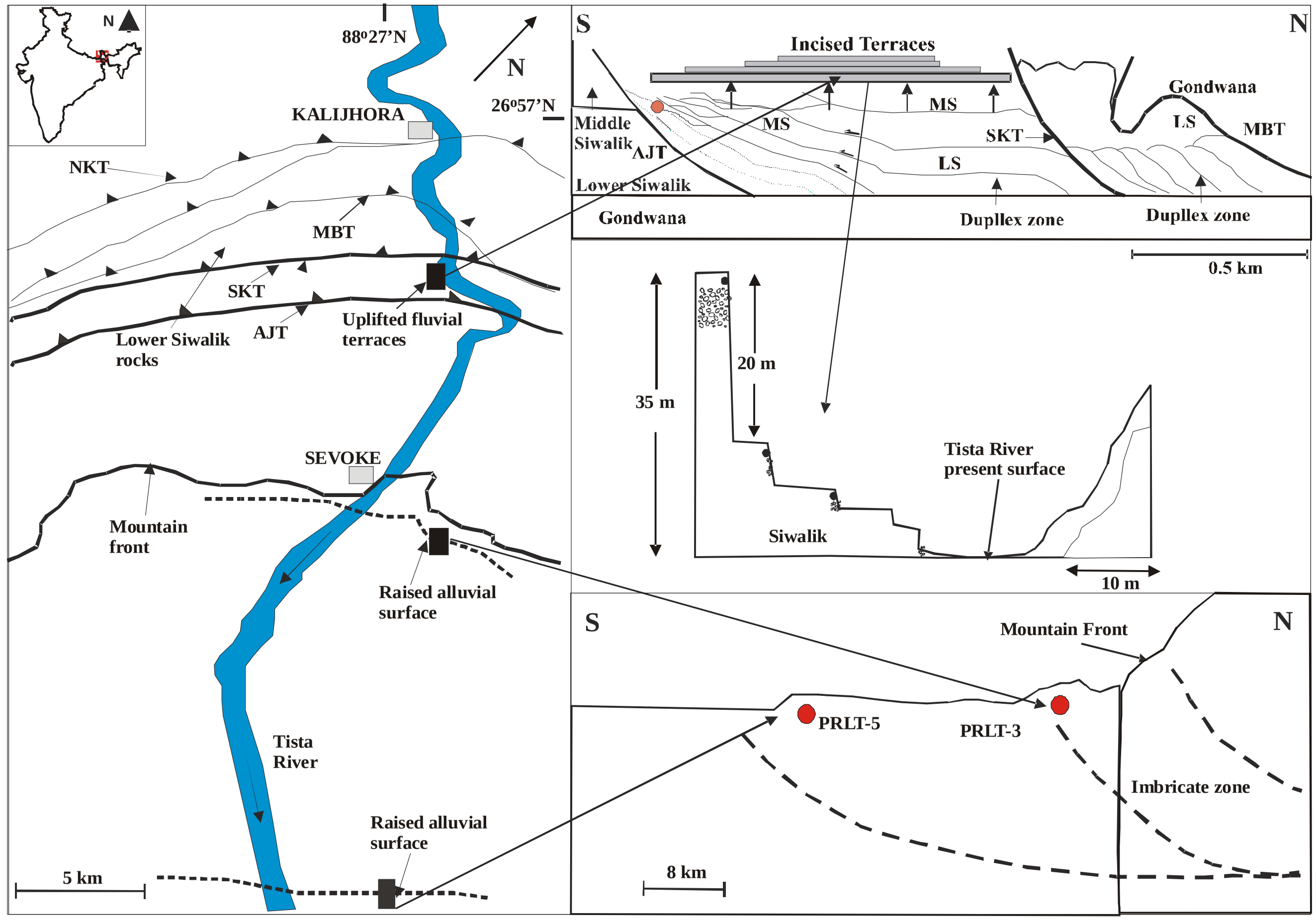

Fig. 5.9. Location and geological setting of the fluvial terraces identified in the vicinity of SKT and MBT. These terraces were formed due to tectonic uplift. Two raised surfaces (PRLT-3 and PRLT-5) were identified in the south of mountain front (After Mukul, 2000) (SKT=South Kalijhora Thrust, NKT=North Kalijhora Thrust, MBT=Main Boundary Thrust, LS=Lower Siwalik, MS=Middle Siwalik, AJT= Anjherijhora Thrust)

References

Acharya, S.K., 1994. The Cenozoic foreland basin and tectonics of the eastern sub-Himalaya: problems and prospects. *Himalayan Geology*, 15, 3–21.

Adams, J., 1980. active tilting of the United States mid-continent; geodetic and geomorphic evidence. *Geology*, 8, 442–446.

Baker, V.R., Kochel, R.C., and Patton, P.C., eds, 1988, *Flood Geomorphology*: New York, John Wiley, 503 pp.

Berger, G.W. and Luternauer, J.J. 1987. Preliminary fieldwork for Thermoluminescence dating Studies at the Fraser river delta, British Columbia. *Geological Survey of Canada Paper* 87, 901–904.

Burnett, A.W. and Schumm, S.A., 1983. Alluvial river response to neo-tectonic deformation in Louisiana and Mississippi. *Science*, 222, 49-50.

Clarke, M.L., 1996. IRSL dating of sands: bleaching characteristics at deposition inferred from the use of single aliquots. *Radiation Measurement*, 26, 611–620.

Dasgupta, S.P., 1975. *The upper Gangetic flood Plain: a regional survey*. National atlas Organization Monograph., Calcutta, 194 pp.

DeCelles, P.G. and Cavezza, W., 1999. A comparison of fluvial mega fan in the Cordilleran (Upper Cretaceous) and modern Himalayan foreland basin systems: *Geological Society of America Bulletin*, 111, 1315–1334.

Gabler, R.E., Sager, R.J. and Wise, D.L., 1997. *Essentials of Physical Geography*, Saunders College Publishing, 587 pp.

Gansser, A., 1964. *The geology of the Himalayas*, Wiley-Inter-science, New York, 289 pp.

Goodbred, S.L.Jr. and Kuehl, S.A., 2000. Enormous Ganges-Brahmaputra sediments discharge during early Holocene monsoon. *Geology*, 28, 1083–1086.

Goodbred, S.L.Jr., 2003. Response of the Ganges dispersal system to climate change: a source-to-sink view since the last interstade. *Sedimentary Geology*, 162, 83–104.

Hasnain, S. I. (1999). *Himalayan Glaciers: Hydrology and Hydrochemistry*. Allied Publishers, New Delhi, 203p.

Horton, B.K. and DeCelles, P.G., 2001. Modern and ancient fluvial mega fans in the foreland basin system of the central Andes, southern Bolovia: Implications for drainage network evolution in fold-thrust belts. *Basin Research*, 13, 43–61.

Ives, J.D. and Messerli, B., 1989. *The Himalayan Dilemma*. Routledge.

Kale,V.S., Singhvi A.K., Mishra P.K. and Banerjee D., 2000. Sedimentary record and luminescence chronology of Late Holocene paleofloods in the Luni river, Thar desert, northwest India. *Catena*, 40, 337–358.

Kale, V.S., Mishra, S., and Baker, V.R., 2003. Sedimentary record of paleofloods in the bedrock gorges of the Tapi and Narmada rivers, central India. *Current Science*, 84, 1072–1079.

Leier, Andrew L., DeCelles, Peter G. and Pellitier Jon D., 2005. Mountains, monsoons and mega fans. *Geology*, 33, 289–292.

Li, S.H. 1994, Optical dating: insufficiently bleached sediments. *Radiation Measurement* 23, 563–567.

Mukul, M., 2000. The Geometry and Kinematics of the Main Boundary Thrust and related Neotectonics in the Darjiling Himalayan Fold-and-thrust belt, West Bengal, India. *Journal of Structural Geology* 22, 1261–1283.

Mukul, M., Jaiswal, M.K. and Singhvi, A.K., 2005. Out-of-Sequence Active Deformation in Lesser Himalaya (submitted).

Murray, A.S., Wintle, A.G., 2000. Luminescence dating of quartz using an improved single aliquot regenerative-dose protocol. *Radiation Measurement*, 32 (1), 57–73.

Nakata, J., 1989. Active faults of the Himalaya of India and Nepal. *Geological Society of America*, special paper 232, 243–264.

Pal, S.K., 1986. *Geomorphology of River terraces along Alaknanada Valley, Garhwal Himalaya.* B.R. Publishing Corporation, Delhi, India, 158 pp.

Press, F. and Siever, R., 1986. *Earth*, W.H. Freeman and company, USA, 656 pp.

Schumm, S.A., 1986. Alluvial river response to active tectonics. *In: Active Tectonics: Studies in Geophysics.* National Academic Press, Washington, DC, 80–94.

Senthil, K., Wesnousky, S.G., Rockwell, T.K., Ragona, D., Thakur, V.C. and Seitz, G.G., 2001. Earthquake recurrence and rupture dynamics of Himalayan Frontal Thrust, India. *Science*, 294, 2328–2331.

Shukla, U.K., Singh, I.B., Sharma, M. and Sharma, S., 2001. A model of alluvial megafan sedimentation: Ganga Megafan. *Sedimentary Geology*, 144, 243–262.

Singh, I.B., 1996. Geological evolution of Ganga plain–an overview. *Journal of Paleotological Society of India*, 41, 99–137.

Singh, I.B., Rajagopalan, G., Agarwal, K.K., Srivastava, P., Sharma, M. and Sharma, S., 1997. Evidence of middle to late Holocene neo-tectonic activity in the Ganga Plain. *Current Science*, 73, 1114–1117.

Srivastava P., Singh I.B., Sharma M., Singhvi A.K., 2003. Luminescence chronometry and late Quaternary geomorphic history of the Ganga plain, India. *Paleogeography, Paleoclimatology, Paleoecology*, 197, 15–41.

Thakur, V.C. and Pandey, A.K., 2004. Active deformation of Himalayan Frontal Thrust and Piedmont Zone south of Dehradun in respect of seismotectonics of Garhwal Himalaya. *Himalayan Geology*, 25, 23–31.

Valdiya, K.S., 1998. *Dynamic Himalaya.* Universities Press, Hyderabad.

Weidinger, T. Johannes, 1998. Case history and hazard analysis of two lake-damming landslides in the Himalayas. *Journal of Asian Earth Sciences*, 16, 323–331.

Wesnousky, S.G., Kumar, S., Mohindra, R. and Thakur, V.C., 1999. Uplift and convergence along the Himalayan Frontal Thrust of India. *Tectonics*, 18, 967–976.

Wobus, C., Heimsath, A., Whipple, K., Hodges, K., 2005. Active out-of-sequence thrust faulting in the central Nepalese Himalaya. *Nature*, 434, 1008–1011.

Chapter 6

Luminescence Chronology of Fluvial Archives: Paleoclimatic and Paleoseismic Implications

6.1 Flash flood and Terrace deposits

Vulnerability of the Himalayan watersheds is attributed to the continued compression caused by the northward movement of Indian plate. This has given rise to rapid upliftment and high incision (Burbank et al., 1996). Aided to this, the region is dominated by southwest monsoon. The central Himalaya has high annual rainfall (1500 mm) and the majority of the precipitation (~80%) occurs during the summer month from the southwest monsoon (Hasnain, 1999). The inherent vulnerability of surface sediments coupled with high rainfall leads to the landslide and debris flow that occasionally create temporary lakes on the river courses. These lakes can last for longtime and eventual breaching of such lakes cause flash floods with catastrophic discharge and sediment load. There are numerous examples of such floods from the Himalayan region. During such unusual events, rivers tend to transport sediments flux that exceeds the annual supply from denudational processes (Cornwell, 1998; Shroder, 1998). In addition to this, flash floods in Himalaya are also reported to have been caused by earthquakes and glacial lake outburst (Monecke et al., 2001). Considering that sizeable number of our population lives on the lower Ganga plain, it is important to ascertain the frequencies of these unusual events in the Himalaya for evolving a mitigation planning. This thesis attempted this by, (i) the identification of paleoflood deposits and (ii) ascertaining their chronology.

In the present study, these aspects were addressed. The age estimate for the known flood event that occurred during 1970 was dated at various places from the origin of the flood to the farthest location at the point of emergence of the Ganga River near Rishikesh. The ages obtained using the least 10% of the paleodoses varied from 0.5 ± 0.1 ka to 7 ± 2 ka (Table 6.1). In view of the short-lived nature of the flash flood, the above ages indicate that sediment bleaching was inadequate to erase the geological luminescence. Considering that 0.5 ± 0.1 ka was obtained from a flood plain deposit located proximal to the origin of flash flood site (at Kaleshwar), it can be suggested that luminescence dating of flood plain sediment can provide reliable ages.

With the above observation, paleoflood history of the Alaknanda River was reconstructed from a flood plain sequence at Srinagar (Fig. 6.1). These deposits are exposed on the left and right flank of the Alaknanda River. Compared to the left flank (Terrace T_1), where four paleoflood deposits of increasing magnitude were identified, the right flank had preserved only one event that is too of lesser magnitude (Fig. 6.1). Using the average of least 10% paleodose, the four paleoflood events on the left flank (from bottom upward) were dated to 6.3 ± 0.8 ka, 2.7 ± 0.7 ka, 0.8 ± 0.1ka and 0.5 ± 0.1 ka. A lone paleoflood event on the right flank was dated to 0.3 ± 0.1 ka. The reliability of luminescence ages is ensured by the fact that they are obtained on, (i) flood plain sediment; (ii) stratigraphically consistent and (iii) the younger age 0.5 ± 0.1 ka is obtained on the flood sediment on which 400 year old Keshav Rai temple was constructed.

In the monsoon dominated Alaknanda basin, the above flood events would in principle imply enhanced southwest monsoon. Paleomonsoon reconstruction based on pollen studies from the adjoining Bhagirathi valley identified three events of enhanced southwest monsoon between 6000 – 4500 cal years BP, 3000 – 1000 cal years BP and 800 cal years BP to present (Phadtare, 2000). These events accords well with the chronology of paleoflood records. The progressive increase in the flood magnitude from 6 ka to 0.5 ka would imply either increasing monsoon strength or gradual increase the magnitude of landslide-induced flash floods in the basin. The present study shows that

Table 6.1. SAR ages based on least 10% of the paleodoses from the samples of 1970's flood and terrace T_1 in Srinagar, Uttaranchal state.

Sample	U (ppm)	Th (ppm)	K (%)	Dose rate (Gy/ka)	Paleodose	SAR age (ka)
KL-1	2.2 ± 0.8	12.3 ± 2.8	1.3 ± 0.1	2.3 ± 0.3	9 ± 1	3.8 ± 0.5
KL-3	2.5 ± 0.7	12.4 ± 2.6	1.2 ± 0.1	2.3 ± 0.3	1 ± 0.3	0.4 ± 0.1
MVW-9	2.5 ± 0.4	7.7 ± 1.3	1.5 ± 0.1	2.2 ± 0.2	9 ± 2	4.2 ± 0.8
MVW-10	4.2 ± 0.6	14.3 ± 2	1.8 ± 0.1	3.2 ± 0.3	0.8 ± 0.2	0.3 ± 0.1
MVW-11	4.4 ± 0.8	12.7 ± 3	1.9 ± 0.1	3.2 ± 0.3	23 ± 4	7 ± 2
MVW-12	4.5 ± 0.9	17.6 ± 3.3	3.1 ± 0.2	4.5 ± 0.4	7 ± 1	1.5 ± 0.2
OTS-1	2.8 ± 0.7	9.7 ± 2.3	1.8 ± 0.1	2.9 ± 0.3	20 ± 1	6.3 ± 0.8
OTS-2	5.5 ± 1.1	11.8 ± 3.8	1.7 ± 0.1	3.6 ± 0.4	3.4 ± 0.5	0.8 ± 0.1
OTS-3	4.4 ± 0.5	24.1 ± 7.2	1.9 ± 0.1	4.4 ± 0.6	18 ± 0.5	2.7 ± 0.7
OTS-4	3.0 ± 0.8	10.2 ± 2.7	1.2 ± 0.1	2.5 ± 0.3	9 ± 3	3.4 ± 1.5
OTS-5	3.4 ± 0.7	14.9 ± 2.4	1.9 ± 0.1	3.5 ± 0.3	1.7 ± 0.1	0.5 ± 0.1
BN-6	6.6 ± 1.1	24.8 ± 3.8	1.6 ± 0.1	4.1 ± 0.4	18 ± 5	4.3 ± 1

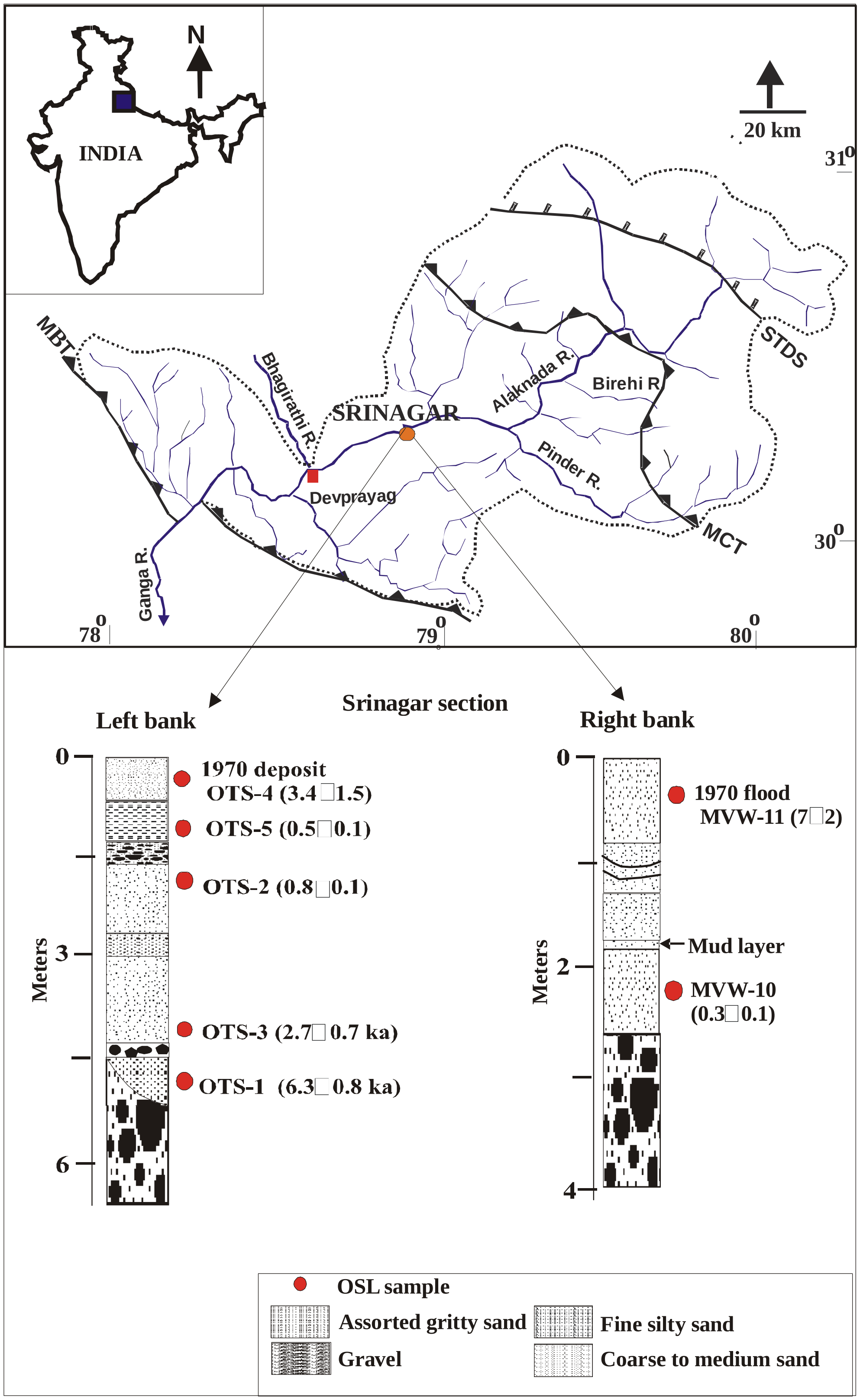

Fig. 6.1. SAR ages obtained from terrace T1 at Srunagar on either bank of the river.

the 1970's flood was of the highest magnitude that was ever recorded in the Alaknanda basin since last 6 ka.

In the last fifty years, increasing deforestation in the upper Alaknanda basin was identified as the cause of the 1970's flash flood (Kimothi and Juyal, 1996). However, considering the tectonically active Himalaya ranges, it has been suggested that deforestation has minimum impact on flash floods (Ives and Messerli, 1989). Due to the paucity of scientific data on paleoflood deposits in the Alaknanda basin, the above debate remained inconclusive. An attempt was made for the first time to reconstruct the geological record of past floods from the Alaknanda basin and ascertain the causes of past floods.

In the present study luminescence dated paleoflood deposits were analyzed for the identification of sediment provenances. This was done using the rare earth tracer ϵ_{Nd} (France-Lenard et al. 2000). The study indicates the paleoflood sediments 6 ka to 0.5 ka (except 0.8 ka) had source in the Higher Himalayan Crystalline (HHC) (Table 6.2) This area lies north of the Main Central Thrusts (MCT), which is a zone of high relief and high physical weathering. Compared to this, during the 1970's flood, majority of the sediment originated from low relief Lesser Himalayan (LH) watersheds (Wasson et al., submitted). This zone is also known as the southern mountain front (Hodges et al., 2004) and had records of deforestation during the recent time. It was observed that the past floods were caused by the natural processes, where as the recent flood was triggered by anthropogenic activity.

6.2 Slack water Deposit

Gangetic plain, a unique geomorphological entity is drained by many large rivers and inhabited by 250 million people. Large and small floods also affect this region during the monsoon. Therefore, an understanding of past floods and their recurrent frequencies is important for better land use and land management strategies. Floods in the Ganga River are associated with the southwest monsoon. The upper catchments of the Ganga River viz. the Alaknanda and Bhagirathi witness high precipitation during June to September (Hasnain, 1999). Though there is limited data on the downstream (Ganga plain), recent studies have demonstrated that majority of the sediment as far as the eastern Ganga plain have source in the higher Himalayan region (Sinha, 2005). Majority of the sediments are transported during the monsoon that are scavenged from the Himalayan watershed by surface runoff and landslides (Wasson, 2003). At times, river courses are blocked temporarily, breaching of such blockades cause flash floods in the lower reaches such as the 1970’s flood (Weidinger, 1998). A recent study suggests that 90% of the total sediment that are transported by the Ganga River originates from the Himalaya (Wasson, 2003).

Evidence of past floods at Raiwala, where 14 vertically stacked flood couplets (slack water deposits) suggests that the upper catchments of the Ganga River in central Himalaya witnessed high magnitude floods in the past. Luminescence chronology using least 10% of paleodoses that are obtained on 8 samples collected from three pits (Pit-1 to Pit-3) suggests that the flood occurred during 2.6 ± 0.6 ka (Fig. 6.2, Table 6.3). This event was observed in both Pit-1 and Pit-2 (Fig. 6.2) and also seen in the Alaknanda basin at Srinagar. Following this a maximum of 6 floods of high magnitude occurred between 2.6 to 1 ka and during 1 ka to 0.8 ka, presence of 8 flood couplets suggests significant increase in flood frequencies. Absence of flood couplet above the 0.8 ka event suggests that flood magnitude since then decreased. Occurrence of 10 couplets during 2.6 to 1 ka suggests the recurrent interval of 260 years for high magnitude flood. However between 1 ka to 0.8 ka, a significant rise in the frequencies of high magnitude flood that comes out to be once in every 25 years. Since floods are associated with high rainfall event, which in our case is the southwest monsoon, thus, it can be suggested that the paleoflood sequence represent fluctuating southwest monsoon during the last 2.6 ka. Evidence based on the peat bog from the central Himalaya indicate a stepwise increase in southwest monsoon after 3000 cal. yrs. BP culminating at 1000 Cal. yrs. BP (Phadtare, 2000). This periods broadly compares well with the event corresponding to 6 flood couplets that were deposited between 2.6 ka and >1 ka. Between 1 ka and 0.8 ka 8 flood events of increasing magnitude suggests frequent flash flood events suggesting stronger monsoonal condition. Speleothem record from Nepal Himalaya (Denniston, et al., 2000) and peat bog data indicate strengthening of southwest monsoon after 1500 year that persisted until >0.8 ka. This period culminated into cold and dry phase around 0.8 ka (Phadtare, 2000) this is

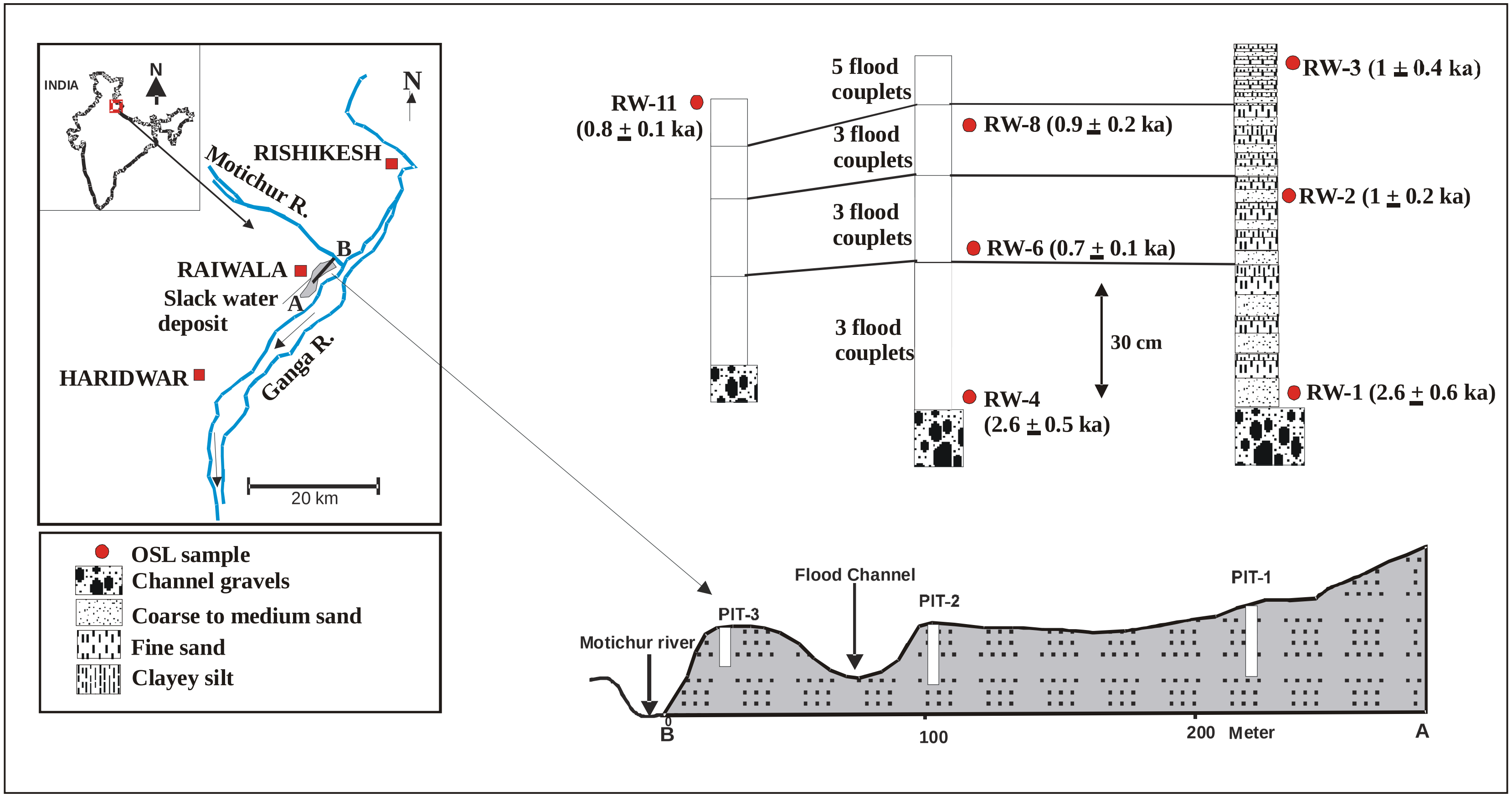

Fig. 6.2. SAR ages from slack water deposit at Raiwala, Haridwar. Ages are suggesting ameliorating monsoon during 2-1 ka, however, the monsoon strength was highest during ~1 ka as suggested by high frequency paleoflood record.

Table 6.2. The sediment contribution from High Crystalline Himalaya (HCH) and Inner Lesser Himalaya (ILH) to the sediment at Srinagar terrace T_1 (after Wasson et al., submitted)

Serial no.	Sample	*HCH%*	*ILH%*
1	OTS-1	78	22
2	OTS-2	52	48
3	OTS-3	86	14
4	OTS-4	45	55
5	OTS-5	86	14
6	Modern	64	36

Table 6.3. SAR ages from slack water deposit at Raiwala

Sample (pit no.)	U (ppm)	Th (ppm)	K (%)	Dose rate (Gy/ka)	Paleodose (SAR)	SAR ages (ky)
RW-1 (1)	3.6 ± 0.7	14.2 ± 2.4	1.9 ± 0.1	3.1 ± 0.3	8.2 ± 1.6	2.6 ± 0.6
RW-2 (1)	5.0 ± 0.8	12.1 ± 2.8	1.3 ± 0.1	2.7 ± 0.3	2.7 ± 0.5	1.0 ± 0.2
RW-3 (1)	3.9 ± 0.9	15.1 ± 3.1	1.7 ± 0.1	3.0 ± 0.3	3 ± 1	1.0 ± 0.4
RW-4 (2)	5.4 ± 0.5	26.1 ± 5.6	2.2 ± 0.1	4.3 ± 0.5	11 ± 2	2.6 ± 0.5
RW-6 (2)	2.2 ± 0.6	19 ± 5.7	2.5 ± 0.2	3.6 ± 0.4	2.5 ± 0.3	0.7 ± 0.1
RW-8 (2)	3.9 ± 1	20.3 ± 7.8	2.4 ± 0.2	3.9 ± 0.6	3.5 ± 0.8	0.9 ± 0.2
RW-11 (3)	4.4 ± 0.8	16.8 ± 2.8	1.7 ± 0.1	3.2 ± 0.3	2.5 ± 0.4	0.8 ± 0.1

manifested in the absence of high magnitude flood after 0.8 ka at Raiwala indicating weakening of the southwest monsoon in the upper catchments of the Ganga River.

6.3. Mega alluvial and Piedmont fan

Srivastava et al., (2003) provided the preliminary luminescence chronology for the mega fan formation. Based on MAAD technique the event of mega fan aggradation was bracketed between 26 - 22 ka. Similarly, the ages on piedmont fan ranged from 8 – 3 ka. Considering the poorly bleached nature of fan sediments, MAAD ages are likely to be overestimate of the real age. In the present study SAR technique was employed for age estimation. Clarke (1996) and Jain et al., (2004) have demonstrated that for older samples, mean paleodose can be considered for age estimation. Because in such samples the unbleached luminescence is insignificant compared to the acquired luminescence during the burial. This is further supported by the low relative standard deviation (20 – 30%) and normal distribution of paleodoses (Fig. 5.6, chapter 5). However, in case of the younger piedmont fan sediments, least 10% paleodose was used for age estimation.

In the field, three events of mega fan aggradation were identified. Due to inaccessibility three samples were dated one from lower episode-I and two from the upper episodes-III. One sample was dated from the upper 3 m sheet deposit (NN-8) (Fig. 6.3). Due to lack of coarse quartz fraction in sample NN-8, MAAD fine grain technique was used. The lower most fan aggradation (episode-I) was dated to 14 ± 3 ka (NN-1, Table 6.4). Initiation of the upper most phase of fan aggradation began at 9 ± 1 ka and terminated at 8 ± 1 ka (Fig. 6.3). The overlying sheet flood deposit occurred after the deposition of the upper most fan sequence was dated to 8 ± 2 ka (Srivastava, 2003). Considering the uncertainty associated with this age, it can be argued that event of surface modification began around <9 ka. In piedmont fan two events were identified in the field stratigraphy. Chronology of these events was ascertained using the least 10% of the paleodoses. Thus ages obtained are 2 ± 0.2 ka for the older episode and 1 ± 0.2 ka for the younger episode (Fig. 6.3).

Table 6.4. SAR ages of the mega and piedmont fan samples (Least 10% for sample KT-5 and KT-6 and mean paleodose were taken for samples NN-1, NN-5 and NN-6 respectively.

Sample	U (ppm)	Th (ppm)	K (%)	Dose rate (Gy/ka)	Paleodose (SAR)	SAR ages (ka)
NN-1	2.5 ± 0.8	10.6 ± 3	1.7 ± 0.1	4.6 ± 0.7	38 ± 11	14 ± 3
NN-5	3.6 ± 0.9	8.2 ± 3	1.7 ± 0.1	2.9 ± 0.3	25 ± 6	9 ± 2
NN-6	2.8 ± 1.1	14.8 ± 4	1.9 ± 0.1	3.3 ± 0.4	25 ± 8	8 ± 2
KT-5	1.8 ± 0.5	5.3 ± 2	0.8 ± 0.1	1.5 ± 0.2	2.6 ± 0.3	2 ± 0.3
KT-6	2.6 ± 0.9	9.6 ± 3	1.0 ± 0.1	2.2 ± 0.3	2.2 ± 0.8	1 ± 0.2

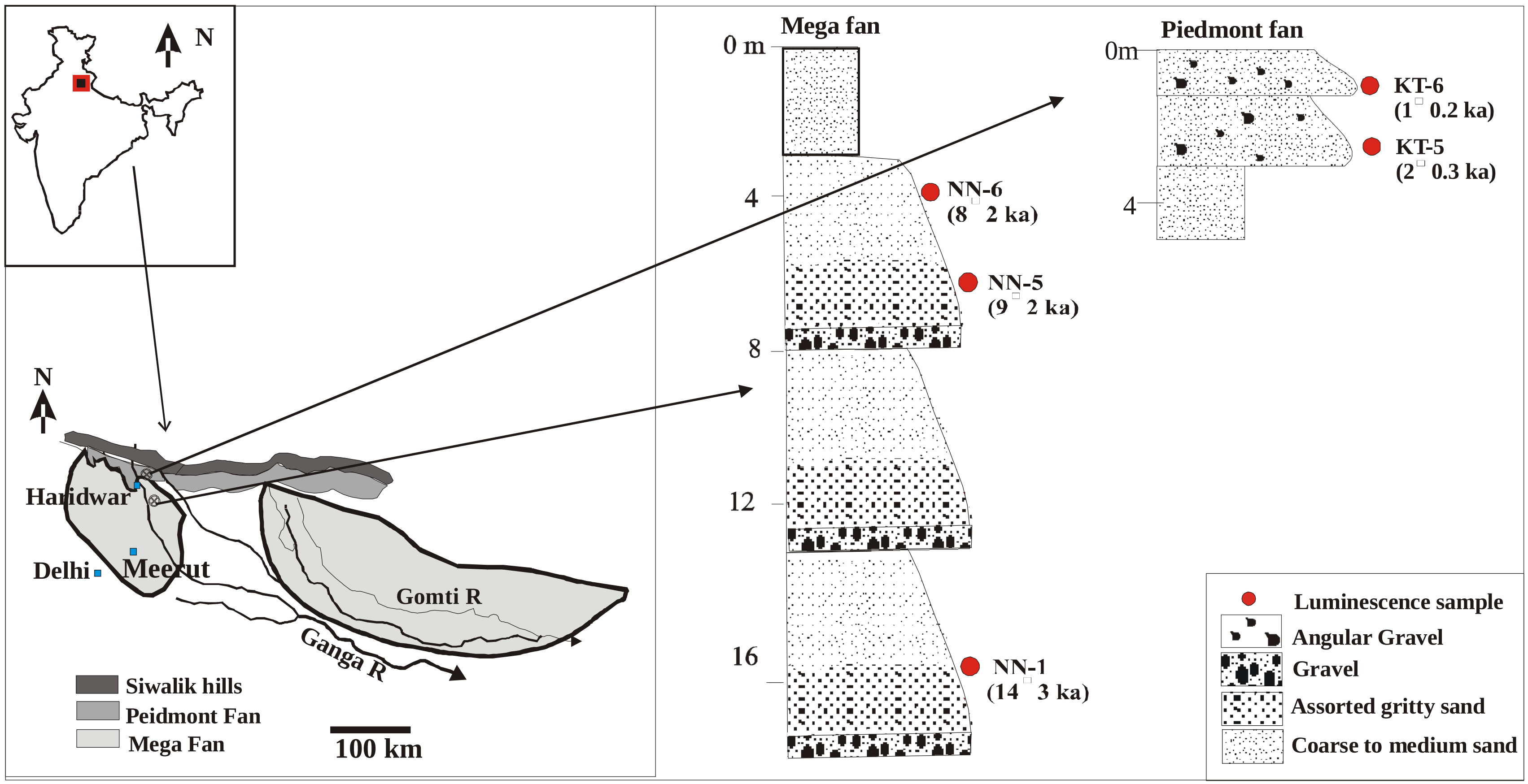

Fig. 6.3. SAR ages obtained for Yamuna Ganga mega and piedmont fan. The ages suggest that the mega fan sedimentation started ~14 ka and terminated ~8 ka. Piedmont fan formed in a short period of time ~2-1 ka. (After Srivastava et al., 2003)

It has been suggested that mega fan aggradation in Ganga plain occurred during the time of the initiation of humid climate that was preceded by a long arid phase when huge amount of sediment from the Himalaya were transported into the Ganga plain (Singh, 1996). Chronology of the mega fan aggradations suggests that the older episodes (I and II) occurred after 14 ka and before 9 ka (Fig. 6.4). The older episode-I corresponds to the reestablishment of southwest monsoon (Sirocko et al., 1993; Overpeck et al., 1996) whereas, the episode-II was deposited after the Younger Drayas cooling event dated to 10.5 ka BP in the Ganga plain (Sharma et al., 2004). Evidence similar to this was obtained from the central Himalayan loess sequences suggesting three phases of loess accretion followed by a period of landscape stability between 16 - 12 ka, 9 – 7 ka and < 1 ka (Pant et al., 2005). The topmost sheet-wash sediments were deposited after 8 ka. Following this incision of the mega fan sediment was initiated in the study area. Observation similar to this was made by Godbred Jr., (2003), who has attributed this period to the hypsithermal event of intense humid climate. Climatically this period corresponds to regionally extensive humid phase that was observed in the central Himalaya (Phadtare, 2000; Sharama et al., 2004; Pant et al., 2005), Central India (William and Clark, 1984), Thar desert (Enzel et al., 1999; Deotare et al., 2004).

Chronology of the younger piedmont fan dated between 2 ka and 1 ka suggests that piedmont fan aggradation post dates the mid-Holocene aridity in the Ganga plain that was dated between 5000 – 2000 (^{14}C) years BP and then followed by ameliorating monsoon (Sharma et al., 2004). The event of piedmont fan aggradation suggests improved moisture regime associated with the improved southwest monsoon. Evidence for improved southwest monsoon is also suggested by the development of paleosol in the central Himalaya (Pant et al., 2005). From the western coast, improved southwest monsoon condition began after 2200 yr BP that continued till today (Caratini, 1994). In the present study it was observed that frequencies and magnitude of floods in the upper Ganga catchments began to increase after 2.7 ka. Thus it can be suggested that piedmont fans aggradation indicate reestablishment of the southwest monsoon after the mid Holocene aridity.

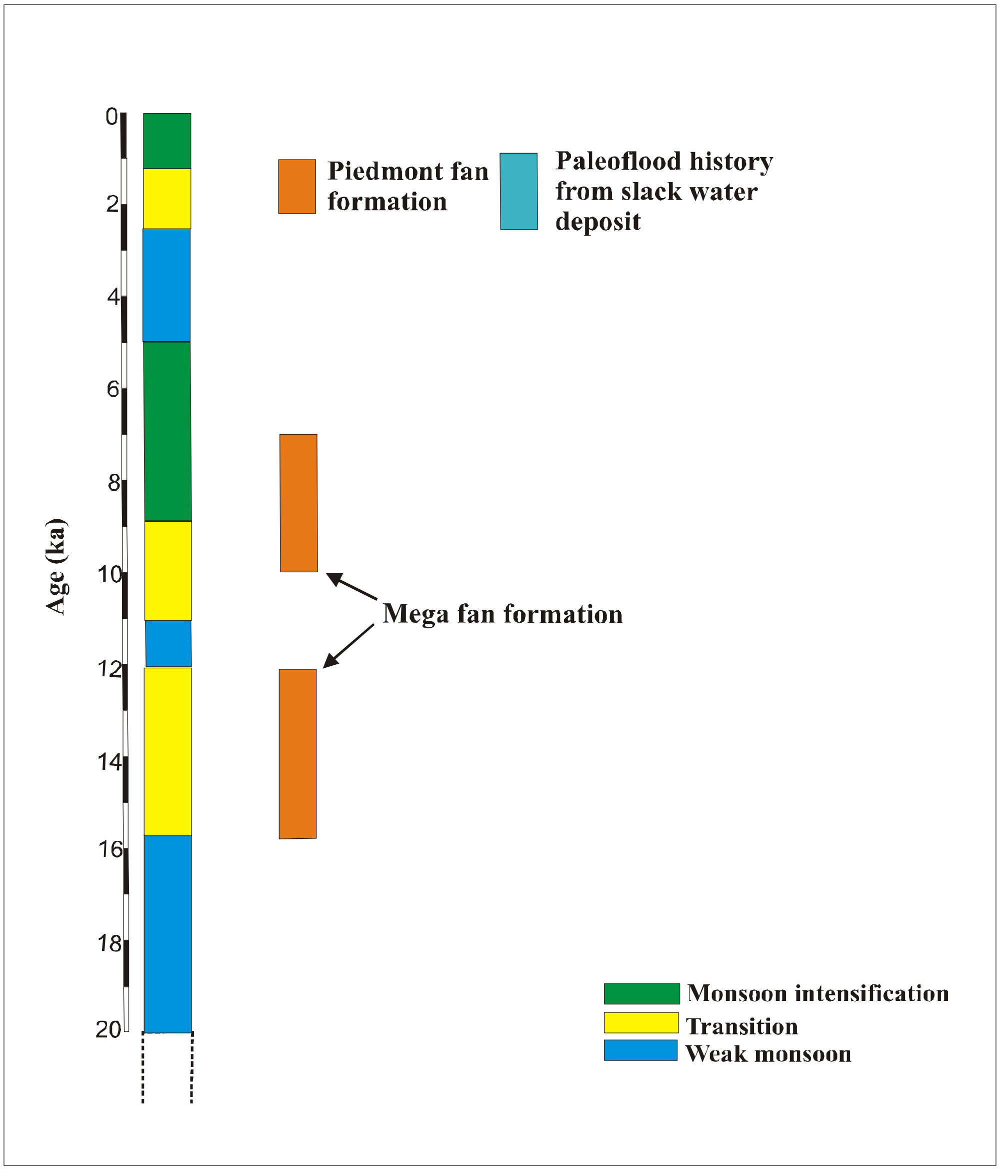

Fig.6.4. Chronology of Yamuna Ganga mega and piedmont fan and their correlation with paleoclimate record from Himalaya. The processess of fan formation accords well with paleocliamte record and also supported by paleoflood record at Raiwala, Haridwar studied in the present work (Phadtare, 2000; Srivastava et al., 2003 and Pant et al., 2005)

6.4 Fault gauge and incised terraces

The surface-breaking faults exhibit brittle deformation fabric. This allows Thermoluminescence (TL) dating of fault gouge (Singhvi et al., 1994) excavated from exposed fault zones in the terrace area. TL dating provides the most recent cataclysmic motion on the faults and assumes that the P-T conditions during faulting reduced the geologically acquired TL to zero or near zero value. TL dates fault gouges from the bounding faults viz. the northern South Kalijhora Thrust (SKT) and the southern Mountain Frontal Thrust (MFT). The fault gauge ages obtained on SKT was 42 ± 10 ka and on the MFT 45 ± 7 ka (Table 6.5). These ages are in conformity with the earlier study carried out in the lesser Central Himalaya (Banerjee et al., 1997) indicating that lesser Himalaya experienced a regional phase of tectonic activity around 40 ka. In addition to this one more sample that was dated from one of the imbricate faults (duplexes) located 0.5 km south of SKT gave TL age of 20 ± 6 ka (Table 6.5). Since the above ages are obtained on the fault gouge that was formed on the host rocks of greater than 2 Ma age (Middle Siwaliks) suggest that the basic premises of zeroing are adequately met for fault gouge samples.

Ages of the incised terraces were obtained using the least 10% paleodoses. The ages obtained are 7.7 ± 1 ka (T_5), 4.4 ± 1 ka (T_4), 1.4 ± 0.3 ka (T_3) and 50 ± 50 a (T_0) (Fig. 6.5). The youngest T_0 sample was collected from the present day Tista River, which has given age of modern sand suggesting that the incised terrace sediments were adequately bleached prior to the deposition. In addition to this, two samples that were collected from 1 km and 20 km south of the mountain (PRLT-3 and PRLT-5) were dated to 14.5 ± 2.4 ka and 6.0 ± 0.6 ka respectively (Fig. 6.5).

Five fluvial terraces of the Tista River are cut into the Siwalik rocks and overlying alluvium (Mukul, 2000). The upper most meter of the alluvium was sampled to date the latest aggradation after which the incision took place and in the process formed a terrace (Fig. 6.5). Terrace (T_5) (~40 m above the present water level) is dated to 7.7 ± 1 ka

Table 6.5. Age table of samples from Tista valley

Sample	U (ppm)	Th (ppm)	K (%)	Dose Rate (Gy/ka)	Paleodose (Gy)	Age (ka)
Raised Terraces						
T-5	5.3 ± 1.3	19.2 ± 8.4	2.9 ± 0.2	5.1 ± 0.7	40 ± 2	7.7 ± 1.1
T-4	6.4 ± 1.3	18.2 ± 8.9	2.7 ± 0.1	5 ± 0.7	22 ± 2	4.4 ± 0.8
T-3	7.0 ± 1.2	19.2 ± 11.4	2.1 ± 0.1	4.8 ± 0.9	7 ± 0.4	1.4 ± 0.3
T-0	3.6 ± 0.8	16.9 ± 6.4	2.2 ± 0.1	3.8 ± 0.5	0.2 ± 0.6	0.05 ± 0.05
PRLT-3	6.8 ± 0.8	20.2 ± 10.3	2.8 ± 0.2	5.3 ± 0.8	77 ± 5	14.5 ± 2.4
PRLT-5	4.7 ± 0.9	7.2 ± 3.1	3.4 ± 0.2	4.6 ± 0.4	28 ± 1	6 ± 0.6
Fault Zones						
SKT-1	5.3 ± 1.2	44.7 ± 19.5	4.2 ± 0.2	13.7 ± 2.4	578 ± 88	42 ± 10
PRLT-1	4.8 ± 1.2	10.9 ± 4.0	3.0 ± 0.2	7.4 ± 1.3	150 ± 38	20 ± 6
PRLT-4	2.9 ± 1.1	14.5 ± 3.6	2.6 ± 0.1	6.5 ± 0.7	293 ± 29	45 ± 7

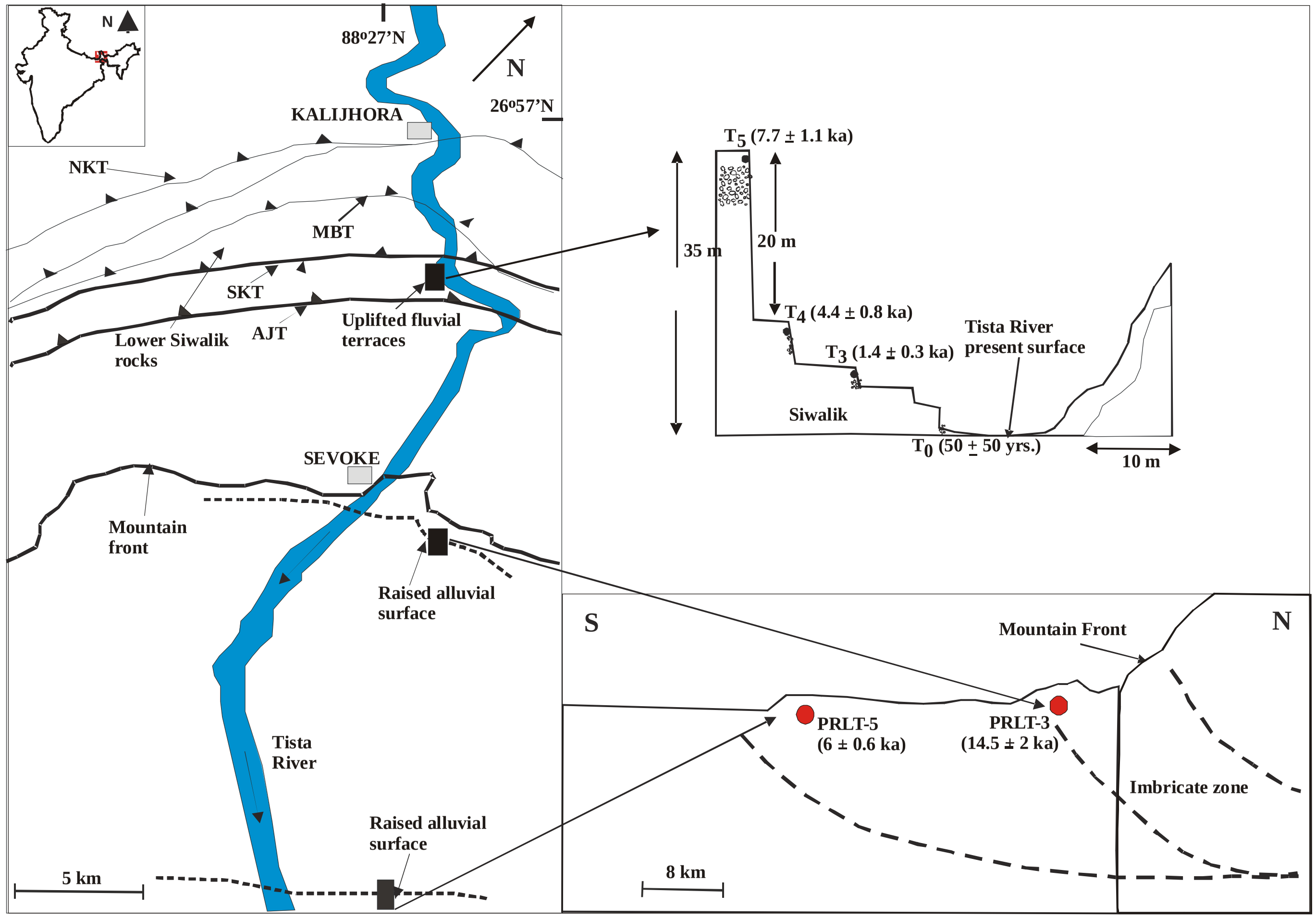

Fig. 6.5. SAR ages of fluvial terraces in Tista valley in the vicinity of MBT. Two raised surfaces (PRLT-3 and PRLT-5) were identified (SKT=South Kalijhora Thrust, NKT=North Kalijhora Thrust, MBT=Main Boundary Thrust, LS=Lower Siwalik, MS=Middle Siwalik, AJT= Anjherijhora Thrust)(After Mukul, 2000)

(Table 6.5). The lower two terraces T_4 and T_3 at ~25 m and ~13 m above the present water level were dated to 4.4 ± 0.8 ka and 1.4 ± 0.3 ka respectively (Table 6.5). The age (50 ± 50 a) of modern samples (T_0) implies that terraces T_2 and T_1, formed in the period between 1.4 ka – 0.3 ka. Given that the area is free from any human interference, and that T_2 and T_1 are practically unvegetated it is suggested that T_2 and T_1 were formed relatively recently. Further, T_3 was vegetated only by bushes whereas T_4, and T_5 were thickly vegetated by bushes and trees (Mukul, 2000). The spatial association of these terraces with the surface breaking imbricates allowed the estimation of the approximate lower (1.4 ± 0.3 ka) and upper (20 ± 6.2 ka) bounds of the age of the active deformation events.

The ages on T_0, T_4, and T_5 (Table 6.5) exhibit an inverted depth-age sequence typical of such fluvial terraces and the sequence $T_1<T_2<T_3$ (1.4 ± 0.3 ka) implies that the out-of-sequence structure has been active from 1.4 ± 0.3 ka till the present. These dates imply local incision rates of 3-10 mm yr^{-1} in the Lesser-Outer Himalaya and are comparable to the incision rates of ~5-10 mm yr^{-1} in the Higher Himalayas (Lave and Avouac, 2001) with higher relief.

Further evidence of blind thrusting south of the exposed mountain front is provided by the presence of fault scarps. Sediments from a scarp about a km south of the exposed mountain front gave an OSL date of 14 ka (PRLT-3; Table 6.5) and about 20 km south of this, sediments from another scarp was dated at 6 ka (PRLT-5; Table 6.5). The combined evidence above indicates that the deformation in the region stalled at the mountain front around 40 ka, and the active deformation front subsequently moved north of the mountain front to the footwall of the MBT around 20 ka. Subsequent deformation and topography building near the MBT then caused additional blind imbricates faults to develop south of the mountain front at 14 ka and 6 ka. The two active fronts may have, therefore, evolved in a coupled manner; with the building of a critical taper in the footwall (Dahlen, 1990) of the MBT driving blind imbrications south of the mountain front at around 14 ka and 6 ka (Mukul, 2005).

References

Banerjee, D., Singhvi, A. K., Bagati, T. N., Mohindra, R., 1997. Luminescence chronology of seismites at Sumdo (Spiti valley) near Kaurik-Chango Fault, Northwestern Himalaya. *Current Science*, 73**,** 276–281.

Burbank, D.W., Leland, J., Fieding, E., Anderson, R.S., Brozoric, N., Reid, M.R. and Duncan, C., 1996. Bedrock incision, rock uplift and threshold hillslopes in Northwest Himalayas. *Nature*, 379, 505–510.

Caratini, C., Bentaleb, I., Fontugne, M., Morzadec-Kerfourn, M.T., Pascal, J.P. and Tissot, C., 1994. A less humid climate since ca. 3500 years B.P. from marine cores off Karwar, western India. *Palaeogeography, Palaeoclimatology, Palaeoecology,* 109, 371–384.

Clarke, M.L., 1996. IRSL dating of sands: bleaching characteristics at deposition inferred from the use of single aliquots. *Radiation Measurement*, 26, 611–620.

Cornwell, K., 1998. Quaternary break-out flood sediments in Peshawar basin of northern Pakistan. *Geomorphology,* 25, 225–248.

Dahlen, F. A., 1990. Critical taper model of fold-and-thrust belts and accretionary wedges. *Annual Review of Earth and Planet Science*, 18**,** 55–90.

Denniston, R.F., Gonzalez, L.A., Asmerom, Y., Sharma, R.H. and Reagen, M.K., 2000. Speleothem evidence for changes in Indian summer monsoon precipitation over the last ~2300 years. *Quaternary Research*, 53, 196–202.

Deotare, B.C., Kajale, M.D., Rajaguru, S.N., Kusumgar, S., Jull, A.J.T and Donahue, J.D., 2004. Paleoenvironmental history of Bap-Malar and Kanod playas of western Rajasthan, Thar Desert. *Proceedings of the Indian Academy of Sciences (Earth and Planetary Sciences),* special issue on Quaternary history and paleoenvironmental record of the Thar Desert in India, 113, 403–425.

Enzel, Y., Ely, L.L., Mishra, S., Ramesh, R., Amit, R., Lazar, B., Rajaguru, S.N., Baker, V.R. and Sandler, A., 1999. *Science*, 284, 125–128.

France-Lanord, C., Derry, L. and Michard, A., 2000. Evolution of the Himalaya since Miocene Time: Isotopic and sedimentological evidence from the Bengal Fan. Treloar, P.J. and Searle, M.P. (eds) *Himalayan Tectonics.* Geological Society Special Publication, 74, 603–621.

Goodbred, J., 2003. Response of the Ganges dispersal system to climate change: a source-to-sink view since the last interstade. *Sedimentary Geology*, 162, 83–104.

Hasnain, S. I. (1999). *Himalayan Glaciers: Hydrology and Hydrochemistry*. Allied Publishers, New Delhi, 203pp.

Hodges, K.V., Cameron, W., Ruhl, K., Schildgen, T. and Whipple, K., 2004. Quaternary deformation, river steepening and heavy precipitation at the front of the higher Himalayan ranges. *Earth and Planetary Sciences Letters*, 7012, 1–11.

Ives, J.D. and Messerli, B., 1989. *The Himalayan Dilemma*. Routledge.

Jain, M, Murray, A.S., Lars, Botter-Jensen, 2004. Optically Stimulated Luminescence Dating: How significant is incomplete light exposure in fluvial environments? *Quaternaire*, 15, (1-2), 143–157.

Kimothi, M.M. and Juyal, N., 1996. Environmental impact assessment of a few selected watersheds of the central Himalaya using remotely sensed data. *International Journal of Remote Sensing*, 17, 1391–1405.

Lave, J. & Avouac, J. P., 2001. Fluvial incision and tectonic uplift across the Himalayas of Central Nepal. *Journal of Geophysical Research*, 106, 26561–26592.

Monecke, K., Winsemann, J. and Hanisch, J., 2001. Climatic response of quaternary alluvial deposits in the upper Kali Gandaki valley, west Nepal. *Global and Planetary Change*, 28, 293–302.

Mukul, M., 2000. The Geometry and Kinematics of the Main Boundary Thrust and related Neotectonics in the Darjiling Himalayan Fold-and-thrust belt, West Bengal, India. *Journal of Structural Geology*, 22, 1261–1283.

Mukul, M., Jaiswal, M.K. and Singhvi, A.K., 2005. Out-of-Sequence Active Deformation in Lesser Himalaya (submitted).

Overpeck, J., Anderson, D., Trumbore, S. and Prell, W., 1996. The southwest Indian monsoon over the last 18,000 years. *Climate Dynamics*, 12, 213–225.

Pant, R.K., Basavaiah, N., Juyal, N., Saini, N.K., Yadava, M.G., Appel, E. and Singhvi, A.K., 2005. A 20 ka climate record from Central Himalayan loess deposits. *Journal of Quaternary Science*, 20, 485–492.

Phadtare, R. N. 2000, Sharp Decrease in summer monsoon strength 4000-3500 cal yr B.P. in the central higher himalaya of India based on pollen evidence from alpine peat. *Quaternary Research*, 53, 122–129.

Sharma, S., Joachimiski, M., Sharma, M., Tobschall, H.J., Singh, I.B., Sharma, C., Chauhan, M.S. and Morgenroth, G., 2004. *Quaternary Science Reviews*, 23, 145–159.

Shroder, J.F., 1998. Slope failure and denudation in the Western Himalaya. *Geomorphology*, 26, 81–105.

Singh, I.B., 1996. Geological evolution of Ganga plain–an overview. *Journal of Paleotological Society of India*, 41, 99–137.

Singhvi, A. K., Banerjee, D., Pande, K., Gogte, V. and Valdiya, K.S., 1994. Luminescence studies on Neotectonic Events in South-Central Kumaun Himalaya-A feasibility study. *Quaternary Science Reviews* 13**,** 595-600.

Sinha, R., 2005. Why do Gangetic rivers aggrade or degrade? *Current Science*, 89, 836–840.

Sirocko, F., Sarnthein, M., and Erlenkeuser, H., 1993. Century-scale events in monsoonal climate over the past 24,000 years. *Nature*, 364, 322–324.

Srivastava P., Singh I.B., Sharma M., Singhvi A.K., 2003. Luminescence chronometry and late Quaternary geomorphic history of the Ganga plain, India. *Paleogeography, Paleoclimatology, Paleoecology*, 197, 15–41.

Wasson, R.J., Jain, V., Jaiswal, M., Juyal, N., McCulloch, M., Sarin, M.M., Singhvi, A.K. and Srivastava, P., (submitted). The mountain lowland debate: forests and sediment transport in the upper Ganges catchment.

Wasson, R.J., 2003. A sediment budget for the Ganga-Brahmaputra catchments. *Current Science*, 84, 1041–1047.

Weidinger, T. Johannes, 1998. Case history and hazard analysis of two lake-damming landslides in the Himalayas. *Journal of Asian Earth Sciences*, 16, 323–331.

William and Clarke, 1984. Late quaternary environments in north-central India. *Nature*, 308, 633–635.

Chapter 7

Conclusions and Future Outlook

7.1. Conclusions and Future Outlook

The objective of the present work was to improve the existing Single Aliquot Regeneration (SAR) protocol, ascertain the bleaching history of the fluvial sediments and develop criteria for the identification of well-bleached aliquots. Finally the ages thus obtained were used to reconstruct the palaeoclimatic and palaeoseismic history of the studied area.

In the SAR protocol, change in sensitivity is monitored by a fixed text dose that follows after the natural OSL measurement and there is no provision to ascertain and monitor the sensitivity change prior to natural OSL measurement. There is a possibility of change in natural sensitivity due to preheat and OSL measurement. Hence an appropriate correction needs to be done for obtaining reliable chronology. This correction is called the natural correction factor (ncf). The present study has shown that ncf can vary between 20 – 30% and in few cases can be as high as 50%. If the samples are not corrected for natural sensitivity changes, it may lead to higher age estimate (~7 – 38%). Based on the above study a modified SAR protocol was developed called as Natural Sensitivity Corrected- Single Aliquot Regeneration (NSC-SAR) protocol. This was successfully applied in all the samples that were investigated in the present study. However, the study done so far is limited to linear and polynomial nature of the growth curves. This needs to be employed on samples that show exponential and exponential + linear nature of growth.

In conventional SAR protocol, enormous TL/OSL reader time is consumed. On an average a sample of ~10 ka would require 4 – 5 days of machine time due to multiple cycles of irradiation, preheat and OSL measurements. It reduces the data throughput in case of partially bleached fluvial sediment in which a large number of aliquots are required for statistical analysis of the distribution of paleodoses. The application of SGC provides an opportunity to produce large number of paleodoses in a short time. The SGC analysis can be applied to any set of sample, where the regression coefficient of a SGC based on 20 aliquots is >90%. Application to samples with lower regression coefficients is likely to be less accurate if one wishes to apply this on very young fluvial sediments where minimum paleodose is considered for age estimation. Most importantly, it was demonstrated that SGC works very well for samples that had minimum lithological variability (single provenance). Considering this, SGC has limited applicability for the Himalayan sediments that originate from complex lithologies.

In high-energy fluvial system, sediments suffer from inadequate bleaching during the flash flood events. A systematic sampling of 1970’s flood sediment along the downstream of the Alaknanda river (source to the ~250 km downstream) yielded ages ranging from 0.4 ± 0.04 ka to 4.3 ± 1 ka. Based on the bleaching study, it was observed that during flash flood events, the distance of sediment transport has limited influence on the extent of pre-depositional bleaching. Instead, it is the nature of transport (suspension load) and depositional environment (flood plain) that is important for erasing the geological luminescence to a residual level.

The paleoflood history has been reconstructed from the Alaknanda basin at Srinagar where five floods of increasing magnitude were recorded since last 6 ka. The 1970’s flood was highest in magnitude. Further it was observed that except for 0.8 ka and 1970, all paleofloods were originated in the higher Himalayan crystalline.

Slack water deposit at Raiwala have provided the record of past flood events in the upper catchment of the Ganga river. A total of 14 floods of increasing magnitude were identified since last 2.6 ka. The results shows that a maximum of 6 floods of high magnitude occurred between 2.6 to 1 ka implying recurrent interval of high magnitude flood was once in a 260 years. The frequencies of flood increased from 1 ka to 0.8 ka during which 8 floods were recorded suggesting one major flood after every 25 years. Absence of flood sediment above 0.8 ka event indicates decrease in the flood magnitude in the upper Ganga catchment.

In the study area the incised fan sequence has preserved three events of alluvial fan aggradations that are bracketed between 14 ka and 8 ka suggesting prevalence of transitional climatic conditions during their formation. The younger piedmont fan aggradations occurred after a prolong hiatus. Luminescence chronology bracketed the piedmont fan sedimentation between 2 ka and 1 ka. This implies that the development of piedmont fan postdate the mid-Holocene aridity in the Ganga plain.

In the recent times there is significant evidences to suggest that sesimicity is concentrated around MBT and MFT. This is very well demonstrated in the Sikkim-Darjiling Himalaya where raised fluvial terraces and gravel bed indicate that the region was active during the Quaternary. However, the geomorphic manifestation of sesimicity lacked absolute chronology.

In the present study activity along the MBT and its splays are chronologically constrain. The ages from fault gouge of South Kalijhora Thrust (SKT) (0.5 km south of Main boundary thrust) and main frontal thrust (MFT) indicated that lesser Himalaya experienced a regional phase of tectonic activity around 40 ka. Following this, the active deformation front subsequently moved north of the mountain front to the footwall of the MBT around 20 ka. Subsequent deformation and topography building near the MBT then caused additional blind imbricate faults to develop south of the mountain front at 14 ka and 6 ka. The two active fronts may have, therefore, evolved in a coupled manner; with the building of a critical taper in the footwall of the MBT.

Further evidence of seismicity are obtained comes from the raised fluvial terraces. Chronology of the fluvial terraces suggests that there were three major event of incision caused by the tectonic activity associated with the splays of MBT viz. the AJT and SKT. These events are dated to 7.7 ka, 4.4 ka and 1.4 ka respectively. This would imply that the terrain is uplifting at rates varied between 3-10 mm yr^{-1}.

As seen from the results from various geological archives discussed above, the sediments have shown partial bleaching. Even though minimum ages have shown considerable luminescence ages supported by paleoclimate records except in a known event of flash flood in 1970, it needs a detailed study. Present study was limited to the grain size of 90-150 micron or more; however, more fine textured grains can be taken for age estimation in a known event on the account of higher suspension time of finer material than coarse textured minerals. Recently developed linearly modulated OSL (LM-OSL) is capable of isolating rapidly bleaching and slowly bleaching component in a shine down curve. Even though initial part of the shine down curve is analyzed for age computation, which is fairly a rapidly bleaching part of the curve, LM-OSL combining with SAR will add new dimensions.

As discussed earlier, Paleoclimatic signatures studied in this work is limited to ~14 ka. In the present work, only a part of the alluvial fan was studied, however, it needs exhaustive study to infer about the older records that can be done by studying core samples at high depth.

Terraces are interplay of tectonic and climatic processes. It was the first time when the geochronology of a terrace in the Himalaya was used for paleoclimatic inferences. This prompts to identify and mapping of the young terraces in the Himalaya to get the paleoflood records in the Holocene. It might contribute to resolve the dilemma of tectonic or climate in such a dynamic area.

Publications

Papers

1. I. B. Singh, **Manoj K. Jaiswal**, A. K. Singhvi and B. K. Singh, 2003. Rapid subsidence of western Ganga plain during late Pleistocene: Evidence from optical dating of subsurface samples. *Current Science,* 84, 451–454.
2. Mark D. Bateman, Charles D. Frederick, **Manoj K. Jaiswal** and Ashok K. Singhvi, 2003. Investigation into the potential effects of pedoturbation on luminescence dating. *Quaternary Science Reviews*, 22, 1169–1176.
3. Mark D. Bateman, Peter J. Holmes, Andrew S. Carr, Benjamin P. Horton and **Manoj K. Jaiswal**, 2004. Aeolianite and barrier dune construction spanning the last two glacial-interglacial cycles from the southern cape coast, South Africa. *Quaternary Science Reviews*, 23, 1681-1698.
4. J.N. Pal, M.A.J. Williams, **Manoj K. Jaiswal** and A.K. Singhvi, 2006. Infrared stimulated luminescence ages for prehistoric cultures in the Son and Belan valleys, north central India. *Journal of Interdisciplinary studies in history and archaeology,* 1, 51-62.
5. M.A.J. Williams, J.N. Pal, **M. Jaiswal** and A.K. Singhvi. River responses to Quaternary climatic fluctuation: evidence from the Son and Belan valley, north central India. (in Press, *Quaternary Science Reviews*)

Abstracts

1. Malay Mukul, **Manoj K. Jaiswal** and A. K. Singhvi, 2003, Neotectonic activity in Darjeeling-Sikkim-Tibet wedge, National Seminar on Himalayan Orogen- Foreland Interaction, January 29-30, 2003, University of Lucknow.
2. A.K. Singhvi, **Manoj K. Jaiswal**, N. Juyal and V. Jain, Luminescence dating studies at the Physical Research Laboratory, International Conference in Luminescence and its Applications, February 9-12, 2004, BARC, Mumbai.
3. Wasson, R. J, Jain, V, **Jaiswal, M**., Juyal, N., Mcculloch, M, Sarin, M.M. Srivastava, P., Singhvi, A. K.The Contribution to the Sediment Budget of Landslides in the Upper Ganga Basin. International Association of Geomorphologists, Regional Conference, Feb. 27-29, 2004, Calcutta.
4. **M.K**. **Jaiswal,** Jain V., Wasson, R.J. Juyal N., and Singhvi A.K. Luminescence characteristics of fluvial sediments from complex lithologies in Himalaya: Implications for SAR and provenance. UK Luminescence and ESR meeting, 2004, St. Andrews University, UK.
5. Martine Simões, Jean Philippe Avouac, Yue-Gau Chen, Ashok K. Singhvi, Yu-Chang Chan, **Manoj Jaiswal**, Sylvain Bernard. Investigating the kinematics of shortening across the Pakuashan anticline, West Central Taiwan. American Geophysical Union, 2004.
6. **M.K. Jaiswal**, Pradeep Srivastava, A.K. Singhvi. Luminescence Chronology of mega and piedmont alluvial fan sequences in Ganga Plain. Indian Association of Sedimentologist, 2005, 21-23 Dec. 2005 at Wadia Institute of Himalayan Geology, Dehradun, India.